HISTOMORPHOMETRIC ANALYSIS OF THE TEMPOROMANDIBULAR JOINT CONDYLE IN YOUNG AND MATURE SHEEP

THE UNIVERSITY OF ADELAIDE
AUSTRALIA

Ryan James Cornish

B.D.S.(Adel.), B.Health Sc.(Hons.), B.Sc.

Thesis submitted in partial fulfilment of the requirements for the degree of Master of Science in Dentistry

Department of Oral Pathology
School of Dentistry
Faculty of Health Sciences
The University of Adelaide
South Australia

August 2005

For my beloved late Grandma

Dorris Maud Bartlett

Men who for truth and honor's sake

Stand fast and suffer long.

Brave men who work while others sleep,

Who dare while others fly-

They build a nation's pillars deep

And lift them to the sky.

Ralph Waldo Emerson

TABLE OF CONTENTS

DECLARATION

I certify that this thesis does not contain any material which has been accepted for the award of any other degree or diploma in any university or tertiary institution. To the best of my knowledge and belief, it does not contain any material previously written or published by another person, except where due reference has been made.

I give consent to the thesis being made available for loan and photocopying, when deposited in the University Library.

Ryan James Cornish

1st August 2005

ACKNOWLEDGEMENTS

I would sincerely like to thank my supervisors Dr. Richard Logan and Dr. Ole Wiebkin for their continual guidance and advice throughout my project. It has been an honour and privilege to have been able to undertake my Masters with such supportive academics. The advice, optimism, enthusiasm and keen interest they have shown were both dynamic and invigorating.

I am most grateful to The University of Adelaide (APA), Faculty of Health Sciences (Winifred S Steel) and Australian Dental Research Foundation (Research Grant) for their provision of scholarships in support of this project.

I gratefully acknowledge Assoc. Professor David Wilson for his encouragement and efforts in providing me with the initial opportunity to study in the department and for teaching me many new aspects of Oral Pathology.

I would also like to express my thanks and appreciation to Dr. Angela Pierce for her short but helpful supervisory assistance and support.

I especially thank Sandie Hughes for her assistance with collection of material and laboratory procedures along with her valued contributions and insights into my project. I appreciate all our many didactic discussions over the years.

I am greatly indebted to Marje Quin and Margaret Leppard for their technical advice in preparation of the histological sections. Thanks also to my Oral Pathology research colleagues for our interesting conversations and your support.

Many thanks must go to Assoc. Professor Nicola Fazzalari and Dr. Ian Parkinson (Institute of Medical and Veterinary Science) for assistance with the Quantimet 500MC. I am also most appreciative of the efforts of Dr. Peter Self, Dr. Meredith Wallwork and Mr. Angus Netting of Adelaide Microscopy for their assistance with the colour macroscopic photomicrographs.

I would also like to thank the many staff at the Adelaide Dental Hospital but especially to those individuals who have greatly assisted me in the completion of my studies including: Assoc. Professor Viv Burgess (Dean), Professor Alastair Goss (Oral Surgery), Professor Grant Townsend (Dental Science), Dr. Peter Telfer (Postgraduate Coordinator), Dr. Tracey Winning, Dr. Bingkui Ma, Dr. Tony Mavrokokki and Dr. Andrew Cheng and for their important contributions over the course of my research.

To my great Dental School mates and research colleagues (aka the executive committee) Dr. Jonathan Race, Dr. Jivajothi Jeyathevan and Dr. Salmin Ladhani, thank you for your endless encouragement and boundless friendship. I would not have achieved the things that I have without you guys. A special thanks must go to Dr. Vivian Liu for your always positive attitude and continued support during my research. Thank you also to Dr. Mariella Alvaro for your friendship and down-to-earth advice throughout my studies. To Dave, Paul, Gianni and my other school mates and university friends, thank you for providing me with light but necessary relief from my studies, especially over the occasional quiet beer.

To my girlfriend Andrea, thank you for your affection, friendship and much appreciated time over the last few months. Finally to my parents and family, I am eternally grateful for your unremitting love, immeasurable support and tireless understanding which make the achievements of this and every academic and life challenge possible.

PUBLICATIONS RELATED TO THESIS

Refereed Journal Articles:

RJ Cornish, DF Wilson, RM Logan, OW Wiebkin.
Trabecular structure of the condyle of the jaw joint in young and mature sheep: A comparative histomorphometric reference
Archives of Oral Biology. Electronic version published 8th June ahead of print.

Refereed Abstracts:

RJ Cornish, OW Wiebkin, DF Wilson, NL Fazzalari
Histomorphometry of trabeculae in the condyle of the jaw-joint: An experimental model involving young and mature sheep
Australian Dental Journal 2002 ADRF Special Research Supplement 43: 3

DF Wilson, OW Wiebkin, J Gardner, NL Fazzalari, **RJ Cornish**
Trabecular patterns in the temporomandibular condyle; the characterisation of a young and older normal sheep model in reference to human specimens.
Australian Dental Journal. In Press

Posters and Presentations:

RJ Cornish: Australian Jaw-Joint Project Scientific Meeting, October 2003
Colgate Australian Clinical Dental Research Centre
Student presentation: Histology and Morphological patterns of the condyle in the sheep

RJ Cornish: Colgate Research Day, August 2004
National Wine Centre
Quantitative histomorphometry of trabeculae in the condyle of the jaw-joint of young and mature sheep

SCHOLARSHIPS AND AWARDS RELATED TO THESIS

Winifred S Steele Faculty of Health Sciences Research Scholar, 2003-2005

Australian Postgraduate Award, 2003-2005

The Pierre Fauchard Undergraduate Award of Merit for best research report, 2003

Faculty of Health Sciences Research Vacation Scholar, 2002-2003

The Pierre Fauchard Undergraduate Award of Merit for best research report, 2002

Australian Dental Research Foundation Undergraduate Scholar, 2001-2002

LIST OF ABBREVIATIONS

AJJP	Australian Jaw Joint Project
AY	Anterior Young (sections)
BS/BV	Bone Surface/Bone Volume
BS/TV	Bone Surface/Tissue Volume
BV/TV	Bone Volume/Tissue Volume
CM	Central Mature (sections)
CT	Connective Tissue
CY	Central Young (sections)
ECM	Extra-cellular Matrix
FZ	Fibrous Zone (of cartilage)
H&EP	Haematoxylin and Eosin-Phloxine
HZ	Hypertrophic Zone (of cartilage)
LM	Lateral Mature (sections)
LY	Lateral Young (sections)
MM	Medial Mature (sections)
MY	Medial Young (sections)
PY	Posterior Young (sections)
SAB	Sub-Articular Bone
TbN	Trabecular Number
TbSp	Trabecular Separation
TbTh	Trabecular Thickness
TM	Total Mature (sections)
TMJ	Temporomandibular Joint
TT	Total Thickness (of cartilage)
TY	Total Young (sections)

LIST OF FIGURES

LIST OF TABLES

LIST OF GRAPHS

ABSTRACT

Much of the literature regarding arthrotic changes in the Temporomandibular Joint (TMJ) is based on the assumption, rather than the demonstration, that joint degeneration is pathologically and biochemically similar to that which has been described for other arthrodial joints. Understanding such changes is axiomatic of an understanding of the specific histomorphometric structure of the normal TMJ, in particular the condyle. Unfortunately, very little has been established about the trabecular bone and cartilaginous morphological patterns in the mandibular condyle as it develops during growth. As a consequence of the obvious practical difficulties in investigations of the human TMJ, the sheep has been variously used as an animal model. In order to augment a fuller characterisation of this animal model, this study focuses on the qualitative and quantitative histomorphometries of the trabecular bone and cartilage in the mandibular condyles of young and mature sheep.

Histomorphometric analyses of cartilage and trabeculae from mature and young sheep condyles were performed on histological sections stained with a modified blue Masson's trichrome and light green Masson's trichrome respectively. Digital photomicrographs of lateral, central & medial sagittal sections, and anterior & posterior coronal sections of the condyle were taken and then analysed using a public domain software programme (ImageJ 1.33u) to measure cartilage thickness as well as a Quantimet 500MC image analysis system programmed to measure 1) cartilage matrix and cellularity of the condyle and 2) structural index values of trabecular bone volume, surface, thickness, separation and number.

The results from this project found that there were strong variations in the range of qualitative morphology seen of both cartilage thickness and cellularity as well as trabecular bone morphology. Analysis of histoquantitation data revealed: 1) a significant decrease in the thickness of the Fibrous Zone, Hypertrophic Zone and Total Thickness of the central region as compared to the lateral and medial regions in the mature sheep, 2) a trend toward a higher cellular component (decreased matrix) in the young sheep as compared with the mature sheep condylar cartilage, and 3) a significant concordance in bone structural index values between lateral, central and medial regions in young and mature sheep as well as anterior and posterior regions in young sheep.

This study provides the first comparative histomorphometric analysis of cartilage and trabecular bone in the mandibular condyle of both young and mature sheep. The findings from this study reinforce the notion that there is constant remodelling of both the condylar cartilage and trabecular architecture throughout growth and development in the postnatal sheep, as well supporting the role of the sheep as a model in studies of the TMJ. Although there is a trend to a reduction in the cellularity of the condylar cartilage with age, a high cellular state still exists in the mature sheep indicative of such continuing growth and regeneration potential. As the thickness of condylar cartilage did not change with increasing age, this is indicative of the importance of cartilage as a method of transferring load to the bone. Nevertheless, the results do suggest that the central region, compared to the poles of the TMJ, has the greatest loads placed upon it over time resulting in increased wear. Finally in regards to the bone as an effective mechanism of distributing load, although qualitative morphological differences with trabeculae aligning perpendicular to the articular surface are seen, quantitatively our results insinuate that it is the distribution of bone, rather than an increase in the quantity of bone that changes with age.

CHAPTER 1:

INTRODUCTION

1.1 Anatomy of the TMJ

1.1.1 Gross anatomy

The temporomandibular joint (TMJ) is a cardinal feature that defines the class Mammalia and separates mammals from other vertebra (Herring, 2003).

The temporomandibular joint (TMJ) is a paired, pressure bearing diarthrodial joint that contributes to the articulation of the lower jaw to the skull. This connection postnatally is comprised of the articular part of the inferior surface of the squamous temporal bone (forming the glenoid fossa and articular eminence) and a convex extension of the mandible, the condylar process (or condyle) (**Figures 1 & 2**). The glenoid fossa is formed by the articular part of the temporal bone and also by part of the tympanic plate posteriorly. The articular eminence in the human is generally convex in the antero-posterior direction and concave in the medio-lateral direction. A capsule surrounds the condyle and the fossa. The joint also has ligaments which limit its movement in a lateral direction whilst the medial surface is limited by the bony fossa wall of the temporal bone. The condyle and temporal bone are separated by an avascular articular fibrocartilage disc which has attachments anteriorly to the lateral pterygoid muscle, laterally to the capsule and posteriorly to the bilaminar zone which is highly innervated and vascular. Thus, two joint spaces are formed (superior and inferior) which contain synovial fluid produced by synovium that has both a lubricative, protective and nutritive function (Piette, 1993).

The TMJ is a true synovial joint and is similar in nature to other synovial joints. However, it is highly specialised as the two joints support the single mandibular bone, making it the only bone to cross the midline that is supported by a joint (cf hyoid bone). The TMJ's are also unique in that they have a movement not only controlled by the

morphology of the joint per se but also by the dentition at the other end of the lever system (Piette, 1993). The TMJ has also been classified as a ginglyarthrodial articulation as it is capable of both hinge type (ginglymos) movements and gliding (arthrodia) movements (McKay et al., 1992). In regards to the size of the TMJ, it has been demonstrated that the dimensions of the TMJ are independent of sex, ethnicity and edentulism but are however related to cranial breadth measurements (Wish-Baratz et al., 1996).

The mandibular condyle can be divided into two gross anatomical parts, its head and neck. The articulating condylar head which is relevant to this histomorphometric study contains two main CT structures: an external cartilaginous covering and an underlying bony support. The structure and function of cartilage and bone will now be reviewed.

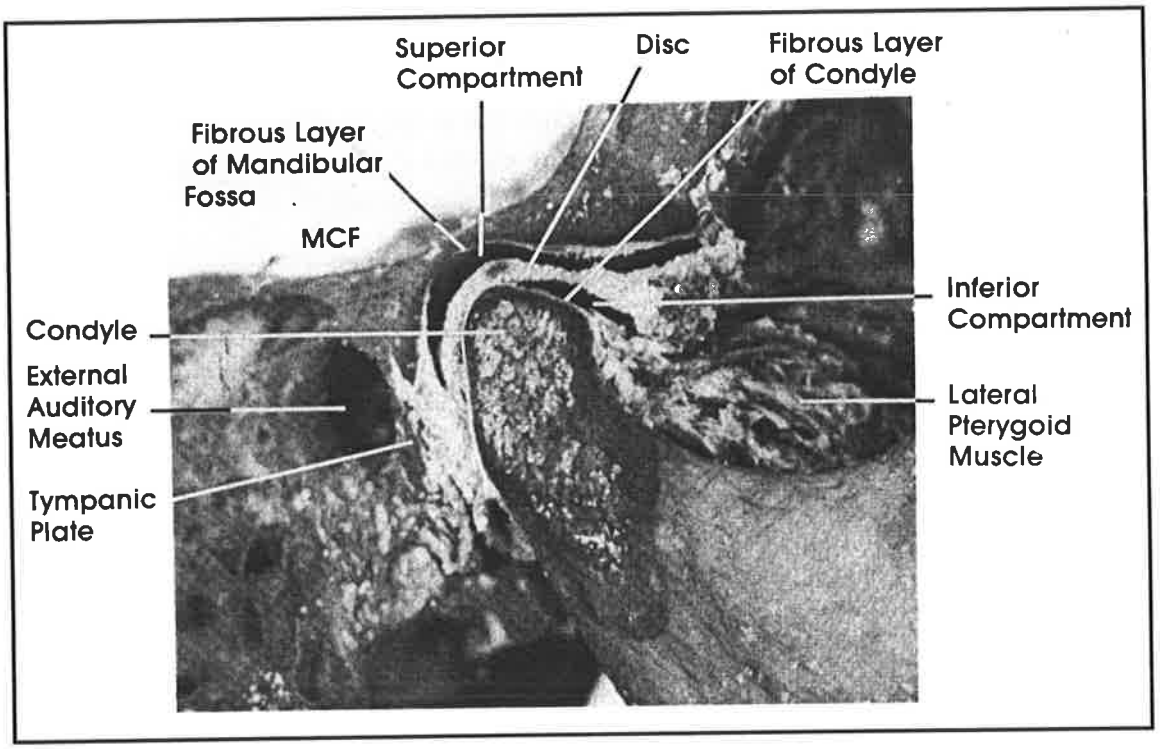

Figure 1: A macroscopic appearance of the Temporomandibular Joint in a human. Taken from Ten Cate, 1989; Oral Histology: Development Structure and Function. St. Louis: Mosby, Ch19: pg 384. (Originally from Liebgott WB. The anatomical basis of dentistry, Philadelphia: WB Saunders, 1982).

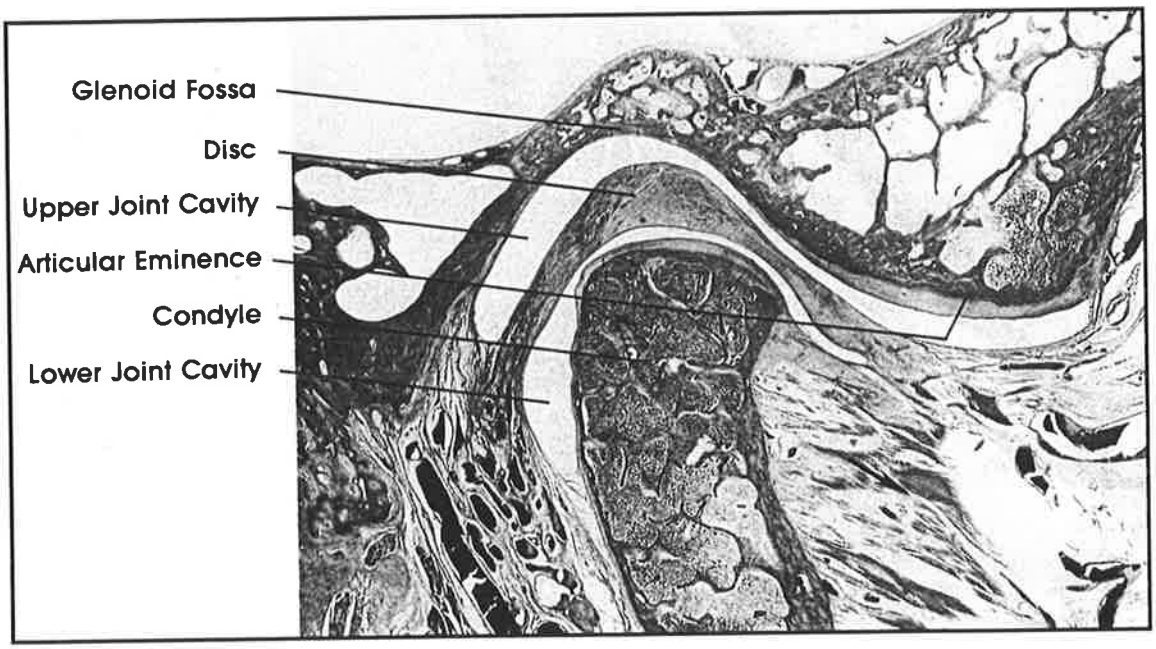

Figure 2: A histological section through the Temporomandibular Joint in a human. Taken from Ten Cate, 1989; Oral Histology: Development Structure and Function. St. Louis: Mosby, Ch19: pg 385. (Originally from Griffin CJ et al. *Monogr Oral Sci.* 1975; **4:** 1).

1.1.2 Microanatomy of the condyle

(a) Tissue and cellular components of cartilage

Cartilage forms the supporting framework of certain organs, the articulating surfaces of bones, and the greater part of the foetal skeleton.

Cartilage is a connective tissue that consists of a fairly dense matrix of collagen fibers encased in an amorphous intercellular substance of the chondroitin sulfate type which is in the form of a very thin gel. This ECM of cartilage is comprised predominantly of water (60-80%), collagen (60% dry weight), proteogylcans and glycoproteins (20-40% dry weight) and structural glycoproteins (non collagenous, non proteoglycan glycoproteins constituting 5-15% of the dry weight). Lipids and inorganic components constitute a negligible part of cartilage (Ten Cate, 2003).

In the matrix are the cellular components of cartilage, which reside in spaces known as lacunae. In a fresh state, the chondrocytes fill the lacunae, whereas in stained sections they often appear shrunken. The cytoplasm contains glycogen and lipid, and the nuclei are spherical with one or more nucleoli. Young immature chondrocytes tend to be rather small and flattened; as they mature they become larger and more rounded (Lamar Jones, 2002).

Hyaline cartilage is the most common type of cartilage and is found in the larynx, bronchus, nose, and as the articulatory surface of joints. When thoroughly lubricated with synovial fluid, the surface of cartilage will take on a high polish, with little friction, and is ideally suited for the bearing surfaces of joints. Fibrocartilage is found in sites such as tendon inserts where the tensile strength of hyaline cartilage alone is insufficient. In the mandibular condyle, unlike the articulating ends of long bones

which consist of hyaline cartilage, the articular surface consists of fibrocartilage that is derived from hypertrophic cartilage present during growth (Oberg and Carlsson, 1979).

The collagen fibers of hyaline cartilage generally do not have a regular pattern, whereas in fibrocartilage they are packed into rows parallel to the direction of the force. Between these collagen fiber bundles lie fibroblasts and rows of chondrocytes and intercellular substances. Cartilage develops from the mesenchymal cells that differentiate into chondroblasts and lay down intercellular substance; they mature into chondrocytes and the cartilage in this form can live for very long periods of time, as it does in joints (Lamar Jones, 2002). Cartilage is also responsible for the growth of bone, such as that of the condyle, see Chapter 1.2.2 (Brighton et al., 1984; Iannotti, 1990).

Luder (1997) reviewed the descriptive studies of the articular tissues in the human condyle and subsequently classified the articular tissue into 4 main zones:

1) A fibrous articular region (superficial zone) consisting of a dense avascular fibrous CT mainly consisting of large bundles of collagen fibers. This layer thins at the periphery of the condyle to blend with the periosteum of the mandible on the condylar neck (Seipp, 1964).

2) A proliferative region (intermediate zone) with a high proportion of polymorphic and flattened cells largely consisting of differentiating cells.

3) A hypertrophic region (deep zone) consisting of hypertrophic cartilage evident by the presence of large round cells in lacunae surrounded by matrix.

4) The calcified cartilage and subchondral bone region as demonstrated by vascular invasion and formation of trabecular bone.

The cartilaginous zones of the condyle are illustrated in **Figure 3.**

Cartilage is distributed in sites throughout the body where the functions it has to perform include having not only tensile strength but also flexibility. However, a permanent rigid type of CT is required to support the body's weight, to maintain its optimal shape and to shield its delicate structures from damage; this tissue is bone.

(b) Tissue and cellular components of bone

Bone is a specialized mineralised CT consisting of 67% mineral (predominantly calcium hydroxyapatite) and 33% organic matrix (including 28% collagen and 5% noncollagenous proteins). Although the values given are approximate and variable (eg as they are in patients with osteoporosis), this 2:1 ratio between hard and soft tissue components is sufficient to provide a degree of elasticity. Bone resists compressive forces best and tensile forces least (Ten Cate, 2003).

Characteristic features of all bones can be seen in the sections of the condyle under the periosteum. These include an outer sheet of dense cortical bone (compact bone) and an inner component representing the cancellous bone (sponge like) that contains a marrow cavity separated by bony trabeculae. In growing children the marrow cavity is filled with haemopoietic tissue which contains a stroma as well as an extensive vascular system. This cavity is not continuous and is interrupted throughout the bone by a network of trabecular bone particularly under the condylar cartilage (Ten Cate, 2003). Although this cancellous bone is always surrounded by compact bone, these internal

trabeculae act as well-banded reinforcement rods to support the outer cortical crust (**Figure 4**).

The inner surface of the cortical bone and entire system of trabecular bone are lined by a soft CT, the endosteum. This is similar to the outer lining, the periosteum but is not as well defined. The endosteum is a single, is a single cellular layer that contains osteogenic cells (Krause and Cutts, 1981). The periosteum contains an inner layer that is composed of bone cells, their precursors and a rich microvascular supply, whilst the outer layer is more fibrous (Ten Cate, 2003).

In both the cortical and trabecular bone, three types of bone cells are described: the osteoblast that forms bone, the osteocyte which maintains bone and the osteoclast that resorbs bone (Krause and Cutts, 1981). All these cells are derived from progenitor cells that reside in the marrow. Osteoblasts are derived from the mesenchymal lineage of the marrow stroma whilst the osteoclasts belong to the haematopoietic lineage of the bone marrow stroma (Ten Cate, 2003). Bone marrow stroma also contains a unique cell population, referred to as marrow stromal cells, capable of differentiating along multiple cell lineages (Bergman et al., 1996; Phinney et al., 1999). In mammalian bone marrow, three types of marrow stromal cells are present including hematopoietic support cells, osteogenic stromal cells and adipocytes.

Bone has many functions, including support, protection, mineral storage, haemopoiesis and permits articulation at its specialised cartilage covered ends (eg the TMJ).

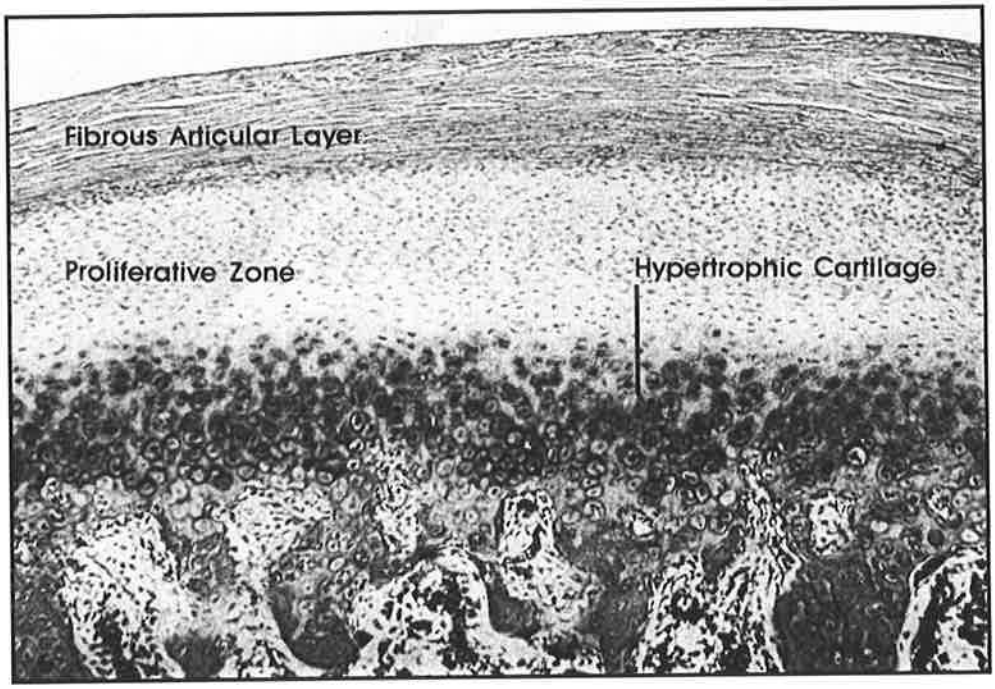

Figure 3: A section through the growing condylar cartilage of a 13-year old child illustrating the different layers present from the external articular surface to the subarticular bone underneath the hypertrophic cartilage layer. Taken from Ten Cate, 1989; Oral Histology: Development Structure and Function. St. Louis: Mosby, Ch19: pg 384. (Originally from Goose, DH and Appleton J. Human Dentofacial growth, Oxford: Pergamon Press, 1989).

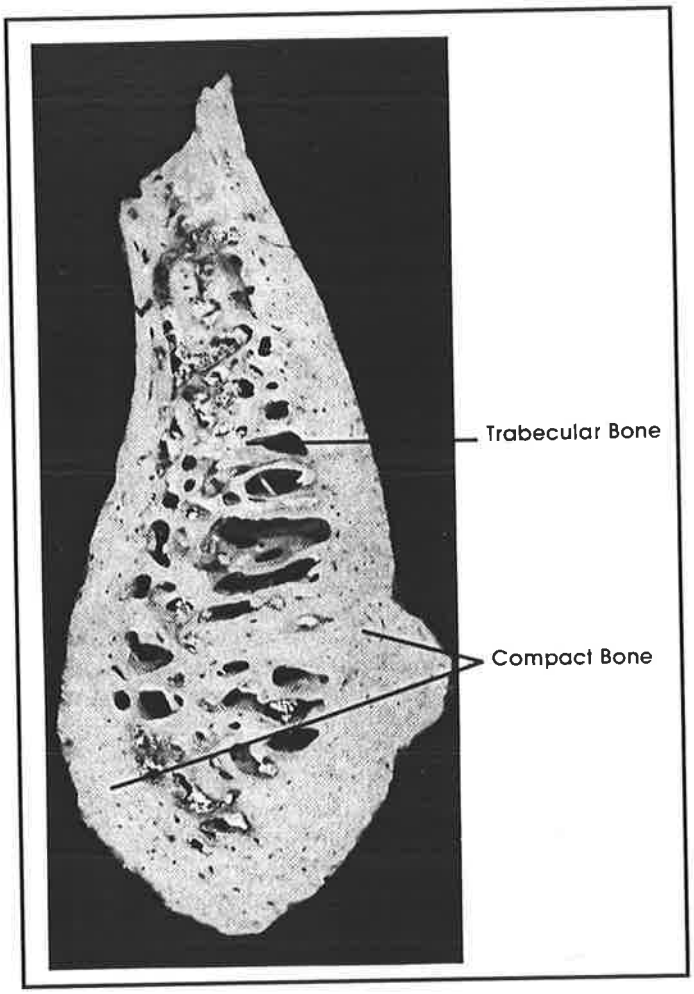

Figure 4: Body of the mandible, gross cross section: the outer layer of compact (cortical) bone and an inner supporting network of trabecular (cancellous) bone can be clearly distinguished. The same gross bony architecture appears in the mandibular condyle. Taken from Ten Cate, 1989; Oral Histology: Development Structure and Function. St. Louis: Mosby, Ch8: pg 116.

1.2 Biology of growth of the condyle

Before assessing the anatomical structure of any given tissue, it is essential to consider its embryological as well as post natal growth and development. The embryology of the TMJ and the method by which the cartilage and bone of the condyle form is pertinent to its final morphological structure. Importantly, the embryonic origin of the TMJ is significantly different from that of other articulations and in phylogenetic terms, the TMJ is actually a secondary joint (Merida-Velasco et al., 1999).

Meckel's cartilage initially provides skeletal support for the developing lower jaw and extends from the midline back dorsally where it terminates as the malleus. This cartilage then articulates with the incal cartilage. In the early jaw, it is between these two cartilages that movement can occur. This primary jaw joint exists for approximately 4 months until ossification of these cartilages occurs and these are incorporated in the middle ear. The primary vertebrate jaw joint is still present however, as the malleo-incal joint, with the bones involved now positioned in the middle ear (Ten Cate, 2003).

At approximately 3 months, the secondary jaw joint (TMJ) begins its development. During this appearance stage, two distinct regions of mesenchymal condensations, the condylar and temporal blastemas are observed. These differentiate into condylar cartilage and temporal bone respectively forming an articulation. Ossification begins first in the temporal blastema while the condylar blastema still consists of condensed mesenchyme. At this stage a cleft appears immediately above it that becomes the inferior joint cavity. The condylar blastema differentiates into cartilage and then a second cleft appears in relation to the temporal ossification that is the upper joint cavity with the primitive disk formed between the two spaces (Ten Cate, 2003) (**Figure 5**).

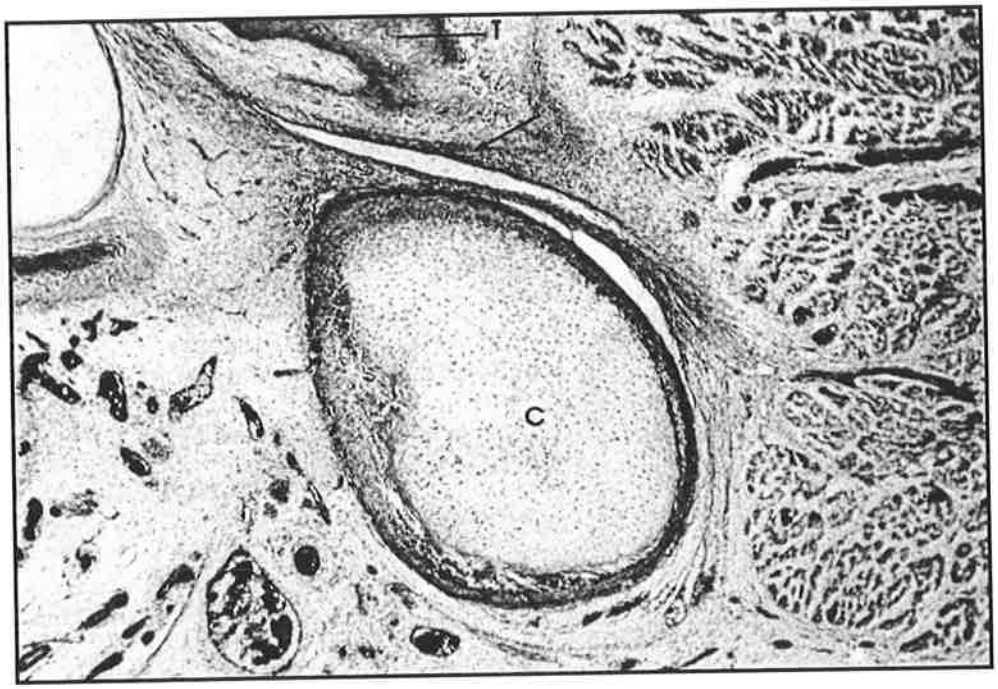

Figure 5: A sagittal section of the temporomandibular joint of a fetus, showing the formation of the superior joint cavity (arrow). Cartilage has formed in the condylar blastema (**C**) and the developing temporal bone (**T**). Taken from Ten Cate, 1989; Oral Histology: Development Structure and Function. St. Louis: Mosby, Ch19: pg 386. (Originally from Perry HT et al. *Cranio*. 1985; **3:** 125).

One interesting feature of the TMJ is its related to its growth. The mandible and the squamous part of the temporal bone do not have an epiphyseal plate. Their growth is affected by nearby cartilaginous structures. In most vertebrates, Meckel's cartilage has been thought to be the cartilaginous structure responsible for this pattern of growth. However, a secondary condylar cartilage also acts as another major growth site in addition to it being an articular covering (Herring, 2003).

1.2.1 Intramembranous ossification of the mandible

In intramembranous bone formation (eg maxilla and body of the mandible), bone develops directly within a soft CT membrane, rather than on a cartilaginous model. Periosteum also has the ability to form bone. Embryonically, the cranial vault, the maxilla and body of the mandible, mesenchymal cells proliferate and condense. As vascularity increases at these sites of condensed mesenchyme, osteoblasts differentiate and begin to produce bone matrix de novo. As more and more bone matrix is deposited, the cells and their processes become trapped in the matrix and are then identified as osteocytes. The initial matrix produced by osteoblasts consists of ECM and collagen fibers. This is called osteoid, which then becomes mineralised to form bone. Once begun intramembranous bone formation forms at an extremely rapid rate (Krause and Cutts, 1984; Ten Cate, 2003).

However, unlike the maxilla, body of the mandible and cranial vault, the bone at the proximal ends of all long bones, vertebra, ribs, as well as that of the mandibular condyle and base of the skull forms from the subsequent replacement of a cartilage matrix scaffold (Ten Cate, 2003). This scaffold is already in the general shape of the bone from which it will be replaced with. This alternative bone forming process of which is pertinent to this study of the condyle is called endochondral ossification.

1.2.2 Endochondral ossification

The formation of bone within the condyle is believed to be due to the process of endochondral ossification. In growing individuals, this pattern of bone formation is recognized both under the periosteum and under the cartilage where blood vessels are present (Ten Cate, 2003). Unlike intramembranous ossification which involves the de novo synthesis of bone from mesenchymal tissue, bone formation involves the replacement of a pre-existing condylar cartilage matrix (Gibson and Flint; 1985; Hunziker et al., 1987; Alini et al., 1992; Brown et al., 1993; Byers et al., 1997). Angiogenesis is recognized as the pivotal event in endochondral ossification with an endothelial cell invasion and migration into hypertrophic cartilage. This cartilage becomes eroded producing a scaffold for osteoblasts to produce bone (Alini et al., 1996). The process of endochondral ossification is considered to occur in two main steps which will now be discussed (Carlevaro et al., 1997).

Firstly, avascular cartilage differentiates into hypertrophic cartilage. The flattened cell layers underneath the articular fibrous CT are the sites of mitotic activity which give rise to cells that undergo endochondral differentiation. Pressure resulting from cell population and matrix production increase cause the articular layer to be displaced further away. The cells in the hypertrophic layer markedly increase their cells size and shape from being flattened to circular and increase their secretary activity, whereby matrix mineralisation proceeds. These cells are eventually lost when their lacunae are invaded by angiogenesis (Luder and Schroeder, 1992). Secondly the invaded hypertrophic cartilage will produce alkaline phosphatase (causing an increase in calcium salts) which causes the cartilage to undergo erosion with degeneration and removal of the unmineralised transverse septal cartilage with the vessels invading into the newly opened lacunar channels. Phagocytosis of the cartilage fragments by

mononuclear cells occurs before osteoblasts deposit bone matrix over any persisting septal cartilage matrix (Brookes and Revel, 1998). There is also degradation of bone and calcified cartilage by osteoclasts in this ossification zone (Lewinson and Silbermann, 1992; Sasaki et al., 1996).

The condylar cartilage scaffold that appears during the twelfth week of development rapidly forms a cone shaped mass that occupies most of the developing ramus. This mass of cartilage is quickly converted to bone by endochondral ossification so that at 20 weeks in utero, only a thin layer of cartilage remains at the condylar head. This remnant of cartilage persists into adulthood and provides a mechanism for growth of the mandible in exactly the same way as the epiphyseal cartilage (growth plate) of long bones (Ten Cate, 2003).

1.3 Age related changes of the condyle

1.3.1 Function of the TMJ

As previously mentioned, the TMJ articulates the tooth bearing mandible to the skull via the squamous part of the temporal bone. The structure of this joint enables it to perform gliding, hinge-like and rotary movements. It is obvious that the most important function of the joint is to enable mastication of food by the teeth of the mobile mandible against the teeth (or anterior hard palate in sheep) of the rigid maxilla. In opening the mouth, both gliding and hinge like actions occur through the rotation of the condyles around a horizontal axis passing through both joints. At the same time, the articular discs are carried orally by gliding on the temporal surfaces. In protrusion and retraction of the lower jaw, only the gliding action occurs. Transverse movement also occurs and consists of a rotary movement about a vertical axis as in mastication and rumination in sheep (Hecker, 1983). In this movement, the disc glides orally on one side and caudally on the other. The mandible is carried across the upper jaw, and a grinding action takes place between the molar teeth (May, 1970).

1.3.2 The mechanical effects of load

Load related changes have previously been described in studies of humans (Atkinson, 1967; Kember and Sissons 1976; Kneissel et al., 1977; Gruber and Rimoin, 1989; Rodriguez et al., 1992; Glorieux et al., 2000; Gong et al., 2005) as well as in various animal species (Hunziker EB and Schenk, 1989; Miralles-Flores and Delgado-Baeza, 1992; Sontag, 1994; Kuhn et al., 1996). The belief that the TMJ is a passive, non-stress bearing suspension has now been considered passé for many years (Standlee et al., 1981). Studies have demonstrated the stress bearing nature of this joint utilizing widely varied methods of investigation. Relevant to the present study is the notion that load is normally applied to the condyle of the TMJ and that it varies in magnitude and

direction. The use of the muscles responsible for masticatory forces and the presence and occlusion of teeth with developmental age are two such examples of how such load may be generated and applied.

The TMJ condyle is believed to be in a constant state of remodelling (cellular and extracellular turnover). The primary function of remodelling is to maintain functional and mechanical relationships between articulating surfaces of the joint. Remodelling is an essential biologic response to normal functional demands, ensuring homeostasis of the joint form, and functional and occlusal relationship (Arnett et al., 1996). Remodelling may result when changes occur in either the host adaptive capacity or when mechanical stresses are placed on the joint structures such that:

Host remodelling capacity + mechanical stress = morphological change in the condyle

In regards to the host remodelling capacity, the factors that have been reported to influence this equation are most importantly age (Silbermann and Livne, 1979), systemic illness (Dick and Jones, 1974) and hormones (Furstman et al., 1965; Arnett and Tamborello, 1990).

Mechanical stress factors occur as a result of the stretch or compression of tissues. Clinical mechanical factors that can have an influence on mechanical stress and consequently initiate change in TMJ structure include: occlusal therapy, internal derangement, parafunction, macrotrauma and an unstable occlusion. Orthodontics (protrusive movements; Ma et al., 2002ab) and orthognathic surgery (sagittal mandibular osteotomies; Arnett et al., 1992) often create mechanical stress factors that can lead to morphological change of the TMJ condyle.

Articular cartilage serves as a load-bearing elastic material that is responsible for the frictionless movement of the surfaces of articulating joints (Huber, 2000). However, it is often stated that the cartilaginous surface of joints is purely a shock absorber. This statement is not true. Although the cartilage is load bearing, it only absorbs a negligible amount. In fact it is predominantly a load transmitter, whereby it distributes load to the underlying bone (Standlee et al., 1981). This notion is reflected in the numerous studies of bone architecture in response to generated loads discussed below.

The trabecular architecture is deemed to be constructed to accommodate such stress since it demonstrates characteristic orientation based upon the location and direction of the stress (Hongo et al., 1989b). Loads created by occlusal compressive forces from the muscular contractures concentration initially in the individual teeth, whereby they are distributed via the periodontal membrane to cortical bone and dense struts of the mandible. Once within the boundaries of the mandibular bone, these loads are transmitted through the ramus to the condyle and eventually to the floor of the skull (Standlee et al., 1981; Teng and Herring, 1995).

Although the precise mechanism of adaptation is uncertain, it is believed that the architecture of trabecular bone corresponds to mechanical loading (Hert 1992; Lanyon, 1992; Turner 1992a,b; Hert 1994; Teng and Herring 1995) and increasing age (Kneissel et al., 1977; Sontag, 1994; Glorieux et al., 2000). The condyle is thought to be the most heavily loaded during chewing as compared with the temporal component of the TMJ (Hylander, 1979; Hylander and Bays, 1979). Compared to cancellous bone from other locations, the trabeculae of the mandibular condyle are quite robust and dense, strongly supporting the notion that the TMJ is heavily loaded (Teng and Herring, 1995). Bone plates and rods align along the lines of principle stress or trajectories (Roesler, 1981).

Trabeculae consequently are equally loaded under tension or compression. This is an ideal property of optimum structures, which combine maximum stiffness with a minimal amount of material (Parkes, 1974). The theory is that these trajectorial structures are due to the process of functional adaptation, in which unloaded bone disappears and mechanical stimulation induces bone formation (Smit et al., 1997).

Judex et al. (2003) showed experimentally that extremely low magnitudes mechanical stimuli induced at high frequencies were anabolic to trabecular bone. For a given input stress, the resultant stresses within trabeculae were more uniformly distributed in the off-axis loading directions of mechanically loaded sheep. Their study summarized that trabecular bone responded to low level mechanical loads with intricate adaptations producing a structure that becomes stiffer and less prone to fracture for a given load.

Previous studies on human TMJ's have also demonstrated a decrease in trabecular bone density and a reduction of trabecular width in the human condyle in edentulous patients whose mandibular loads are absorbed by dentures (Hongo et al., 1989a) and with advancing age (von Wowern and Stoltze, 1980; Hongo et al., 1989b).

Age related changes between those observed in the adult compared to the growing individual have also been reported on the architecture of the articular tissues of the condyle (Wright and Moffett, 1974; Thilander et al., 1976; Oberg and Carlsson, 1979), suggesting that profound maturational changes occur after cessation of growth. During life, the temporal, condylar and discal articular surfaces undergo remodelling (Piette, 1993). However questions about the nature and time course of such maturational changes have remained open.

In a pioneering qualitative histological study by Thilander et al (1976), sections from TMJ's of 61 humans, aged 2 days to 27 years were examined. Four layers of the condyle were studied in detail. The outermost layer was richly vascularised in new-borns but by 3 years of age it becomes avascular and contains few cells. In neonates the cartilage layer constituted a large part of the condyle but soon decreased in thickness and by 5-6 years of age it constituted only a thin zone of the top of the condyle. In the proliferative zone, mitoses occurred up to 13-15 years of age. This zone then decreased in thickness; the number of cells decreased, while the amount of intercellular substance increased. At birth, the temporal component was flat and was lined by vascularised connective tissue which became richer in collagen with increasing age. The cartilage layer was lacking in the fossa but was present on the tuberculum. A proliferative zone in this cartilage could be seen up to the age of 17-18 years and cartilage having only few cells was found in adults. Remodelling processes were seen in all components of the joints.

The ability of bone to adapt to mechanical loads, generally referred to as Wolff's Law (1892), provides each bone or component (such as the mandibular condyle) with a bone architecture that optimally suits its individual needs (Smit et al., 1997). This information plays an obvious important role in relevance to understanding the function of such bones as well as in the clinical diagnosis of pathology.

1.3.3 Architectural changes causing TMJ pathology

The integrity of a joint is dependent upon its architecture (geometry) of cartilage and bone, its supporting structures. Disease is therefore as a result of alterations in the architecture, components or the support of the joint. The alterations in joint shape that

occur with age are usually related to changes in the activity of remodelling of the articular surface of joints with age (Bullough, 2004).

In humans, any pathology associated with the articulating components of the TMJ is often referred to as a temporomandibular disorder (TMD) (McNeill, 1993). There is extensive literature on a variety of well-recognised TMD's, including joint degeneration which has been classified as osteoarthrosis (de Bont and Stegenga, 1993). However, controversy exists in some of the literature regarding these changes, since it is based on the assumption, rather than the demonstration, that this degeneration is pathologically and biochemically similar to that described for other joints (eg excessive loading of compromised joints like the hip and knee). Such controversy has led to the questions of whether degeneration of the TMJ can result from changes in (i) disc position, (ii) from changes in the articular tissues that occur as a consequence of cartilage-driven change or (iii) whether bony structural changes are responsible. Thus, central to any understanding of degenerative TMJ pathologies and their experimental models is the need for a sound knowledge of the structure and biomechanics of bony components of a normal model joint.

The effects of stress on the joint are still not fully understood. Often the joint undergoes arthrosis in response to heavy use with functional stresses concentrating in the condylar neck, but reduced in the condylar head due to its elliptical shape (Standlee et al., 1981). Biomechanically, the development of osteoarthrosis is more likely related to the magnitude and frequency of stresses applied on the cartilage. Joint movements produce tractional forces that may cause shear stresses contributing to cartilage wear and fatigue. Tractional forces are generally the result of frictional forces caused by the cartilage surface rubbing, and plowing forces caused by the translation of a stress-field

through the cartilage matrix, as the intra-articular space changes during motion (Palla et al., 2003). The stress directions within the condyle however do not seem to be preferential and vary with mandibular position (Standlee et al., 1981). This supports the idea that the condyle is designed to receive light varied forces rather than heavy unidirectional forces, which can damage the joint (Standlee et al., 1981; Giesen and van Eijden, 2000).

TMD's are usually characterized by joint degeneration and facial pain. Histological as well as arthroscopic studies have documented that, at the early ages of the disorders, the tissues of the joint undergo a change resembling osteoarthritis (De Bont et al, 1986). At late stages the joint can become inflamed, with synovitis and bone erosion resembling an inflammatory arthritis (Puzas, 2003).

Osteoarthritis is a common disorder of synovial joints. It is characterised pathologically by focal areas of damage to the articular cartilage, centred on load-bearing areas, associated with new bone formation at the joint margins (osteophytosis), changes in the subchondral bone, variable degrees of mild synovitis, and thickening of the joint capsule (Pritzker, 2003). When this disease is advanced it is visible on plain radiographs, which show narrowing of joint space (due to cartilage loss), osteophytes, and sometimes changes in the subchondral bone (Watt and Doherty, 2003). Osteoarthritis can arise in any synovial joint in the body, but is most common in the hands, knees, hips, and spine. A single joint could be involved, but more commonly several joints are affected. This condition is strongly age-related, being less common before 40 years, but rising in frequency with age, such that most people older than 70 years have radiological evidence of osteoarthritis in some joints (Petersson, 1996).

The tissue that has attracted most attention in relation to the pathogenesis of this disease is articular cartilage, largely because of the striking changes in this tissue in advanced osteoarthritis. The surfaces of joints are covered by a thin layer of articular cartilage resting on subchondral bone. Cartilage does not have nerves or blood vessels, whereas both are plentiful in bone. Healthy joint cartilage distributes static and dynamic joint loading and decreases friction. Sparsely distributed cartilage cells maintain a cartilage matrix rich in collagen and proteoglycans. The quality of this matrix is critical for maintaining the functional properties of the cartilage. Changes in the joint cartilage associated with osteoarthritis include gradual proteolytic degradation of the matrix, associated with increased synthesis of the same (or slightly altered) matrix components by the chondrocytes (Sandy, 2003). These events at the molecular level result in early morphological changes: cartilage surface fibrillation, cleft formation, and loss of cartilage volume (Heinegard et al., 2003).

Concomitant events in bone are less well understood, but include the development of osteophytes at the joint margin, through ossification of cartilage outgrowths, and major changes in the vascularity and turnover of the subchondral bone (Burr, 2003; Westacott, 2003). Subchondral bone changes could be an important part of the pathogenesis of progressive joint destruction (Dieppe et al., 1993; Felson et al., 2003; Mazzuca et al., 2004), partly because the bone has far greater ability to repair, adapt, and change the shape of the joint than cartilage. Whether events in cartilage precede those in bone, are concomitant with them, or whether subchondral bone changes can actually cause early cartilage damage is uncertain.

With advancing age, the articular surface of the mandibular condyle can show morphological changes. Ishibashi et al (1995) showed that some changes occurred

unilaterally to condyles that had minimal areas of occlusal contact on that side. Their findings suggested that a decrease in the cellular components with advancing age could play a critical role in the development of degenerative changes. However, Stratmann et al (1996) reported that the condylar cartilage did not seem be affected by age in relation to its thickness in a mediolateral direction. Their results supported the notion that the joint is seemingly loaded along its entire articular surface and that a lateral disc perforation in older individuals could be due to a physiological process of wearing rather than to a pathological sequel of functional disorders.

Nevertheless, clinical manifestations associated with pathological and radiographic changes often include joint pain related to use resulting in inactivity, stiffness of joints, pain on movement with a restricted range, and crackling of joints (crepitus). Pain is particularly important, and osteoarthritis is thought to be the biggest cause of the high rate of regional joint pain suffered by older persons (Peat et al., 2001).

1.4 Histomorphometry of tissues

1.4.1 General principles

Both two dimensional (2D) and three dimensional (3D) techniques are available for the imaging and analysis of tissues. Analysis of biological hard tissues can be performed by medical physicists and radiologists using 3D techniques which include serial sectioning, X-ray tomographic methods, and NMR scanning (Odgaard, 1997). These techniques have the advantage in that they are non-invasive and are ideally suited to clinical studies. However, these techniques have problems of their own. For example, serial sections are extremely time consuming as was noted in the first reported 3D rcconstruction of a vertebral body by Amstutz and Sissons (1969). X-ray CT and NMR methods are expensive and have a limited resolution, with 8 microns being the highest resolution published for cancellous bone (Bonse et al., 1994).

Revealing internal anatomical structures with 2D methods usually involves some form of serial slicing where the 3D space is derived from the 2D images (Mayhew, 2000). Stereomorphology of tissues, such as bone, involves applying a set of clear sampling rules and simple estimation tools that allow 3D quantities to be calculated using chance events (eg intersections, profiles, outline). Structural analysis usually requires measurement of area and perimeter from samples of histological tissues (Parkinson and Fazzalari, 1994). One such technique is the use of a digitized quantitative image analysis system. This technique has saved enormous amounts of time in comparison to conventional counting techniques. This very attractive way to measure structural parameters of bone and cartilage will now be discussed.

1.4.2 Quantitative image analysis

Quantitative image analysis started in the early 1960's, applying stereological axioms

by point counting (Weibel, 1979). The application of stereological methods was based on two requirements: firstly the identification of the objects being measured and secondarily the actual measurements and calculation of parameters derived from these primary data. Over time, manual point counting has been replaced by computers and segmentation of tissues (ie the field of interest) is carried out by electronic aid, either by interactive tracing of the objects or by automatic procedures. (Oberholzer et al., 1996). The enormous time savings of automated morphometry make this a very attractive way in which to measure structural parameters

The main steps of any image analysis system are image capturing, image storage (compression), correcting imaging defects, image enhancement, segmentation of objects in the image and finally image measurements. Digitisation is usually made with a camera. The numerical information consists of a grey values describing the brightness of every point within the image, termed a pixel. This information is stored in bits with eight bits equaling one byte. Therefore, grey values can be achieved between 0 and 256 (or 2^8) with image analysis systems, as compared with the human eye with an approximate five bit image capability (corresponding to 64 different grey values) (Oberholzer et al., 1996).

Image analysis systems such as the Quantimet 500MC have previously been used (Parkinson and Fazzalari, 1994) to measure digital entities by creating a binary representation of the original image on an X by Y pixel array. This can be achieved by setting the binary threshold to a grey level that detects the entire stained trabecular bony matrix but none of the background of the section. The program then provides the total pixel count of the binary image against a translucent background of the slide.

Trabecular bone with its cancellous structrure and cartilage with its matrix scaffold have long been studied by morphometrists. Histological sections allow all components of tissue structure to be examined including the size and shape of the individual cells, to what structures they form and in what spatial arrangement they exist. In regards to trabecular bone, structural analysis involves the measurements of area and perimeter and along with the total measuring frame (as outlined by the X and Y pixel array) are applied to formulae derived from the parallel plate model of cancellous bone to yield structural parameters that describe it. This Euclidean based geometric model proposed by Parfitt et al (1983) is most commonly used where the cancellous bone is deemed to be composed of parallel plates with interconnecting rods.

In a study by Flygare et al (1997) using image analysis, the aim was to develop a reproducible method for bone histomorphometry with the aid of a computerized image analysis program, and to examine the variation when assessing total and trabecular bone volume parameters. Histologic sections of TMJ's from eighteen autopsy specimens were read interactively using a cursor. The two parameters (total bone and trabecular bone volume) of the condyle and the temporal component were estimated twice by one observer using three different threshold settings: an automatic, a semi-automatic and a manual technique. The threshold was based on the gray-scale distribution of the image. Their findings showed that the intra-observer variation ranged between 1.9% and 7.1% for the automatic threshold setting technique and between 2.8% and 8.7% for the semi-automatic technique. The manual technique however, resulted in a high intra-observer variation with a coefficient of variation between 5.2% and 19.9% creating a statistical difference between the estimates of the two observers. Interestingly they also found that the intra- and inter-observer variation was higher in the temporal component than in the condyle. In conclusion they stated that automatic

and semi-automatic techniques resulted in comparable intra-observer variation with a lower bias in the estimates of the semi-automatic technique. They also felt however, that it was possible to achieve fast and reproducible analysis of the total and trabecular bone volume using the manual technique as long as strict boundaries and parameters were defined and assessed prior to quantitation.

A study by Hacket et al (1997) also confirms the findings of Flygare et al (1997). In this study a colour based imaging system for accurate quantitation of articular cartilage was used. They demonstrated this through the reproducibility of quantitative results with precision analysis of intraobserver and interobserver variability when measuring cultured perichondral cells implanted in a polylactic acid matrix in the rabbit femoral condyle.

Indeed, other studies of complex 3D gridworks such as the architecture of the TMJ using image analysis stereomorphometry have been performed (see section 1.5.3). This methodology has offered a reliable way of quantifying cartilage (Luder, 1997; Luder, 1998; Ma et al., 2002a) as well trabecular bone volumes, surfaces, lengths and numbers in the TMJ condyles involving experimental animal models such as the sheep (Ma et al., 2002b) and pig (Teng and Herring, 1995).

Architecture of tissues changes readily in response to disease. The disease process may result in alteration to the normal mechanical stresses acting on a particular site where the alteration may be in both magnitude and direction. For these reasons, the application of image analysis techniques for the analysis of histology and histopathology are developing rapidly, particularly where it is possible to prepare high contrast histology sections. Bone and cartilage are two such tissues that commonly

undergo degeneration and are studied throughout the literature. These tissues however, require stains that enable them to be adequately contrasted and quantitated.

1.4.3 Histological stains for cartilage and bone quantitation

(a) Routine and specific stains

Because of the mineral content of teeth, bone and calcified cartilage, some modification of the methods used for the preparation of sections of other tissues is necessary. Although the preparation of special undecalcified hard tissue sections is possible (such as the von Kossa silver stain), the removal of calcium salts is generally required before sectioning using one of a number of demineralization solutions for histological purposes.

The standard counterstain technique employed universally is the Haematoxylin-Eosin stain (H&E). The Ehrlich's Haematoxylin nuclear stain with corresponding eosin counterstain is used for general assessment and demonstration of tissues and their pathologies. Modifications of the routine H&E counterstain can include the addition of Phloxine B (maximum absorption 546-548) to the Eosin counterstain (maximum absorption 515-518) giving a greater intensity of transmitted light to the counterstain (appears pinky orange) (Lillie, 1969). Also the combination of Weigert's Haematoxylin nuclear stain with van Gieson's stain is popular, but the staining of collagen red with other tissues staining yellow does not provide the widest degree of contrast of stains available (Drury and Wallington, 1967).

Collagen in cartilage and bone may be stained by Mallory's aniline blue stain for collagen, the Schmorl's picro-thionin method, Heidenhain's azan stain, Lillie's allochrome method or metachromatically with safranine, methyl violet or toludine blue.

However, these techniques either require a special fixative solution or lack the variation in colour intensities and differential, especially in regards to distinguishing between tissue components like collagen fibers (such as those in cartilage matrix) and cellular cytoplasm (Culling, 1974).

Collagen also stains strongly with acid dyes, due to the affinity of the cationic groups of the proteins for the anionic reactive groups of the acid dyes. These can be demonstrated more selectively by compound solutions of acid dyes (eg van Gieson) or by compound solutions of acid dyes (Lamar Jones, 2002).

The Masson's trichrome technique is an excellent example of an acidic dye that stains intensely and has a good colour differential between tissue components. The use of such a technique is particularly necessary if the array and intensity of transmitted light of the individual tissue components is required as in the case of using digitized image analysis systems for histoquantitation. This technique will now be discussed in further detail.

(b) Masson's trichrome

The term trichrome stain is a general name for a number of techniques the selective demonstration of collagen, muscle, fibrin and erythrocytes. By implication, three dyes are employed, one of which may be a nuclear stain. The Masson's trichrome staining technique of 1911 provides differential staining typically in red and green/blue. This technique allowed the retention of negatively charged arylmethane dyes in different tensional states of collagen, due to the availability of positively charged amino acid groups, which act as ionic receptors of the dyes.

As an entity, all coloured substances absorb light of certain definite wavelengths and transmit the rest. The absorption spectrum is essentially the inverse of that which is transmitted. Therefore the colour of light which reaches the eye after transmission through a coloured substance is complementary to the colour of light absorbed by that substance. The absorption maximum is quite characteristic of any dye and thus yields a colour density of the complementary colour (Lillie, 1969). A number of different dyes (with different absorptions) have been used for the Masson's trichrome technique with the most common being a red plasma stain (ponceau 2R/acid fuchsin) with either a green (light green) or blue (aniline blue) fiber stain (see Appendix I).

Although collagen can be stained equally well with ponceau 2R/acid fuchsin or light green or aniline blue if the dyes are used independently. However experiments designed to test the basis of differences in dye retention indicate that more positively charged amino dye-binding sites are available in the cytoplasm and tensioned collagen than in relaxed collagen where they appear to be closely associated with adjacent carboxyl groups on the collagen fiber. It has been proposed that the differences in charge distribution on the collagen of the two situations is related to the piezo-electric effect demonstrable on stretched collagen. It is for this reason that historically techniques such as the Masson's trichrome stain have been used effectively in creating trichromic staining of animal tissues (Flint et al., 1975).

1.5 Animal models in TMJ research

1.5.1 Animal models in general

The issue of choosing the correct animal model to test particular hypotheses in biomedical research is not straightforward. As Festing (2000) summarised, the issues concerning the choice of the most appropriate experimental model to address a defined scientific hypothesis, and the way in which results can be extrapolated from experiments using different animal models to answer a hypothesis are complex and not straightforward. Furthermore there are no rules regarding the choice of a proper animal model or extrapolating results between species or man (van der Gulden et al., 1993).

In answering whether or not a given animal model is appropriate obviously depends on what problem the model is supposed to address. A perfect animal mimic of human function is an impossibility, because the human TMJ is unique in several features, such as the comparatively enormous lateral pterygoid muscle (Herring, 2001).

The use of animal models in TMJ research has been well established as the availability and preservation of the TMJ components from healthy subjects is obviously limited. Many animal models have been used in experimental research of the TMJ condyle. The TMJ has not lagged behind in comparison to other joints utilising animal models, being only second to the knee joint (Herring, 2003). One major problem in researching the TMJ however, is that there is no single ideal experimental animal model due to species polymorphism. Morphological, functional, ethical, economical, and availability of material are all important considerations when choosing a suitable model.

Despite its status as a mammalian identifier, the TMJ does show remarkable morphological and functional variation in different species. This is likely to reflect not

only the mammalian adaptive feeding mechanism but also a freedom from constraints such as bearing body weight (Herring, 2003). The relative size of the joint is exceedingly variable. Soft tissues such as the capsular ligaments (Herring et al., 2002) and discal components (Gillbe, 1973) are highly species specific. The anatomical differences in the TMJ are clearly tied to biomechanics. The differences generally correlate with loading of the joint (represented by the size of the articular surfaces) or movement (joint orientation) or a combination of the two (Herring, 2003).

Loading of the TMJ is a reaction force arising from the contraction of jaw muscles; its magnitude depends strongly on the position of the bite point relative to the muscle action line (Herring, 2003). The evolution of the TMJ is thought to have coincided with a period of low reaction loads during chewing (Crompton and Parker, 1978). Many common laboratory animals, especially rodents still have a minimal loading of the TMJ during chewing. In contrast however, higher loading has repeatedly evolved such that primates are sustaining TMJ loads greater than that of rodents but not as much as those of carnivores such as dogs (Herring, 1995).

Primates have previously been used as the preferred animal model in TMJ research due to their perceived similarity in structure and function (Tominaga et al., 2002; Herring, 2003). Nevertheless, the relative proximity of the monkey and human lineages is no guarantee of similarity in TMJ function. Recently however, the use of primates as animal models has diminished. The most likely reason for this is due to ethical considerations and pressure from animal protection groups along with the financial costs involved.

The pig has often been used as a model in TMJ research because of its similarity to that of higher primates and humans (Fontenot, 1985; Nickel and McLachlan, 1994; Herring et al., 2002). Bermejo et al (1993) suggested that cattle and pigs have a similar functional shape to humans. The main disadvantage with the pig however, is its poor joint accessibility when performing surgery (Bermejo et al., 1993).

Experimental animals also have to be maintained and housed. Apart from travel and expense this creates issues in relation to achieving fresh material. In an experiment whereby time is critical this makes smaller animal models more important due to their ease of handling and housing on site. Generally larger animals must be reared elsewhere and brought to the laboratory. This could potentially have effects in relation to the results. Hence, many small animal models have been used in studies of the histological and biochemical analysis of the TMJ condyle such as the rabbit (Fujisawa et al., 2003), rodent (Oztan et al., 2004), and guinea pigs (al-Mobireek et al., 2000). However when researching the long term effects of an experiment time is not as essential to control and thus the use of larger animal models is favourable.

It is also generally easier to use an animal model when studying one functional component of the joint as compared with the whole joint, although animals with a similar size, structure and function are preferred.

1.5.2 The sheep model

The value of the sheep as an experimental animal for TMJ studies has been established (Bosanquet and Goss, 1987; Ishimaru and Goss, 1992). Generally, the ungulate such as the sheep is mostly favoured for material property measurements and for the more elaborate surgical procedures that formerly utilised primates and carnivores (Herring,

2003). Sheep as experimental animals also have the advantages of being readily available (either as live animal model or supplied from an abattoir), inexpensive, and attract a high level of ethical approval (cf primates).

Sheep (along with goats and cattle) are closely related ruminant artiodactyls and have essentially identical TMJ's. Although the sheep has a jaw apparatus specialised for an herbivorous diet (food is ground with a lateral motion with unilateral contact, Bosanquet and Goss, 1987) loading of facial bones has been well described (Lieberman and Crompton, 2000; Thomason et al., 2001). The reason for this being that the animal chews up to 23 hours per day (Finn, 1995). Mandibular movement in the sheep is primarily mediolateral, which enables the crushing and grinding of the food to break up cellulose fibers (Dovitch and Herzberg, 1968). The disc and intra-articular components of the TMJ are also similar to humans with a biconcave disc separated by two planes (Bosanquet and Goss, 1987).

Differences highlighted between sheep and humans are also well defined by Bosanquet and Goss (1987). The significant difference between humans and sheep in terms of gross anatomy of the TMJ is that the condylar process is not as much of a separate entity in the sheep. The TMJ is placed laterally to the skull as opposed to being inferior to it. Sheep have a fairly flat mandibular condyle, with the medio-lateral dimension being larger and wider than the anterior-posterior (Ma et al., 2002a). No prominent articular eminence exists in the sheep, with the condyle moving excursively within the fossa that lies lateral to the middle cranial fossa during function. The sheep also has a much larger coronoid process that extends posteriorly and superiorly to the condyle, compared with that of humans which is completely anterior to the condyle (May, 1970). Bosanquet and Goss (1987) stated that as long as the differences and limitations are

acknowledged then the sheep provides a useful model for human comparisons in TMJ research.

To be a relevant surgical model for the human condition, the condyles of the sheep also need to reflect 1) degenerative joint pathology or osteoarthrosis (Ishimaru and Goss, 1992) and 2) orthodontic reactive responses (simple functional modelling and remodelling such as hypermandibular propulsion) (Ma et al., 2001; Ma et al., 2002a,b).

In contrast to other models, the anatomy, morphology, size, and function (cf rodents) and joint accessibility of the sheep (cf pigs) are similar to the human joint with any differences being well defined. Apart from anatomical similarities, it can be argued that the sheep is also an excellent animal model in regards to other physiological systems such as the cardiovascular, respiratory, renal, reproductive and endocrinological when making comparisons to humans (McMillen, 2001).

1.5.3 Histomorphometry of the TMJ condyle

One of the first studies to quantitatively analyse tissue in the condyle was that done by McNamara and Carlson (1979). In an experimental study they studied the TMJ adaptability to alteration of the biomechanical environment in rhesus monkeys by modifying the functional position of the mandible. They showed that the growth of the condylar cartilage can be increased in comparison to control level values through the insertion of an appliance which prompted the jaw to function in an anterior position. In measuring the effects on the condylar cartilage, they analysed sagittal sections (stained with H&E) of rhesus monkeys and measured the thickness of cartilage in two regions termed the articular cartilage (dense fibroelastic CT) and the growth cartilage (proliferating chondroblastic and maturing chondrocytes in the chondroblastic layer).

The thickness of the layers was measured perpendicular to the articular surface at the posterior, postero-superior, and superior regions along the circumference of the sagitally dissected condyle (**Figure 6**). The measurements were averaged for both control and experimental groups using a two-tailed t test and their results showed that an adaptive response was evident within 2 weeks following treatment with a functional appliance being most pronounced in the posterior region. The relevance and importance of this study was that it was one of the first to descriptively measure the thickness of condylar cartilage into corresponding regions based on its histomorphological appearance.

In order to investigate whether dentofacial orthopaedic treatment influenced the growth of the TMJ in sheep, a previous study measured the changes in condylar cartilage thickness with functional appliances (Ma et al., 2002a). A consistent quantitative protocol was adapted from McNamara and Carlson (1979) to measure the thickness in response to the experimental functional appliance treatment. Sagittal sections of the condyle were used to measure the thickness of condylar cartilage perpendicular to the articular surface in anterior, intermediate and posterior regions from each section (**Figure 7**). These thicknesses were then averaged to determine if there was any variation between the growth of control animals and those that had orthopaedic treatment. The findings from this study showed that there was proliferation of both the proliferative and hypertrophic zones in cartilage, especially in the anterior region. This observation was in agreement with that of Kantomaa (1984) in rabbits but differed to those of McNamara and Carlson (1979) in monkeys and Charlier et al. (1969) in rats.

A study by Paulsen et al (1999) used SEM histomorphometry to study the human condylar cartilage and bone tissue changes in relation to age. To determine the

possibility for adaptive growth in human condyles, they quantified the thickness of cartilage and the constitution of cells with potential activity, as well as measuring the trabecular bone volume. Human condyles from 20 individuals 18-31 years of age were studied. Correlative analysis showed a moderately statistical significant correlation between age and fibrocartilage thickness, trabecular bone volume and hypertrophic chondrocyte numbers. They concluded that condylar growth potential existed in the human up to 30 years of age with continued activity of hypertrophic chondrocytes and turnover of trabecular bone, albeit that there was some declination with age.

Luder (1998) also found that some age changes of condylar articular tissue had occurred in a semiquantitative light microscopy study. In his study, he focused on the superficial, intermediate and deep articular tissue zones and recorded results arbitrarily on the basis of the tissue absence (score of zero) to its continuous presence (score of ten) plotted against age. From 15-30 years of age it was noted that there was a decrease in hypertrophic growth cartilage, a decline in endochondral ossification and thickening of the superficial zone from formation of cartilage. However, he also noted frequencies of a second group of tissue features that only occurred from middle to old age including a decrease in the prominence of the intermediate zone as well as a reduction in its cellularity. Both of these maturational and later age changes were noted as being dependent markedly on articular load bearing. This statement was reflected by the fact that the above changes were noted to have occurred along the whole of the latero-medial dimension and at the load bearing anterior slope, but not from that of the non-load bearing posterior slope.

In a quantitative and morphological study of the trabecular bone pattern in condyles of Japanese mandibles, Hongo et al (1989b) assessed the structure of bone with advancing

age. The condyles were removed from cadavers from several age groups and changes in the trabecular bone structure were compared. They found that the trabecular bone density and trabecular width in the condyle was only slightly different between age groups with no major changes observed.

Kawashima et al (1997) performed an interesting study whereby trabecular bone was compared between dentulous and edentulous cadavers to clarify what changes occur in the trabecular structure due to a loss of teeth. The results from their study showed that at all sites, the density, width, extent and index indicating the complexity of the trabecular bone had higher values in dentulous specimens than in edentulous ones. Another study by Hongo and colleagues also compared the bone morphology measurements of the trabecular bone in the condyle of dentulous and edentulous cadavers (Hongo et al., 1989a). This study was in accordance with that of Kawashima et al (1997) with a lower bone density and trabecular width in edentulous specimens along with less rod formation and interlocking of plates.

In study by Giesen and van Eijden (2000), the cancellous bone of the mandibular condyle was studied to see if it was inhomogeneous and anisotropic. For this purpose, they used 11 mandibular condyles that were scanned in a micro-CT system. Within each condyle several bone parameters were calculated to describe the morphology from different medio-lateral and supero-inferior regions. They showed that the cancellous bone of the condyle is approximated by parallel plates that were almost vertically oriented relative to the sagittal plane (ie perpendicular to the condylar axis). In regards to trabecular bone indices measured, they assessed the bone volume fraction, trabecular thickness and trabecular number. Their results showed no medio-lateral differences in bone morphology, but superiorly, central regions contained more bone than peripheral

regions. They concluded that the presence of a plate-like structure indicated that the condyle is optimally adapted to sustain loads from all directions in a plane perpendicular to the condylar axis. Toward the neck however, the trabeculae were more aligned suggesting that stresses act predominantly in one direction which is in agreement with Standlee et al (1981).

Animals have also been used to study the histomorphometry of the TMJ condyle. Teng and Herring (1995), quantitatively analysed trabecular bone patterns in the pig. They concluded that the condyle was heavily loaded with robust and dense trabecular bone. The domestic pig has also recently been used as a model to quantitate cartilage in the condylar process during growth and differentiation (Leidhold et al., 2004). Interestingly, the aim of their study was to examine the extent to which the ratio of the growth components of cell volume to matrix production was subject to age dependent and animal specific changes in the condylar cartilage. This was assessed in different ages of young pigs ranging from 0-24 months. Although they did not use an image analysis system, a special squared measuring grid was used to determine the average section area of the cartilage cells and the number of cut cells per unit area to work out cell and matrix volumes from stereological calculation algorithms for ellipsoids. Their results showed that the relative increase in cell volume is predominant until the juvenile stage at 11 months (2.55:1, increase in cell volume to matrix volume) whereby in late puberty the matrix synthesis exceeds the cell volume (0.91:1 cell volume increase to matrix volume). Comparisons with other stereological growth studies showed that the investigated ratio has a similar aging behavior to that in the rat (Charlier et al., 1969; Luder, 1994) but in the monkey (Carlson et al., 1978; Bosshardt-Luehrs and Luder, 1991) matrix synthesis was predominant. This suggests that the thickness of condylar cartilage during growth and development is not only age dependent but is also animal

specific. However, this study did not assess animals older than 24 months and no study has used the sheep to measure cellular and matrix volumes of the condylar cartilage.

In another study by Ma and colleagues, the trabecular bone of young sheep was histomorphometrically analysed in response to forward mandibular displacement growth modification using functional appliances (Ma et al., 2002b). Trabecular bone indices including bone volume density, bone surface density, trabecular thickness, separation and number were measured using the Quantimet 500MC image analysis system. Fluorochromes were also used to estimate variables associated with bone formation and resorbing activity in the subchondral region and central region of each section. This study found regional differences in the adaptive responses within the mandibular condyle from a complicated alteration of the mechanical environment. They concluded that the findings could not be explained by the magnitude of the mechanical force alone, but future studies should concern the orientation and pattern of the force as well.

Although the sheep has been used as an animal model in TMJ research, there is a dearth of quantitative data regarding the histomorphometry of the trabecular and cartilaginous patterns during growth and development in the mandibular condyle of both young and mature sheep; particularly in relation to the thickness of condylar cartilage, cell and matrix proportions of condylar cartilage, and trabecular bone parameters.

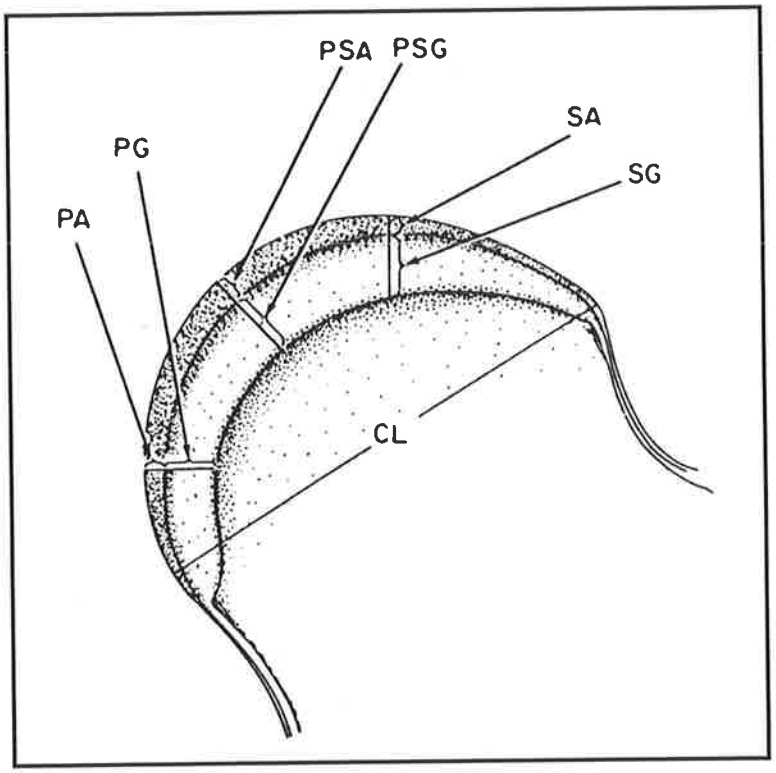

Figure 6: Regions measured in the determination of cartilage thickness across the length of the condyle (**CL**) in a study by McNamara and Carlson (1979). **PA**, Posterior articular cartilage; **PG**, posterior growth cartilage; **PSA**, posterosuperior articular cartilage; **PSG**, posterosuperior growth cartilage; **SA**, superior articular cartilage; **SG**, superior growth cartilage. Taken from McNamara JA Jr and Carlson DS. *Am J Orthod.* 1979; **76:** 596.

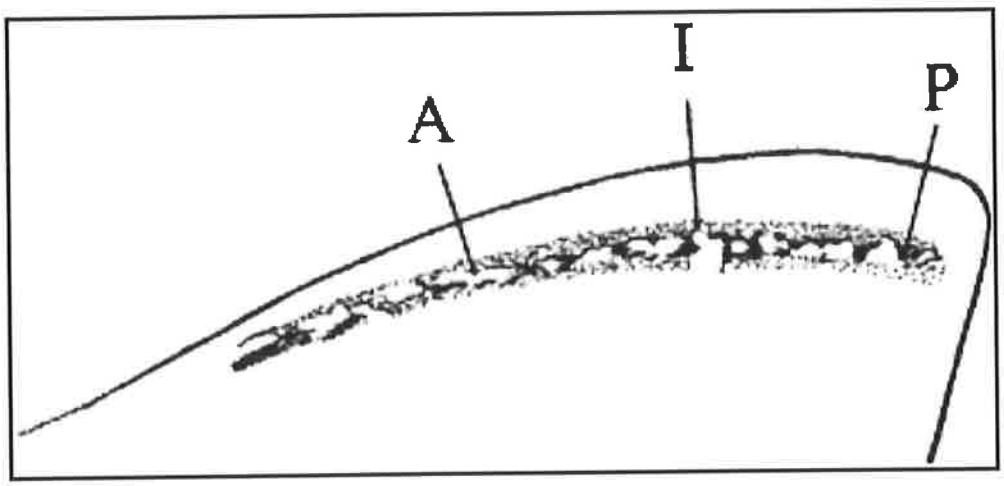

Figure 7: Illustration of how condylar cartilage thickness was measured on sagittal sections of sheep as published by Ma et al. (2002). The measurements were made perpendicular to the articular surface at anterior (**A**), intermediate (**I**) and posterior (**P**) regions from each section using bright-field light microscopy with a 4× objective and an ocular graticule (accuracy 20μm). Three mid-sagittal sections were selected for each condyle and the average thicknesses of the condylar cartilage was calculated. Taken from Ma et al. *Arch Oral Bio.* 2002; **47(1):** 78.

1.6 The present study

1.6.1 Investigative rationale

The Australian Jaw Joint Project (AJJP) was established at The University of Adelaide to create a dynamic multi focussed centre for TMJ research. The sheep has been used as the prime animal model for experimental research with the AJJP (Bosanquet and Goss, 1987; Ishimaru and Goss, 1992, Ma et al., 2002a,b). Although a number of studies have focussed on the surgical and orthodontic aspects of the sheep TMJ, research pertaining to the morphometry of the condyle during growth and development are lacking. Broadly, the contributions of this project have been to provide further knowledge and contribution to the international literature in researching the histological stereomorphology of the trabecular bone and cartilage of the TMJ in the young and mature sheep. This is important in the context of describing a normal, aged and degenerative joint structure to provide further understanding of metabolism in health and disease of the whole TMJ complex.

1.6.1 Objectives to be fulfilled

Specifically, the purpose of this study was to analyse and fulfil the following:

1. To develop and implement a standardised protocol for the histoquantitation of various condylar cartilage and trabecular bone measurements.

2. To become competent in the use of an image analysis system (Quantimet 500MC) in measuring condylar cartilage and trabecular bone.

3. To quantitatively and quantitatively analyse the thickness of articular cartilage in the Fibrous zone (FZ), Hypertrophic zone (HZ) and the Total Thickness (TT) of the condyle in various anatomical regions in both young and mature sheep.

4. To quantitatively and quantitatively analyse the proportions of the matrix and cellular components of condylar cartilage in various anatomical regions in both young and mature sheep.

5. To qualitatively and quantitatively analyse the cancellous bone of the condyle including bone volume density, bone surface density bone surface/bone volume, trabecular thickness, trabecular separation and trabecular number in various anatomical regions in both young and mature sheep.

6. To reinforce the practicality and appropriateness of the sheep as a useful animal model in studies of growth and development on the morphological architecture of the condyle.

1.6.3 Hypotheses to be tested

The broad hypothesis being tested is that developmental and functional changes of the cartilage and trabecular bone in the mandibular condyle of young sheep will be reflected in their qualitative and histoquantitative morphology when compared with that of the mature sheep.

Specifically, the hypotheses being tested are:

1. There is a significant reduction in the thickness of condylar cartilage in sheep with age.

2. There is a significant decrease in the cellularity of condylar cartilage in sheep with age.

3. There is a qualitative morphological difference in the arrangement of the condylar trabeculae in mature sheep as compared with young sheep.

4. There will be quantitative differences in the trabecular bone indices of the condyle between age groups for the same anatomical region in sheep.

CHAPTER 2:

MATERIALS AND METHODS

2.1 Selection of material

2.1.1 Animals

Twelve young and ten mature Merino skinned sheep heads (**Figure 8**) were obtained fresh from a commercial source (Economy Meats, SA). All animals were collected together at the same time of year. The sheep heads were collected within twenty four hours of the animal being killed. No importance was placed on the selectivity of animals in regards to their sex in this study as there has been no evidence of sexual dimorphism described for the condyle of the TMJ.

2.1.2 Habitat

The specimens were standardized as much as possible relating to habitat. All specimens were collected from animals reared in local regional pastures which do not have a large variation in climate and thus provide a consistent source of food (ie winters are mild and summers still provide some rain). Sheep from remote areas were excluded as these areas are prone to both floods and droughts. The specimens were collected from animals that were reared on either the Lobethal or Crystal Brook regional private paddocks.

2.1.3 Diet

All specimens came from sheep that were pasture grazing animals (ie grass fed). No grain or concentrates were additionally supplied in supplement to their grazing. Thus, any bias pertaining to differences in chewing patterns and loading on the TMJ amongst animals used in this study was minimised.

2.1.4 Age determination

The usual method of determining the age of sheep is from the teeth (May, 1970). In this

study, the age of each animal was primarily determined by assessing its level of dental development with respect to the erupted mandibular teeth present.

The dental formula for the deciduous teeth is

$$2\ (\text{dI } 0/4,\ \text{dC } 0/0,\ \text{dP } 3/3)$$

The dental formula of the permanent teeth is:

$$2\ (\text{I } 0/4,\ \text{C } 0/0,\ \text{P } 3/3,\ \text{M } 3/3)$$

Table 1 shows the average eruption times of the dentition in the sheep:

TOOTH	AGE OF ERUPTION
First deciduous incisor	1 month
First molar	3 months
Second molar	9 months
First Incisor	10-12 months
Third Molar	18 months
Second Incisor First premolar Second Premolar	18-24 months
Third Incisor Third Premolar	2 – 2.5 years
Fourth Incisor	3-4 years

Table 1.

In regards to the young sheep, ten of the twelve animals had 4 deciduous incisors and 2 erupting molars on each side of the mandible with the other two animals having 3 dcciduous incisors and an erupting permanent central incisor with 2 erupted molars on each side of the mandible. Thus according to **Table 1**, at an extreme the ages could vary between 9 months as the earliest onset for all of the deciduous incisors and erupting first and second molars, and between 10-12 months for the "one toothed" animals. Also, as

the animals were collected in the month of August with these animals born in the preceding year's spring in the southern hemisphere (the farmer is rearing such animals for optimal commercial meat gain), the variation in ages was determined to range from between 9-12 months with the average age determined to be about 10 ± 2 months.

All of the animals in the mature age group had all their permanent mandibular premolars and molars fully erupted suggesting their age be at least 2½ years according to **Table 1**. The extreme age constraint for mature animals used for commercial meat produce from the private paddocks where the animals were collected was 3-4 years ie "four toothed animals" (due to the farmer is rearing these animals for meat production without them ageing and the quality of meat decreasing). Thus, the mature age group can be considered to have an average age of 3 years ± 6 months.

This grouping of the sheep related to the dental age of the animals used in this study ensures a significant difference in regards to age between the young and mature groups without a vast variation within the mature group.

2.2 Tissue preparation

2.2.1 Tissue sampling and fixation

Preparation and dissection of the specimens from the animals was performed in the Oral Pathology Research laboratory at The University of Adelaide. The mandible from each skinned sheep head was initially separated from the surrounding muscle and soft tissue structures with a scalpel (**Figure 9**). The jaw was then disarticulated with the condyles subsequently being separated from the rest of the mandible using a diamond saw

(**Figure 10**). Each condyle was then marked for subsequent identification and fixed in a solution of 10 per cent neutral buffered formalin (see Appendix II) for a minimum of 48 hours to allow for adequate penetration of the tissues.

2.2.2 Demineralisation and radiological analysis

After formalin fixation, the condyles were placed in a solution of Decal® (Surgipath Inc, USA) to demineralise the tissues. The condyles were left in Decal® until complete demineralisation occurred which was determined by radiographic examination. Specimens were said to have been completely demineralised when no radio-opaqueness could be seen on the exposed film (**Figure 11**). All radiographs were taken with a Pendo-Diagnost Super 50CP® unit (Phillips, USA) at 52kV, 8mAs for 24ms each with fine focus using Curix Ortho HT-G film in a 18x24 extremity cassette (AGFA, Belgium). If a specimen had any visualised area of radio-opacity, it was placed back in Decal® solution for 1 week and subsequently checked by radiographic examination for complete decalcification (**Figure 12**).

2.2.3 Dissection of the condyles

After complete decalcification, condyles from six of the twelve young sheep and condyles from the ten mature sheep were sectioned with a scalpel into medial, central and lateral sagittal blocks (**Figure 13**). The dissection was performed consistently such that the central cut was made in the centre of the head of the condyle, whilst the lateral and medial cuts were made 5mm in from the respective sagittal edges. This allowed for comparisons between different regions within each of the two age groups, as well as between each of the groups. The condyles from the remaining six young sheep were also dissected into anterior and posterior coronal blocks (**Figure 14**). The two cuts were made consistently such that it divided the head of the condyle into equal coronal thirds.

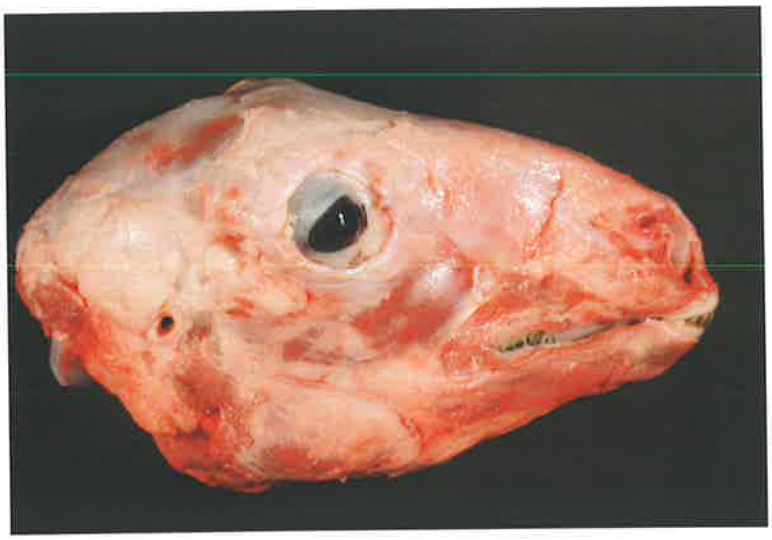

Figure 8. A fresh skinned sheep head as obtained from the commercial supplier.

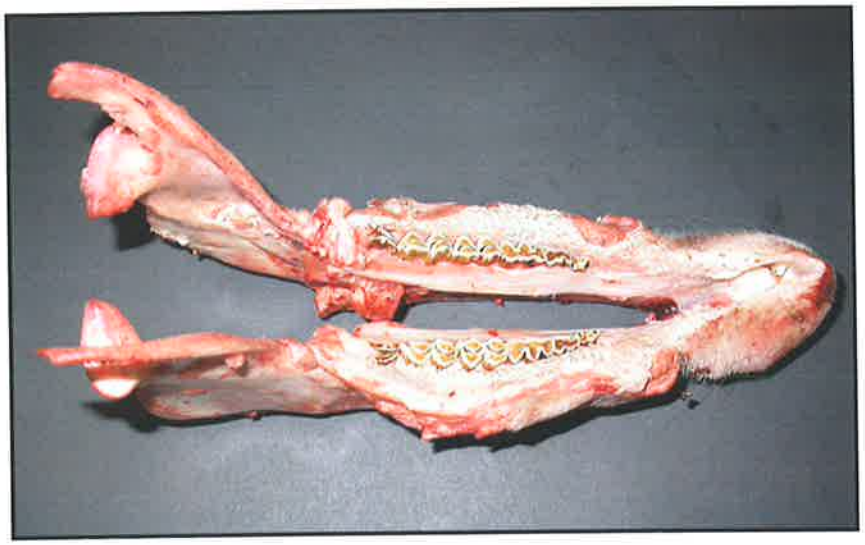

Figure 9. The disarticulated mandible after separation from the surrounding muscle and soft tissue structures. The two condyles are still attached.

Figure 10. The resected condyles ready for fixation

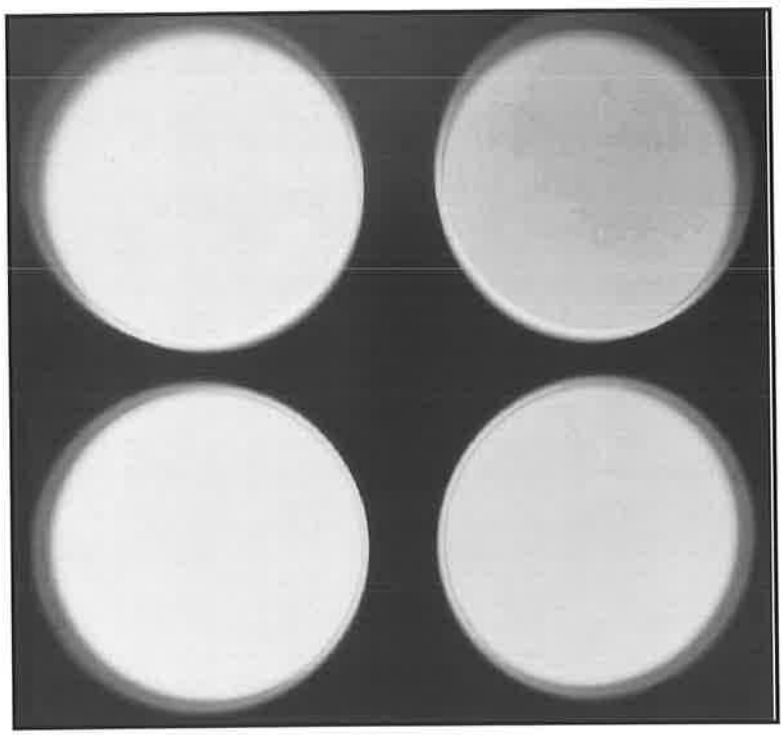

Figure 11. A radiograph of 4 specimen containers containing mandibular condyles soaking in Decal® solution. No radio-opacity can be seen in any of the specimens confirming complete demineralisation.

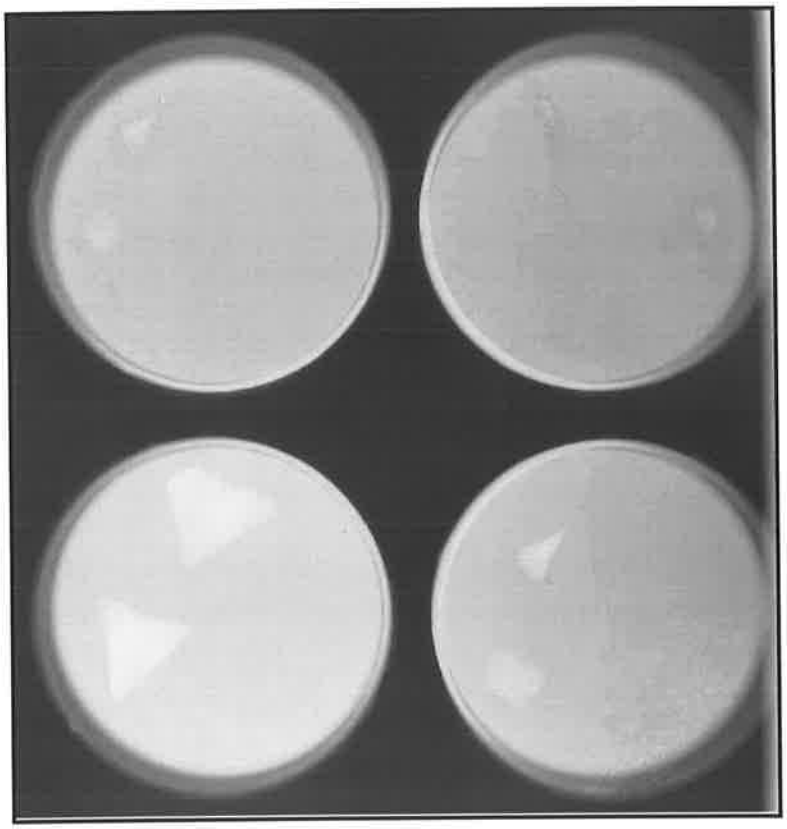

Figure 12. A radiograph of 4 specimen containers containing mandibular condyles soaking in Decal® solution. Varying degrees of radio-opacity can still be seen for each pair of condyles confirming incomplete decalcification.

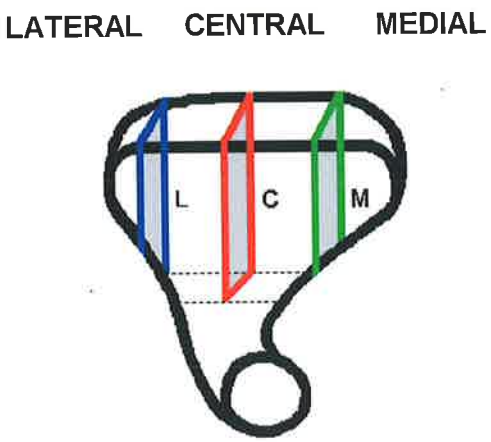

Figure 13. Schematic diagram showing the plane of section of the mandibular condyles used to produce each of the three sagittal blocks from the lateral (**L**), central (**C**) and medial (**M**) aspects of six young sheep and ten mature sheep.

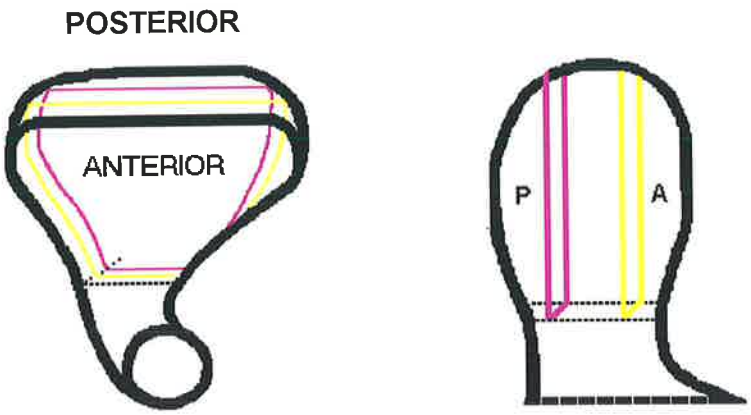

Figure 14. Schematic diagram showing the plane of section of the mandibular condyles used to produce each of the two coronal blocks from the anterior (**A**) and posterior (**P**) aspects of six young sheep.

2.2.4 Tissue processing and embedding

All specimens were placed into labelled processing cassettes (Tissue-Tek Mega-Cassettes®, Miles Laboratories Inc, USA) and processed in an automatic processing unit (Shandon Citadel 2000®) according to the protocol outlined in Appendix III.

The tissue blocks were then subjected to automated wax penetration, followed by immersion in a beaker of Blue Ribbon Tissue Infiltration Media® (Surgipath Medical Industries Inc, USA) at 60C° and held in vacuum (25 in of Hg) for 12 hours. Specimens were then removed from the cassettes and embedded in Surgipath Embedding Media® (Surgipath Medical Industries Inc, USA) at 60C° in steel moulded trays using a Reichert HistoSTAT® Tissue Embedding Centre. Specimens were then placed in the refrigerator to cool prior to sectioning for at least 24 hours.

2.2.5 Sectioning

After sufficient cooling, blocks could then be trimmed of excess wax. The blocked specimens were then faced from the original dissected surface of the condyle and histological sections of 5μm were cut using a Leitz 1512 microtome with a stainless steel feather microtome blade. Slides were then mounted on an APT (3-amino propyltriethoxysaline) coated glass slide (ie subbed slide) to aid adhesion of the specimen (see Appendix IV). One section was mounted per slide and a number of serial sections were cut for appropriate staining. Slides were then placed in a heated slide drying oven (Dishwarmer®, Photax Ltd, England) for at least 30 minutes then cooled before staining for improved adhesion.

2.3 Staining methods

Two main types of staining were used in this study to qualitatively and quantitatively analyse the cartilage and trabecular morphology of young and mature sheep.

2.3.1 Routine histological staining

Sections were initially stained with Haematoxylin and Eosin-Phloxine for gross orientation and structural component evaluation of the sections (**Figure 15**). Also, an initial examination was done and if any structural or pathological abnormality was detected in any specimen then the specimens from that animal were excluded from the study. The procedure for Haematoxylin and Eosin-Phloxine staining of specimens is outlined in Appendix V (a).

2.3.2 Masson's trichrome staining techniques

Masson's trichrome stains were performed for quantitative purposes as they enhanced collagen distribution, structural arrangement and provided good contrast.

The sections were stained using a Masson's trichrome technique that incorporated a light green fiber and red ponceau/fuchsin contrasting plasma stain as well as a haematoxylin nuclear stain. This stain enabled the qualitative and quantitative (bone indices) analysis of the trabecular bone stereomorphology.

A slightly different type of Masson's trichrome stain was devised to qualitatively and quantitatively analyse the cartilage histomorphometry. An aniline blue fiber and red ponceau/fuchsin contrasting plasma stain was performed, but without the nuclear stain. This modified Masson's trichrome stain was created in order for a colour contrast between the matrix (staining blue) and the cellular components (staining red) of the

cartilage without any haematoxylin nuclear stain causing any blue-black staining. The fact that these sections had a contrast between the blue staining matrix (as compared with light green) and the red staining cytoplasm was important for measurements pertaining to the cartilage matrix and cellularity of cartilage (see section 2.4.3b). The procedure for the two protocols are outlined in Appendix V (b) and (c).

2.4 Tissue examination

2.4.1 Initial examination

The H&EP stained sections were initially examined macroscopically and then microscopically using an Olympus CH microscope, with an eyepiece magnification of 10X and an objective lens of 4X. Gross orientation and structural component evaluation of the sections were observed along with any unusual or unexpected morphological findings. Photomicroscopy was performed with a Leica DM6000 B light microscope with a Leica DFC 480 digital camera attached. In one of the coronally dissected young sheep specimens a cartilaginous neoplasm was discovered and this animal was excluded from any further involvement in the study (**Figure 16**).

2.4.2 Qualitative histology and tissue parameters

H&EP sections were examined using light microscopy with an Olympus CH microscope with an eyepiece magnification of 10X and objective lenses at 4X, 10X, 25X and 40X. Qualitative comparisons were made regarding cartilaginous and trabecular morphological patterns between the sections.

Each of the Masson's trichrome stained sections was also examined to help delineate tissue parameters including: 1) the different zones of condylar cartilage & 2) cancellous

bone (trabecular bone) as distinct from cortical bone (non-trabecular bone).

For cartilage, the following zones are described (**Figure 17**) as adapted from that reported by McNamara and Carlson (1979), Luder (1998), and Ma et al (2002):

1) The Fibrous zone (**FZ**): This is represented by the distance between the external articular surface of the condyle to the internal boundary of the proliferative cartilage layer (flattened cells), or similarly to the external boundary of the hypertrophic cartilage layer (rounded cells). Thus this zone incorporates the avascular fibrous articular CT layer and the proliferative cartilage layer.

2) The Hypertrophic zone (**HZ**): This is represented by the distance between the external boundary of the hypertrophic cartilage layer to the internal boundary of the hypertrophic cartilage layer, or similarly to the external boundary of the subarticular bone (presence of vascularisation and angiogenesis).

3) The total thickness of the condylar cartilage (**TT**). This is represented by the distance from the external articular surface of the articular fibrous CT, to the external boundary of the subarticular bone (similarly by summation of FZ & HZ).

For bone, the cancellous bone incorporating the trabeculae in plates and rods was defined as having widely spaced areas as compared with the cortical bone, which was generally more homogeneously thick and dense. The reference point for quantitation of the trabeculae in this study was where the cancellous bone united with the cortical bone (**Figure 18**). The standardised trabecular bone structural index values recorded with the Quantimet 500MC from the raw pixel data are given in **Table 2**.

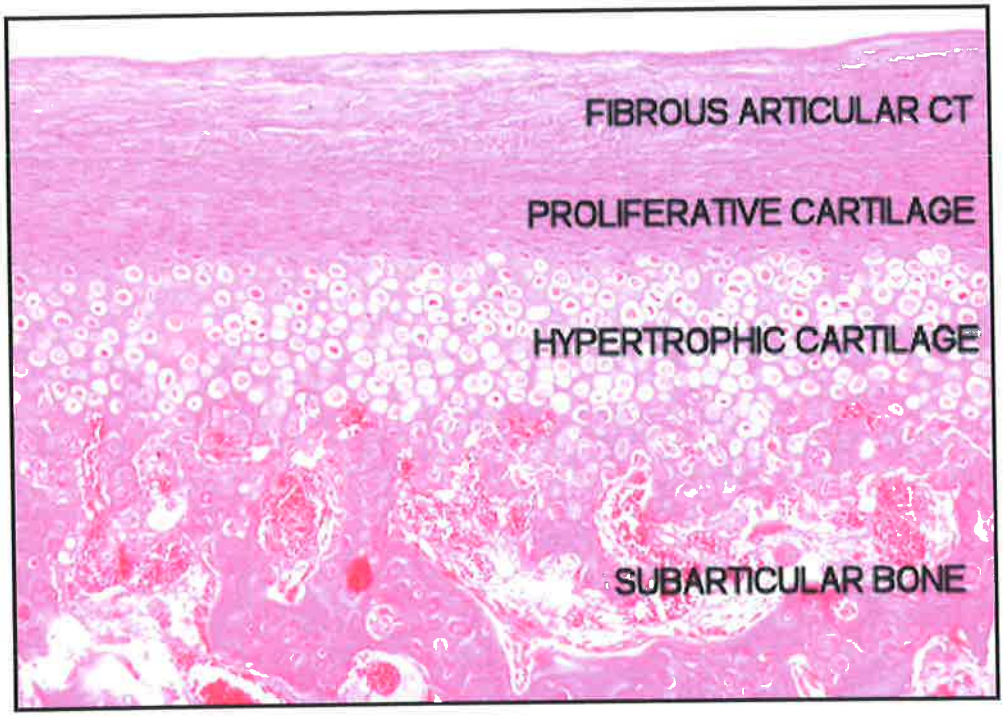

A

B

Figure 15: Photomicrographs of H&EP stained sections which were used in the initial examination of the tissues including orientation and structural component evaluation. **A.** A section of the articular covering of the condyle including the different cartilaginous layers and underlying subarticular bone as demonstrated by vascularity of the tissues (100X). **B.** This photomicrograph demonstrates the parallel plate method of trabecular bone with the presence of parallel plates (**P**) with interconnecting rods (**R**) (50X).

A

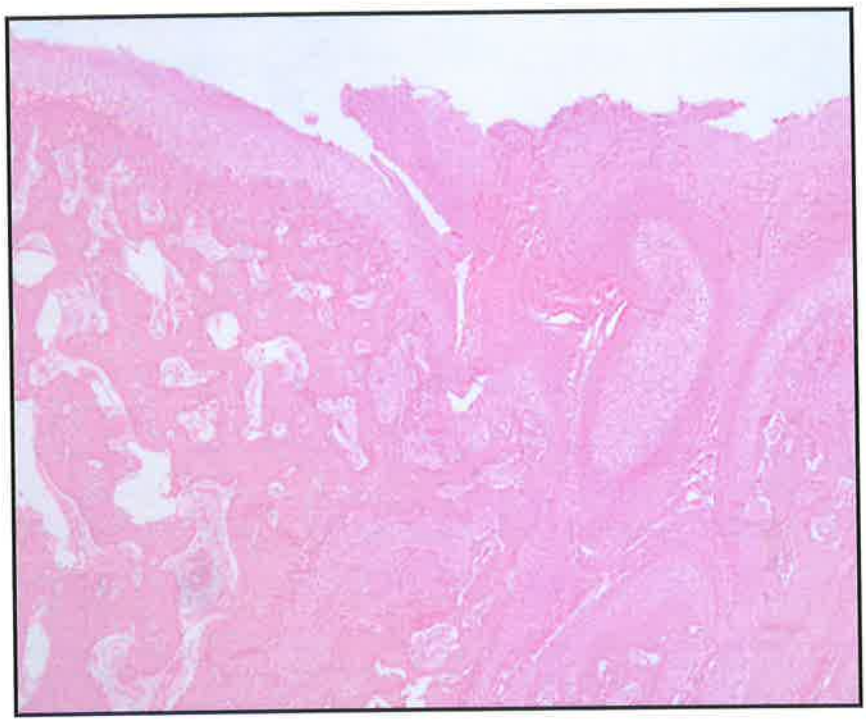

B

Figure 16. **A.** A composite photomicrograph of an incidental finding (lateral pole) of a cartilaginous neoplasm (H&EP) from a coronally sectioned young sheep condyle taken with a Nikon DXM camera on a Nikon Eclipse TE300 microscope with the images combined using the computer programme analySIS®, Soft Imaging System, Germany. The disruption to the architecture and morphological appearance of the condyle is easily seen macroscopically in **A** as well as microscopically as in **B** (25X). This animal was excluded from the study.

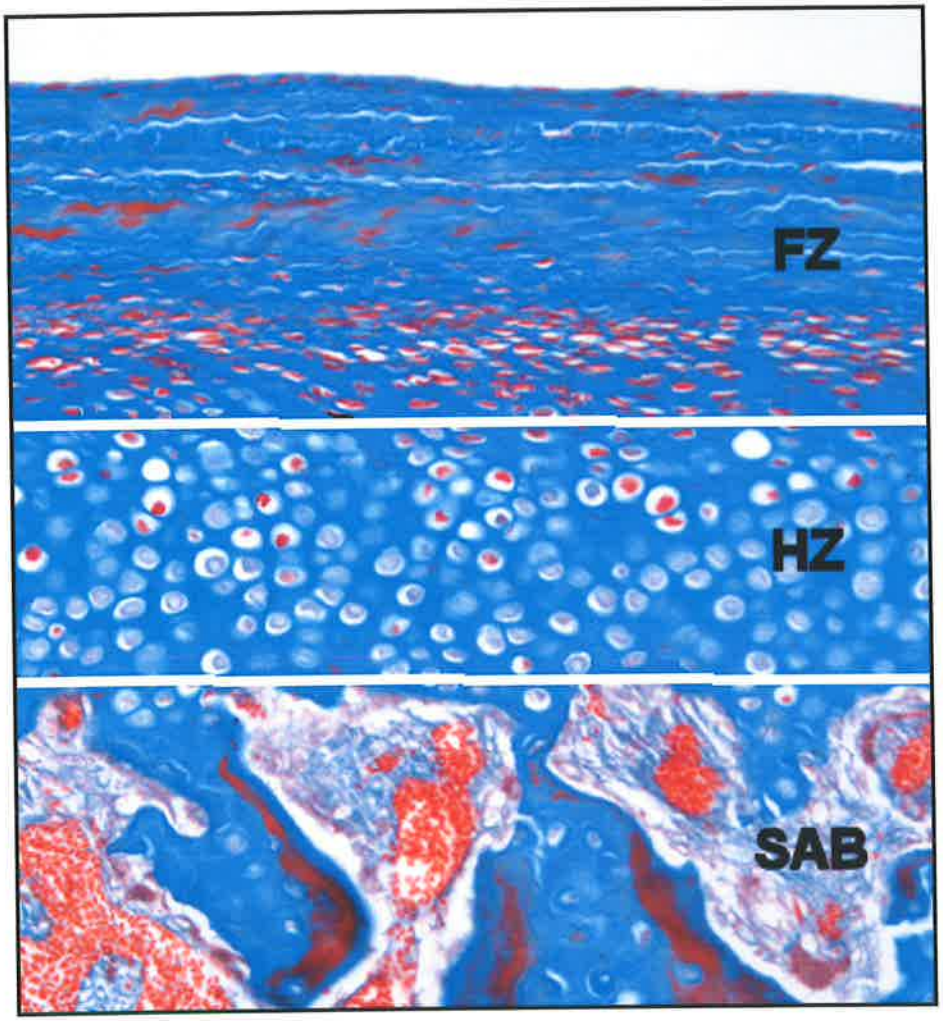

Figure 17. Photomicrograph of the condylar cartilage as stained with a modified blue Masson's trichrome outlining the different morphology and boundaries of the regions defined in this study (200X). The top zone (from the articular surface) is the Fibrous Zone (**FZ**) as illustrated by many flattened cells of the proliferative cartilaginous layer under the articular CT layer. The middle of the three defined zones with its presence of rounded chondroblasts demonstrates the Hypertrophic Zone (**HZ**). The Bottom segment represents the subarticular bone (**SAB**) as displayed by evidence of vascularisation and angiogenesis. The summation of the FZ and HZ represent the Total thickness (**TT**) of condylar cartilage.

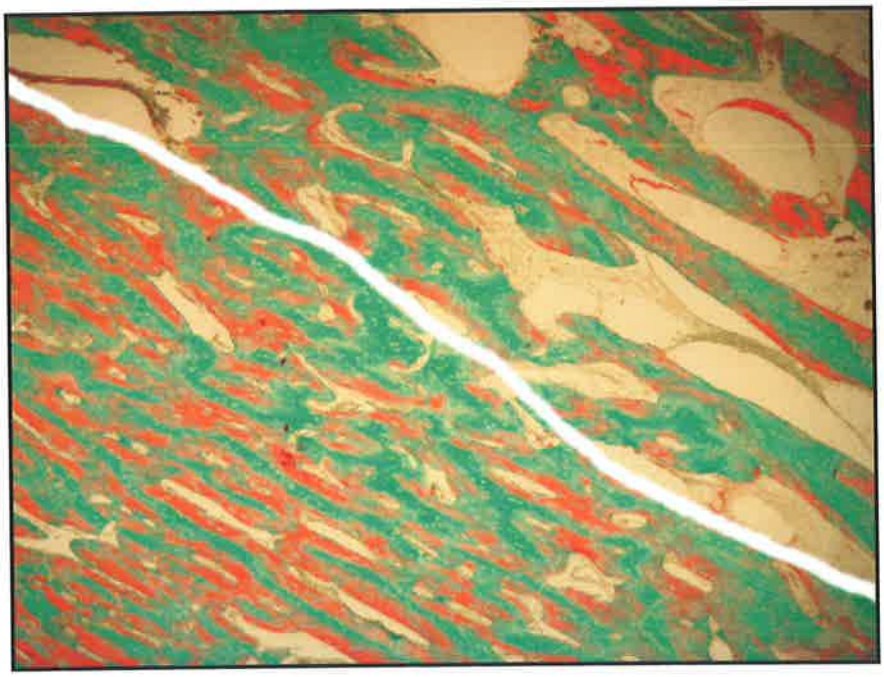

A

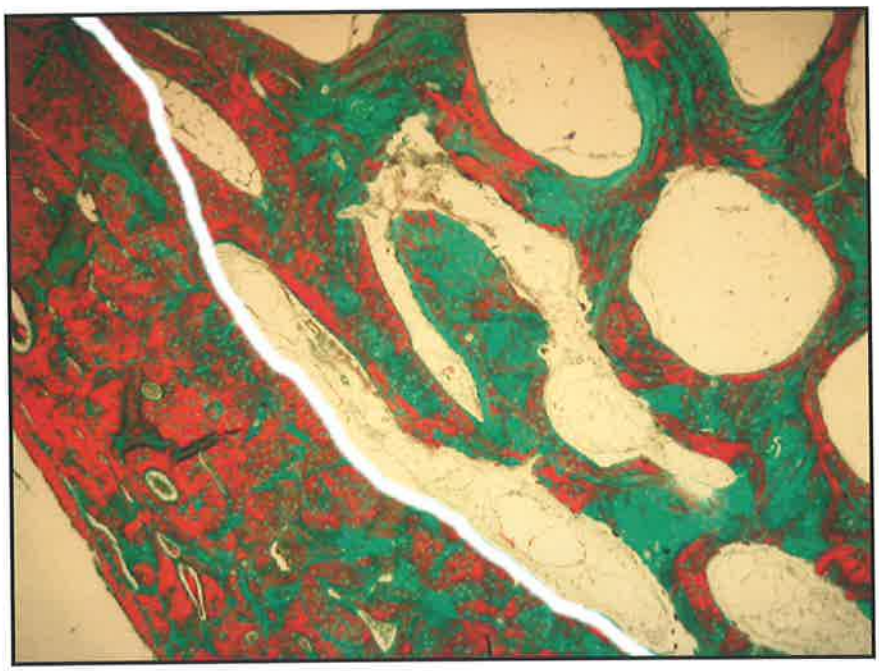

B

Figure 18. Photomicrographs of histological sections of young and mature sheep mandibular condyles (**A** and **B** respectively) stained with a light green Masson's trichrome (50X). Note the widely spaced cancellous bone (upper right) containing the trabeculae compared with the thick and dense cortical bone (lower left). The reference point for quantitation of the trabeculae in this study was where the cancellous bone united with the cortical bone (outlined in white). This border was well differentiated in some sections (**B**) but more indistinct in others (**A**).

Bone structural index value	Abbreviation	Measures	Defined as	Units
Bone volume density	BV/TV	The ratio of bone volume over tissue volume	Area/Field Area x100	%
Bone surface density	BS/TV	The ratio of bone surface area to total tissue volume	Perimeter/Field Area x1000	mm^2/mm^3
Bone surface/Bone volume	BS/BV	The ratio of the bone surface to the bone volume	Perimeter/Area x 1000	mm^2/mm^3
Trabecular thickness	Tb.Th	The average width of the trabeculae	$\frac{BVTV/100}{0.5 \times BSTV}$	mm
Trabecular separation	Tb.Sp	The average distance between the edges of trabeculae	$\frac{1 - (BV/TV/100)}{0.5 \times BSTV}$	mm
Trabecular number	Tb.N	The average number of trabeculae	$\frac{BVTV/100}{Tb.Th}$	#/mm

Table 2. Standardised structural bone index values recorded with the Quantimet 500MC for the region of interest (cancellous bone).

2.4.3 Quantitative histomorphometry

Histoquantitation of both cartilage and trabecular bone was performed on eleven young sheep and ten mature sheep using a Quantimet 500MC (Leica, Cambridge) image analysis system (**Figure 19**).

The software package measures the contrast differences of tissues compared to the background, as well as comparing between differing tissues. The Quantimet 500MC measures features by creating a binary representation of the original image on an X and Y pixel array. Setting the binary threshold to a grey level allows the entire tissue substance to be detected but none of the background of the slide. Sections stained with Masson's trichrome were used to enhance contrast between the tissues as well as against the background for Quantimet analysis.

Slides were placed on a Leica DM6000 B light microscope and imaged by a closed circuit digital camera (Leica DFC 480) which was set at a fixed magnification (200X for cartilage and 25X for trabecular bone) and distance from the analysed specimen. This calibration value was kept constant for all histoquantification measurements. The digital camera then recorded the images of the slides at the appropriate magnification.

The region of interest of the tissue for each specimen (termed the field) was firstly determined, and then outlined, by manually highlighting on the recorded image the boundary (or perimeter) of the field. This area was then scanned ensuring a reasonable reflection of the tissue of interest was captured. Any digital editing of unwanted areas was easily performed at this stage.

A total pixel count of the binary field image and the perimeter pixel count of the binary-

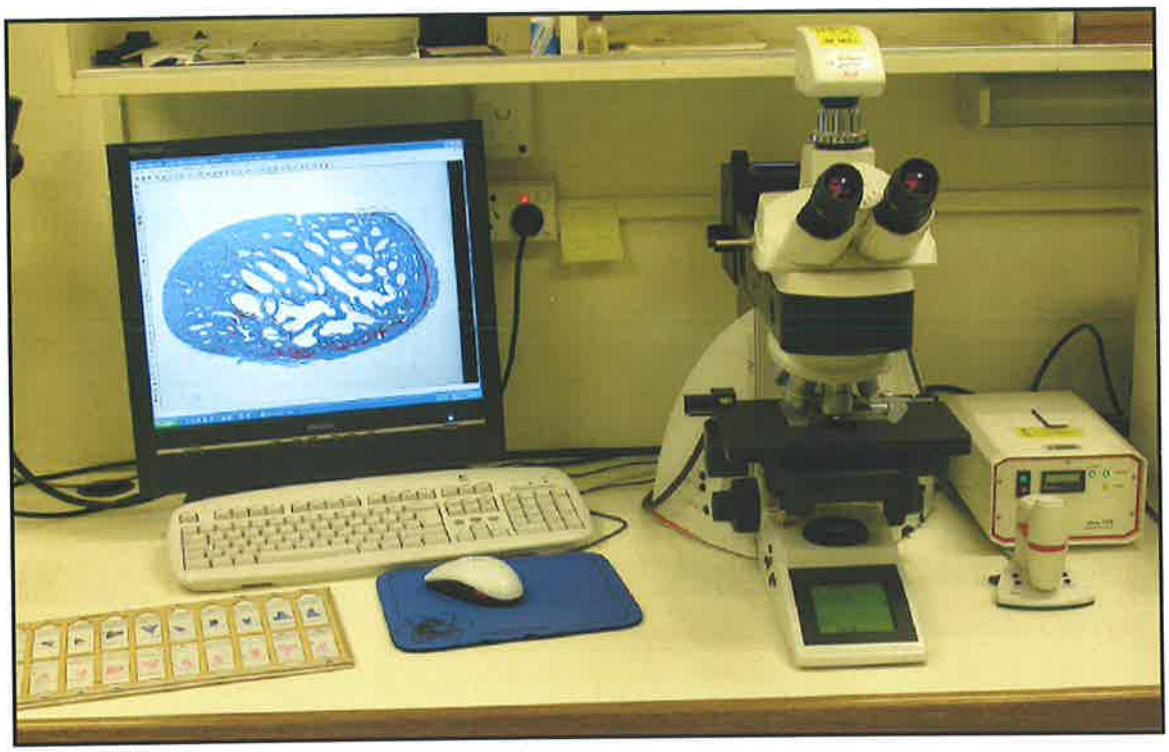

Figure 19. The Quantimet 500MC image analysis system with a Leica DM6000 B microscope and a Leica DFC 480 closed circuit digital camera used to histoquantitate cartilage and trabecular bone.

image could then be calculated. Specific procedures in quantitating each of the various histomorphometric measurements are now further explained.

(a) Cartilage thickness

Three digital photomicrographs were taken of each slide using the Quantimet 500MC setup at 200x magnification to outline the whole thickness of condylar cartilage on the modified blue Masson's trichrome section as assessed by prior microscopic examination with the H&EP stained sections.

Linear lines were then drawn with a public domain software programme (ImageJ 1.33u, National Institute of Health, USA) on the digital images to measure the average thickness (in pixels which was subsequently converted into microns based on prior calibration of the Quantimet) of the HZ, FZ and TT regions for each digital image. All measurements were performed perpendicular from the highest point present on the external articular surface, to the cartilage-bone interface according to an adapted method described by McNamara and Carlson (1979).

For every histological section, three digital images (and thus measurements) were taken across the span of the cartilage bearing region (according to an adapted method described by Ma et al 2002), but not within 1 mm of its attachment and fusion to the mucoperiosteum of the condylar neck. The data were then arranged collectively into lateral, central, and medial modalities for both young and mature sheep as well as anterior and posterior modalities for the remaining young sheep. The mean and standard deviation was established for each collective group.

(b) Cartilage matrix and cellularity

The same digital images of the condylar articular surface that were used to measure cartilage thickness were also subsequently used to determine the proportions of cartilage matrix (in this study defined as the cartilage matrix proper plus fibrous CT components) to cellular components. The area and perimeter of the total measuring frame (ie the field represented by X and Y planes) incorporated the total thickness (TT) of the condylar cartilage (ie FZ+HZ, but not SAB) at 200x magnification for each measured field. The digital photomicrograph was then highlighted to outline only the blue staining matrix (cf cellular components staining red) of the condylar cartilage on the section (**Figure 20**). This was achieved by setting the Quantimet to only highlight those regions that appeared blue (ie only reflected blue light from the matrix was identified by the Quantimet and so highlighted as the field of interest). As no other tissue component stained blue except matrix, this was a very useful method to measure the matrix compared to the cellular tissue components. For consistency, a cartilage width of 500μms was used for each measurement. Any artefact of the cartilage on the slide was digitally edited from the highlighted field of interest.

The aniline blue staining method also provides a more accurate measurement than the light green stain when comparing it to the red staining cytoplasm when quantitating the proportions of cartilage matrix and cellular components in this fashion. Firstly, because the wavelength (λ) of the transmitted blue light (455-492nm) from the stained matrix is further away from the transmitted λ of red light (622-780nm) from the stained cytoplasm, as compared with transmitted green light (492-577) from a green Masson's trichrome. Secondarily, there is a narrower range of λ with blue light as compared with green light, creating less potential for false positive measurement.

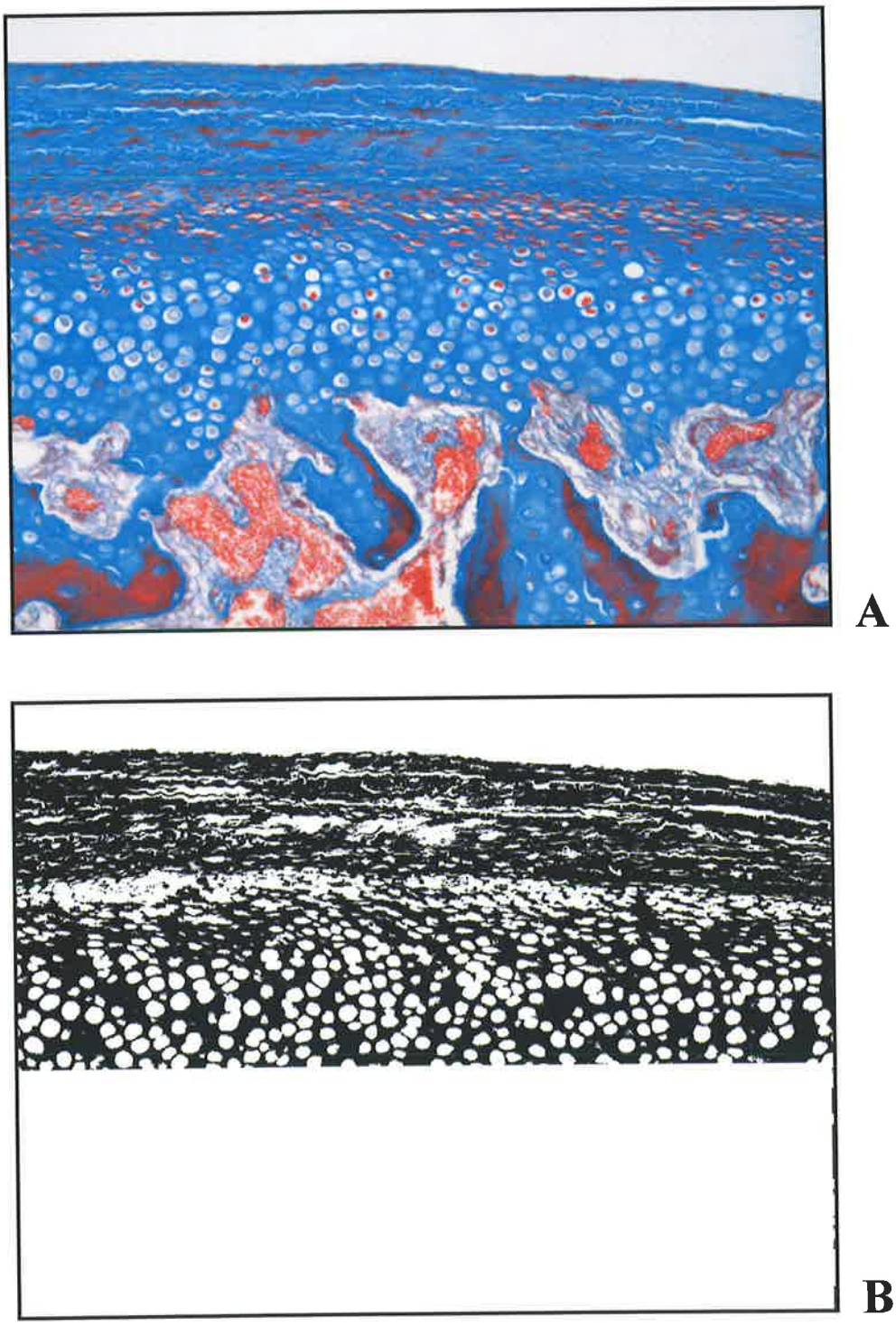

Figure 20. **A.** Photomicrograph of sagittal section of a young sheep condyle illustrating the condylar cartilage as stained with a modified blue Masson's trichrome. (200X). **B.** A binary image highlighting only the blue staining cartilage matrix within the defined field from articular surface to subarticular bone (cf the red staining cells within that area) as measured by the Quantimet 500MC. The proportions of cartilage matrix and cellular components could be measured (at a consistent width of 500μm) using this method by comparing the two percentages of each compared to the selected field as drawn on each image.

For each histological section the matrix area was measured three times across the available span of cartilage, but not within 1mm of each end. The data were arranged collectively into lateral, central, and medial modalities for both young and mature sheep as well as anterior and posterior modalities for the remaining young sheep. The mean and standard deviation was established for each collective group.

(c) Trabecular bone indicies

The scanned image was digitally highlighted to outline the cancellous trabecular bone field on the light green Masson's trichrome (cell and matrix) section as assessed by prior microscopic examination with the H&EP stained sections (**Figure 21**).

The area and perimeter of the total measuring frame (ie the field represented by X and Y planes) were calculated and then applied to formulae based on trabecular bone being composed of vertical plates with interconnecting rods (Parfitt et al., 1983). The standardised trabecular bone structural index values were recorded with the Quantimet 500MC from the raw pixel data.

The data were arranged collectively into lateral, central, and medial modalities for both young and mature sheep as well as anterior and posterior modalities for the remaining young sheep. The mean and standard deviation was established for each collective group.

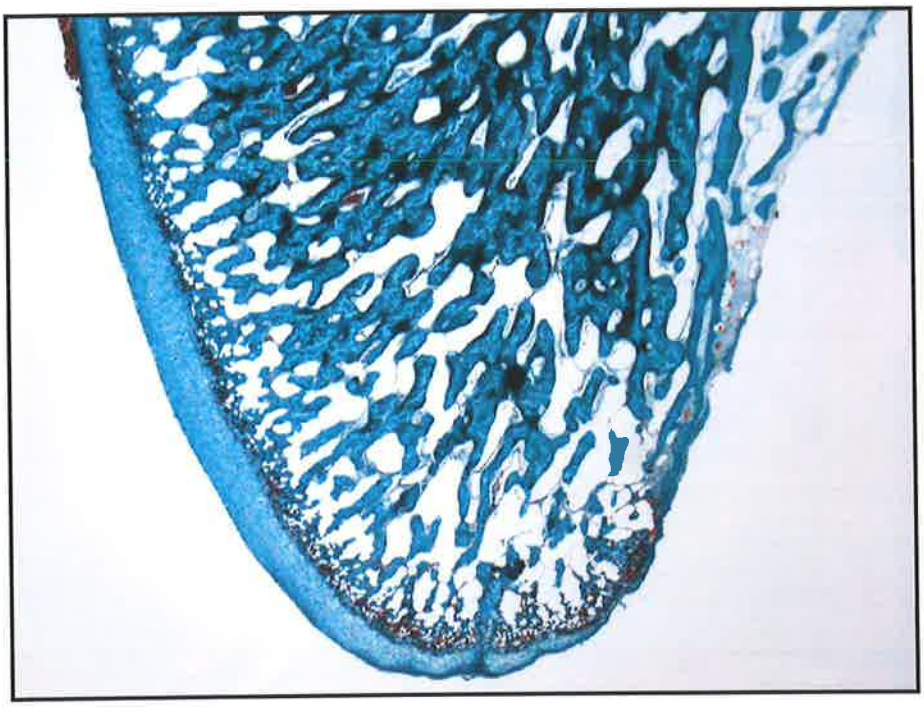

A

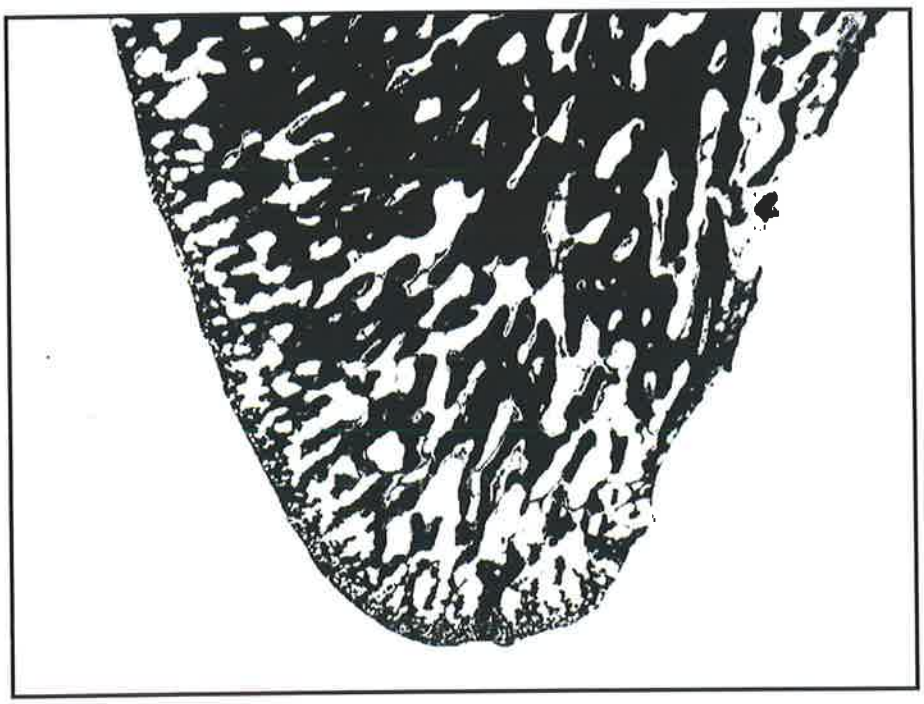

B

Figure 21. **A.** Photomicrograph of a sagittal section of a young sheep condyle illustrating trabeculae as stained with a light green Masson's trichrome (25X). **B.** A binary image highlighting only the trabecular bone (in white) within the defined total cancellous bony perimeter as measured by the Quantimet 500MC. The trabecular bone indices were then calculated from formulae derived from the parallel plate model of bone.

2.5 Statistical analysis

2.5.1 Tissue data analysis

For cartilage, statistical analysis involved testing for significant variation of 1) the thickness of cartilage (hypertrophic, fibrous and total) and 2) the cartilage matrix and cellular proportions of cartilage for regional variations within each age group The following regions were compared: a) lateral *vs* central *vs* medial sections for mature sheep, b) lateral *vs* central *vs* medial sections for young sheep and c) anterior *vs* posterior coronal sections for young sheep. Tests for significance of the means for both thickness, and proportions of cartilage matrix and cellularity in each regional group between the two age groups (eg mean young lateral *vs* mean mature lateral) were also performed. The significance of each cartilage measurement for the combined values of all regions (lateral, central and medial) between young and mature sheep condyles was also tested.

For trabecular bone, statistical analysis initially involved testing for significant variation of each bone structural index value for regional variations within each age group (ie lateral *vs* central *vs* medial regions for mature sheep; lateral *vs* central *vs* medial regions for young sheep *&* anterior *vs* posterior coronal regions for young sheep). Tests for significance of the means for each bone structural index value in each regional group between the two age groups (eg mean young lateral *vs* mean mature lateral) were also performed. The significance of each bone structural index value for the combined values of all regions (lateral, central and medial) between young and mature sheep condyles was also tested.

For all tissue data pertaining to the measurement of variables in similar regions, statistical analysis was performed using a Student's t-test (two sample assuming unequal variances) with a significance level of $p<0.05$ adopted for each case. All tests were performed with Microsoft Excel 2000.

2.5.2 Variability of the measurements

For evaluation of error between linear measurements performed using digital images and a public domain software programme (ImageJ 1.33u, National Institute of Health, USA) pertaining to the thickness of condylar cartilage, the error was calculated according to that published by Dahlberg (1940) using a random sample of sections:

$$S = \sqrt{\sum d^2 / 2n}$$

Where S is the measurement error, d is the difference between the repeated measurements and n is the number of the repeated measurement.

To test for variability when quantitating cartilaginous and trabecular histomorphometric data using the Quantimet 500MC, a random sample of sections were remeasured according to the previously described methodology. Statistical analysis was performed with a Student's t-test (two sample assuming unequal variances) between the original data and those of the remeasured data. A significance level of $p<0.05$ for each case was accepted as relevant. All tests were performed with Microsoft Excel 2000.

CHAPTER 3:

RESULTS

3.1 Qualitative histomorphology

3.1.1 Cartilage

The modified aniline blue and ponceau-fuchsin Masson's trichrome technique generally stained cartilage blue with bone a contrasting red. This stain not only contrasted between these two tissues but also contrasted between the cartilage matrix (including fibrous CT) staining blue and the cellular components staining red of the condylar cartilage (**Figure 22**). The general cartilaginous structure and presence of both the FZ and HZ remained unchanged, except for the tapering of the cartilage at the ends of the articular surface where the HZ narrowed and disappeared as the FZ fused with the mucoperiosteum of the neck of the condyle. Nevertheless, differences were noted in the FZ, HZ & TT proportions and morphological patterns between different regions and different animals, particularly in the mature sheep (**Figure 23**). In the young sheep, one animal had an unusually large medial FZ region however; as this was not considered to be pathological this animal was not precluded from the study. Another qualitative difference noted was that the articular surface often appeared more undulating and friable in the mature sheep as compared with the young sheep (**Figures 23 & 24**).

In regards to the levels of cellular and matrix components seen, variability was obvious with some specimens displaying a highly cellular morphological appearance whilst others had a more solid matrix architecture with smaller diameters of the chondrocytes. A greater variation tended to be seen in the mature age group (**Figure 25**). Examination of the specimens for blue and red staining of the cartilage matrix and cellular components respectively revealed little variation within the same animal. Comparisons however, between the young and mature age groups did demonstrate some qualitative differences, particularly in regards to the colour saturation of the stains used (**Figure 24**).

3.1.2 Trabecular bone

The light green and ponceau-fuchsin Masson's trichrome technique generally stained cartilage green with bone displaying a little more variability in the uptake of the two stains (green and red). However, this stain did give a high level of contrast between the stained tissues and the background (**Figure 26**).

As a general morphological perception of trabecular patterns of condylar bone between young and mature sheep, qualitative differences were noted (**Figure 27**). Condylar trabeculae appeared thick and dense in the young sheep with many small trabecular separations often displaying a poorly aligned connection of bony plates and rods. In the mature sheep however, the trabeculae tended to form longer and thinner cortical plates. Although the trabeculae still appeared denser, the more widely spaced trabeculae were usually aligned in a parallel fashion toward the articular surface.

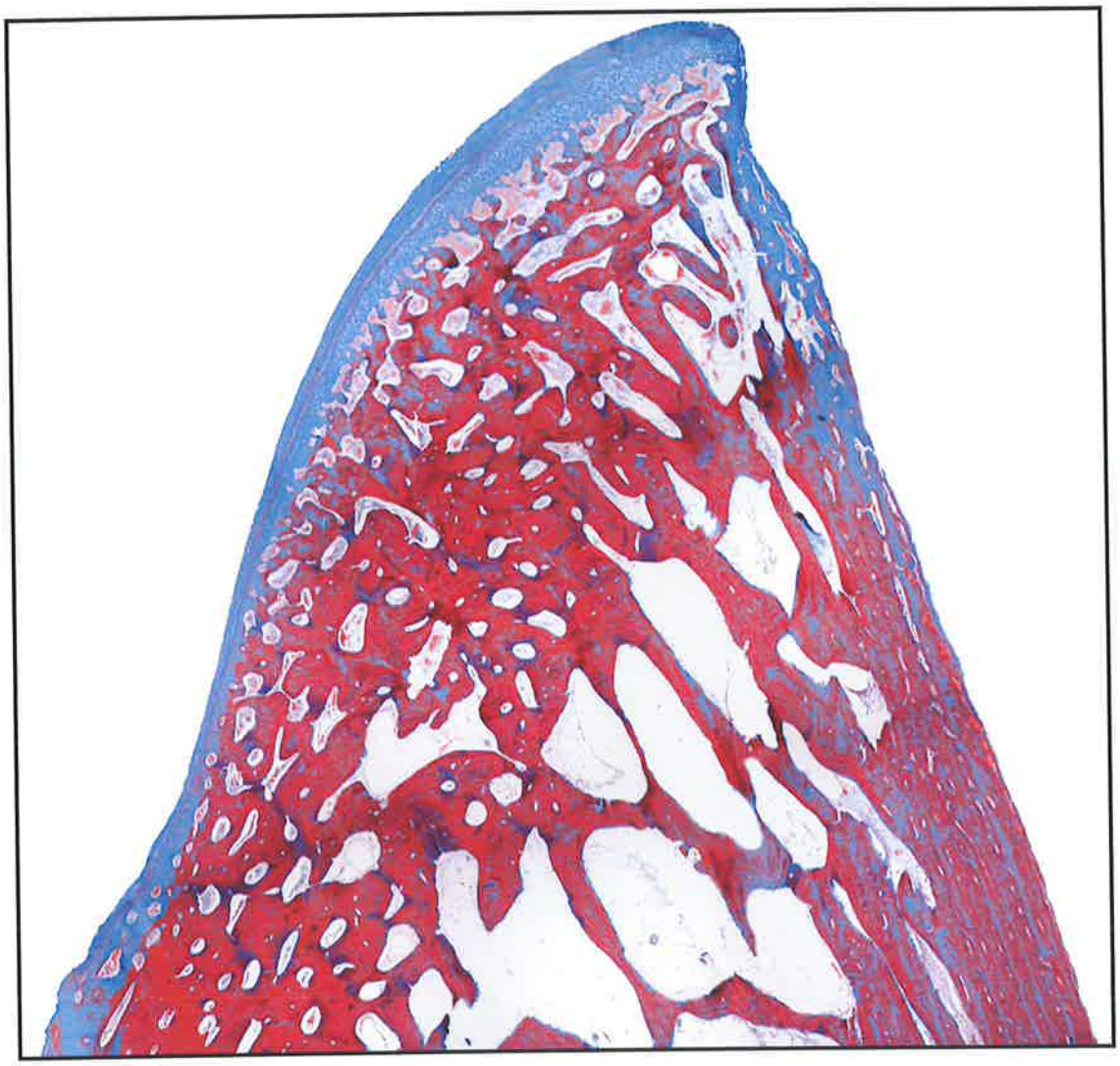

Figure 22. A composite photomicrograph of a lateral sagittal section taken from a young sheep condyle as stained with a modified aniline blue and ponceau-fuchsin Masson's trichrome technique that predominantly stained cartilage blue and bone red. This stain was not only valuable in delineating between these two types of tissues, but was also necessary for making comparisons between the matrix (inc fibrous CT) and cellular components of the condylar cartilage. Images were taken with a Nikon DXM camera on a Nikon Eclipse TE300 microscope with the images combined using the computer programme analySIS®, Soft Imaging System, Germany.

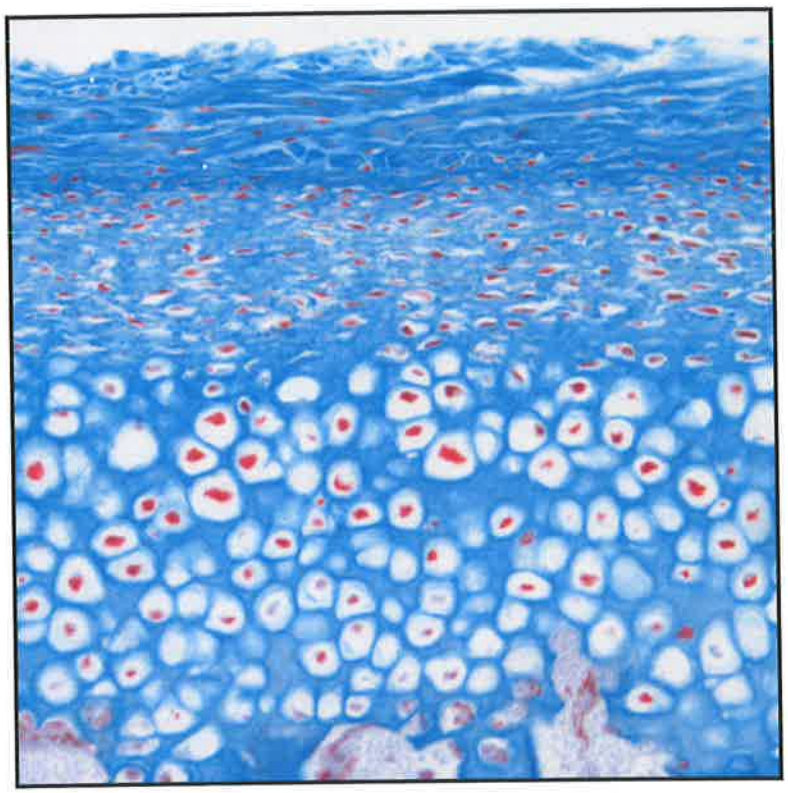

A

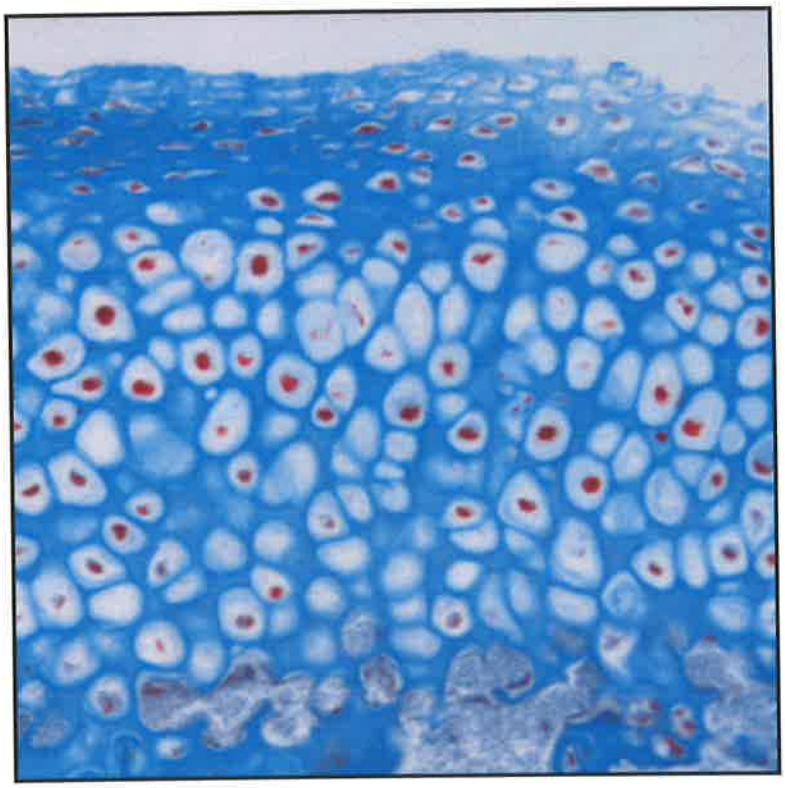

B

Figure 23. Photomicrographs of histological sections from the medial (**A**) and central (**B**) regions of the same mature sheep condyle as stained with a modified blue Masson's trichrome (both 200X). These pictures illustrate the variability of the thickness of the FZ region, with the central region being much thinner than that of the medial region, leading to a decrease in the FZ thickness and TT of the central section. However, the levels of cellularity observed remain similar for both sections. Also note the friable (**A**) and undulating (**B**) surface of the condyle.

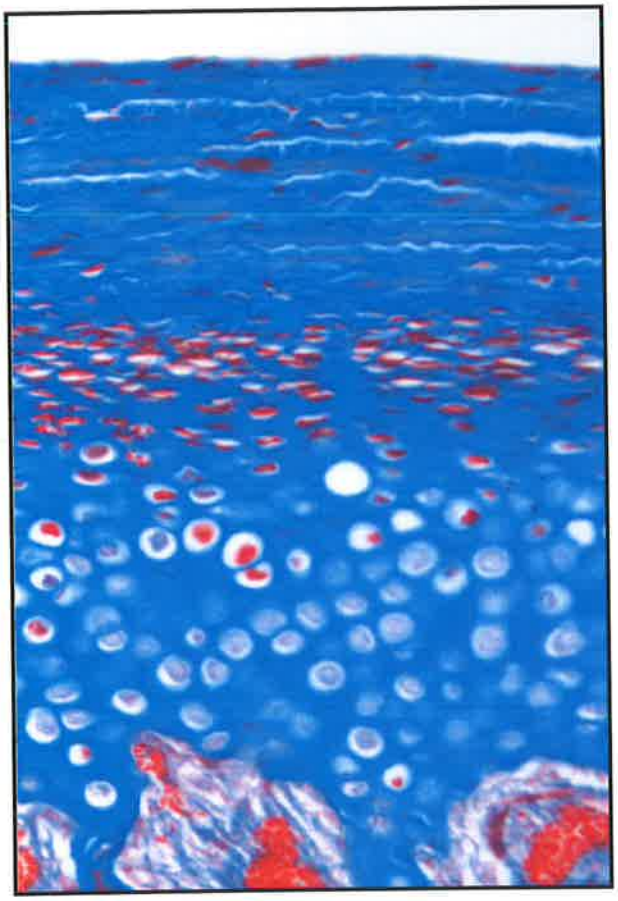

A

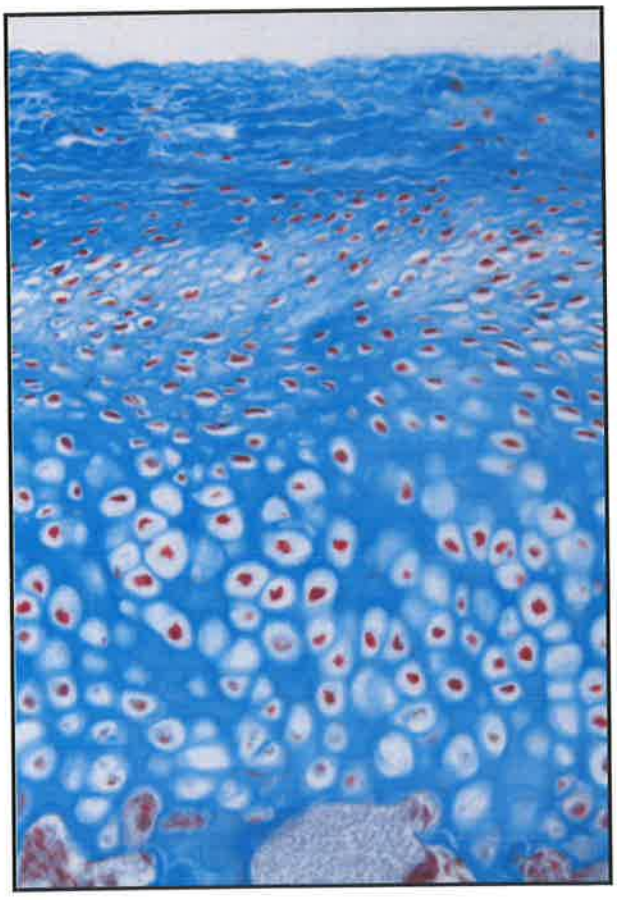

B

Figure 24. Photomicrographs of histological sections of condylar cartilage from a young sheep (**A**) and a mature sheep (**B**) as stained using a modified aniline blue Masson's trichrome (both 200X). The general structure of the condylar cartilage seen is similar with the presence of both the FZ and HZ, although the proliferative group of cells is more compact in this illustration. Although some difference regarding the colour saturation of the sections is visible, the cartilage matrix still stained blue whilst the cellular components stained red for both age groups. Note the more undulating articular surface in the mature sheep.

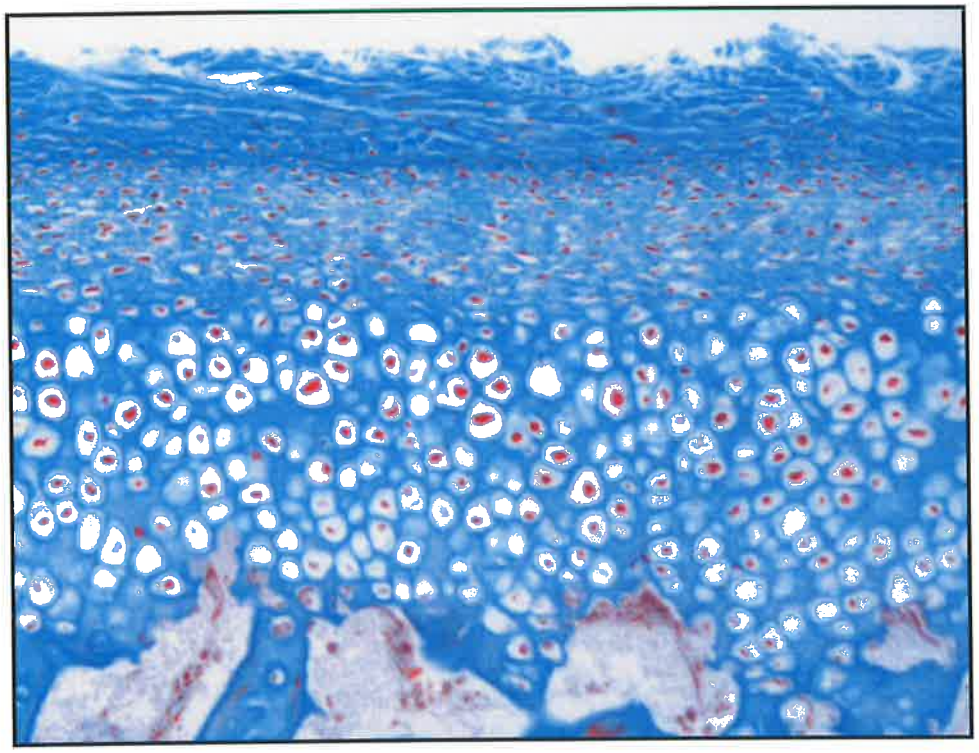

A

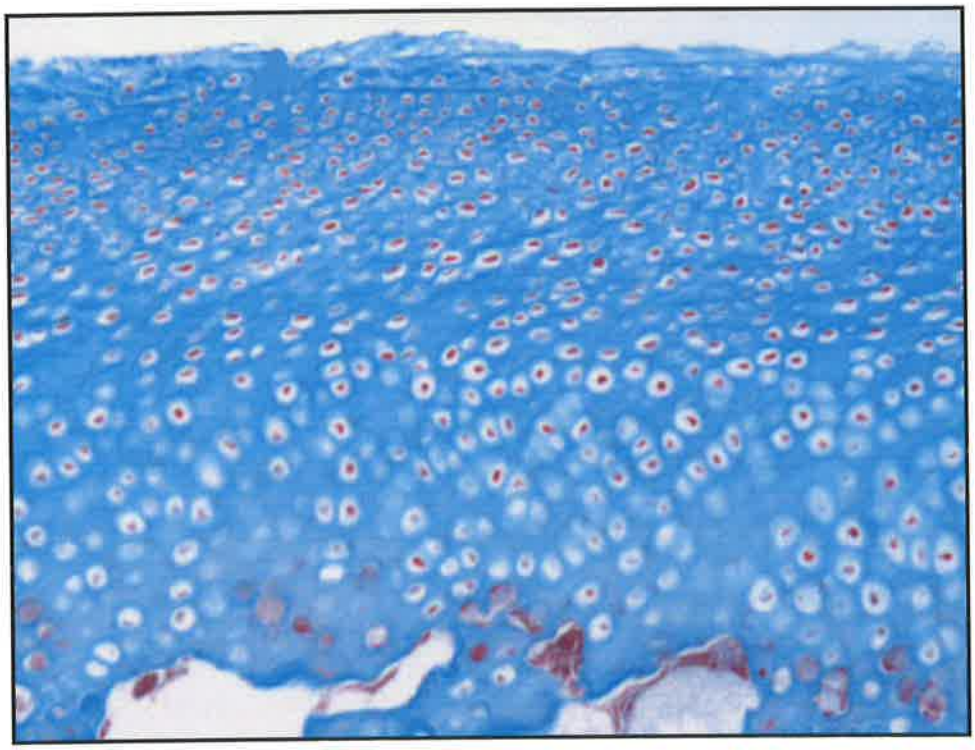

B

Figure 25. Photomicrographs of histological sections stained with a modified blue Masson's trichrome from two different mature sheep condyles, illustrating the differences in the levels of cellularity observed (both 100X). **A.** displays a highly cellular morphological appearance whilst **B.** displays a more solid matrix architecture with smaller diameters of the chondrocytes. Note that in both sections the matrix stains blue whilst the cellular components stain red.

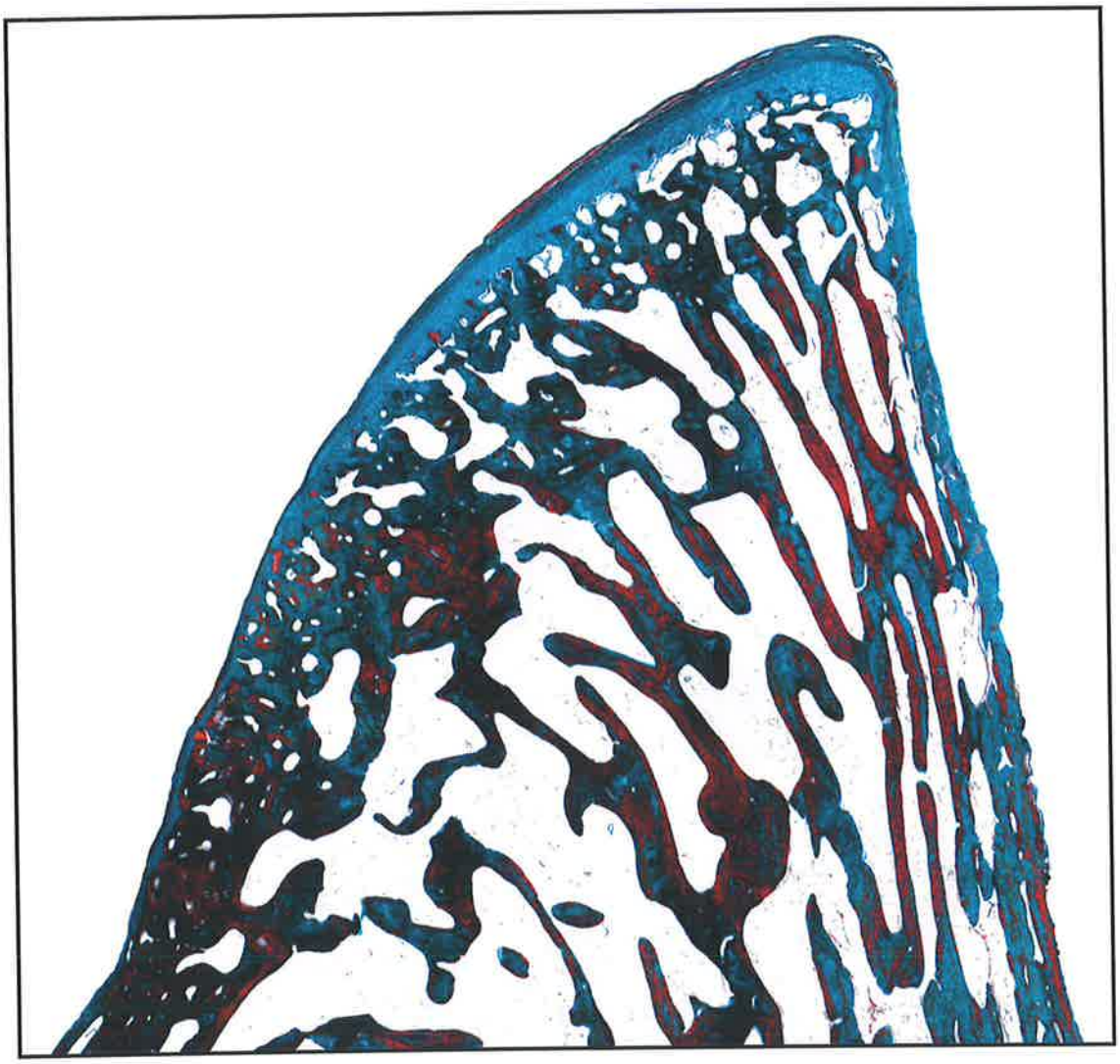

Figure 26. A composite photomicrograph of a medial sagittal section taken from a mature sheep condyle as stained with a light green and ponceau-fuchsin Masson's trichrome technique. There was more variability of the tissues in the uptake of the two stains however, this stain does give a high level of contrast between the stained tissues and the background. The images were taken with a Nikon DXM camera on a Nikon Eclipse TE300 microscope with the images combined using the computer programme analySIS®, Soft Imaging System, Germany.

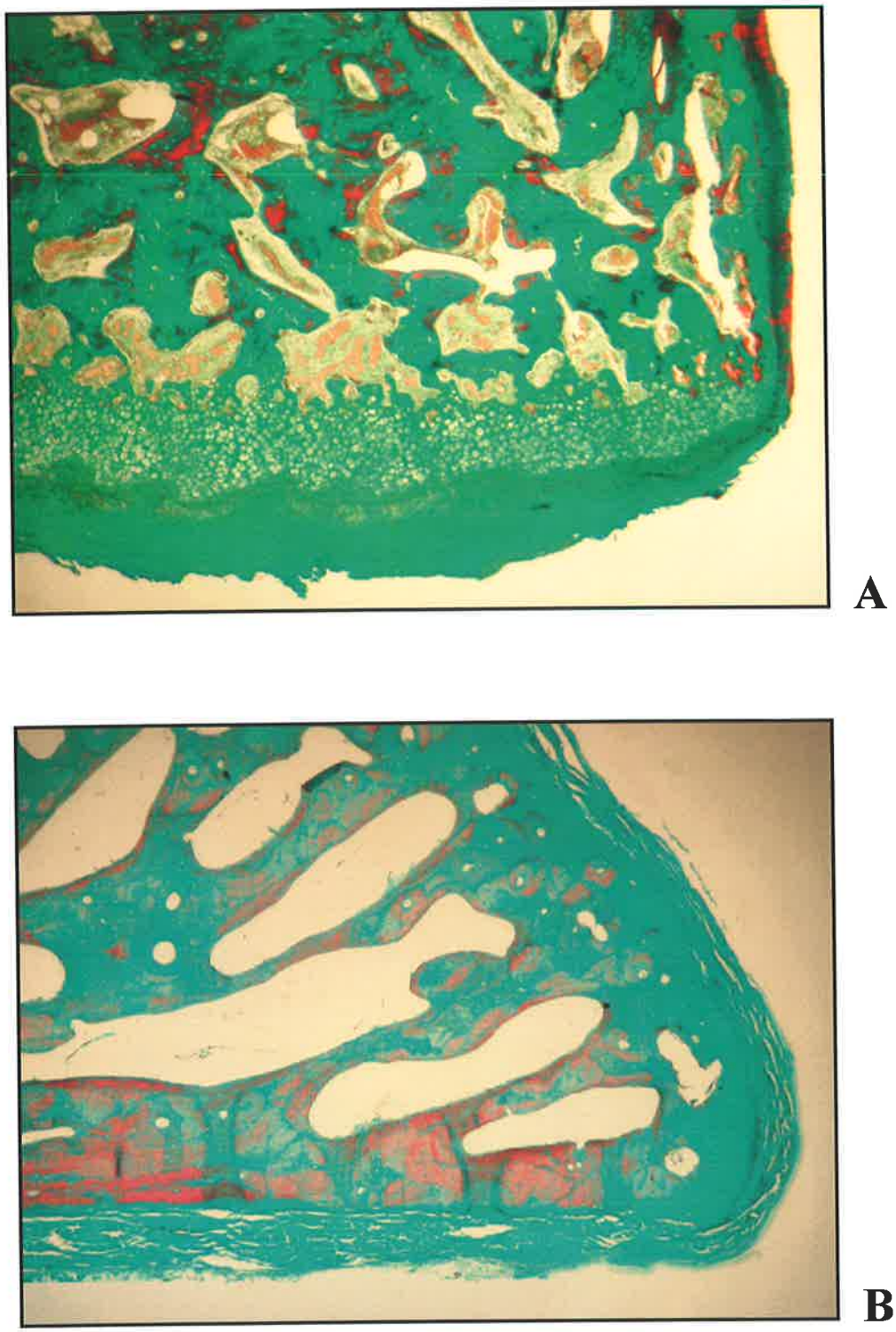

Figure 27. **A**. Photomicrograph of a histological section of a young sheep condyle stained with a light green Masson's trichrome (40X). Note the thick and dense condylar trabeculae that form a poorly aligned connection of bony plates and rods. **B**. Photomicrograph of a histological section of a mature sheep condyle also stained with Masson's trichrome (40X). Note the difference in the morphological pattern of the condylar trabeculae where the trabecular plates are longer and thinner and are aligned in a parallel fashion towards the articular surface.

3.2 Cartilage thickness

The mean and standard deviation for the thickness of Fibrous Zone (FZ), Hypertrophic Zone (HZ) and the Total Thickness of condylar cartilage (TT) for the lateral, central and medial sagittal sections in young and mature sheep are given in **Table 3.** In addition, the mean and standard deviation of these thicknesses for anterior and posterior coronal sections in young sheep are given in **Table 4.** A summary of the significant differences of these data appear in **Table 5.** In regards to the variability of linear measurements using ImageJ 1.33u, the measurement error for condylar cartilage thickness was estimated to be 12.16μm for the FZ and 13.01μm for the HZ (see Appendix VI).

3.2.1 Fibrous zone (FZ)

The FZ means and standard deviations for all anatomical regions measured including the combined sagittal totals for both young and mature sheep ranged from 110-207μm (41.3-123.6) and are presented in **Graph 1** (Abbreviations for all graphs: **LY** lateral young; **CY** central young; **MY** medial young; **AY** anterior young; **PY** posterior young; **LM** lateral mature; **CM** central mature; **MM** medial mature; **TY** total young; **TM** total mature). The only statistically significant ($p<0.05$) regional variation for all thickness measurements within the young sheep age group was found between the lateral and medial sagittal section FZ thicknesses (see Appendix VII). In regards to the mature sheep age group statistically significant regional differences were also found, but in this instance between the central and lateral regions as well as between the central and medial regions (see Appendix VII).

3.2.2 Hypertrophic zone (HZ)

The HZ means and standard deviations for all anatomical regions measured including the combined sagittal totals for both young and mature sheep ranged from 119-150μm

(24.1-60.4) and are presented in **Graph 2**. Again a statistically significant regional difference was found within the mature age group between the central and lateral region (see Appendix VII).

3.2.3 Total thickness (TT)

The TT means and standard deviations for all anatomical regions measured including the combined sagittal totals for both young and mature sheep ranged from 240-326μm (58.5-107) and are presented in **Graph 3**. Consistently, the significant regional difference occurred between the central and lateral regions in the mature sheep as well as that between the central and medial regions analogous to the FZ thickness findings (see Appendix VII).

GRAPH 1

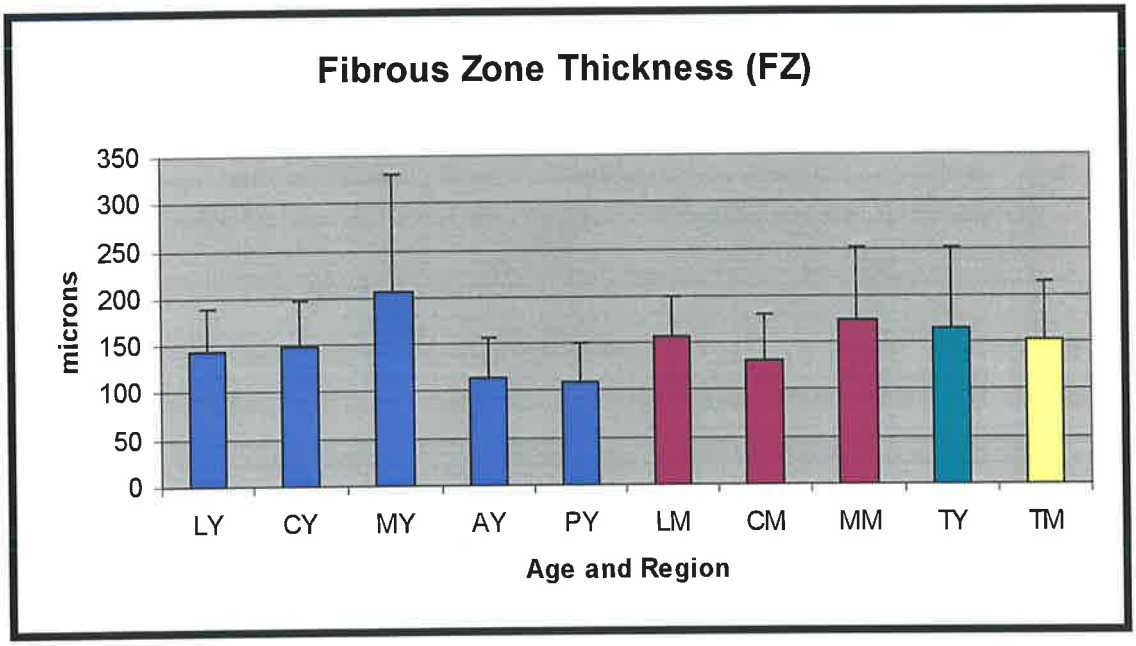

GRAPH 2

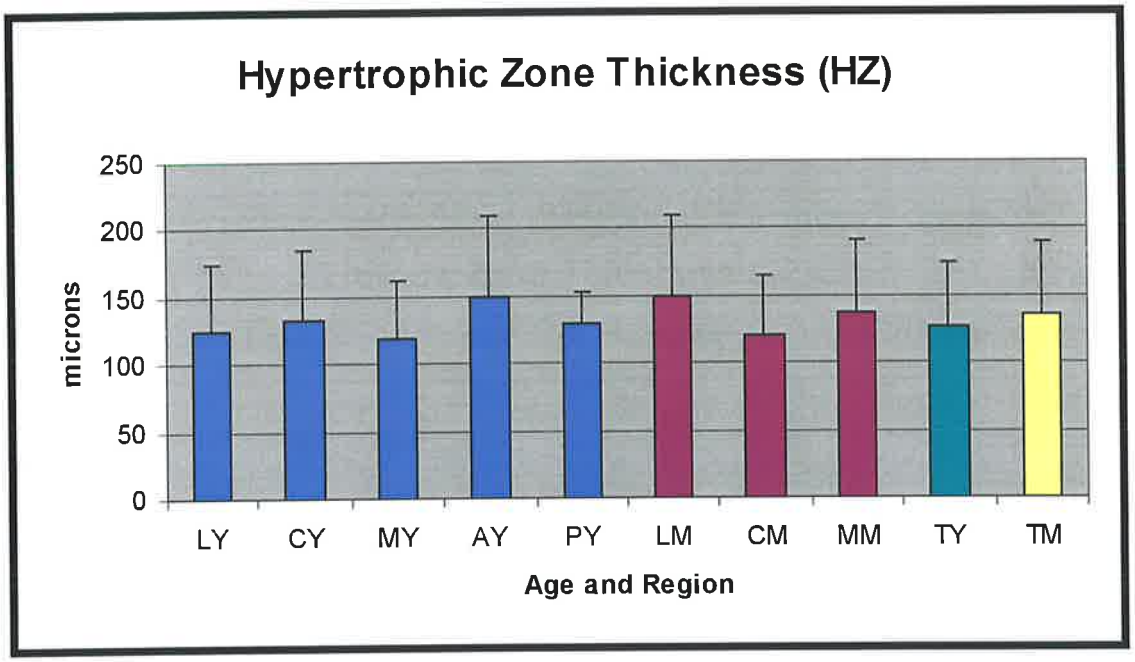

GRAPH 3

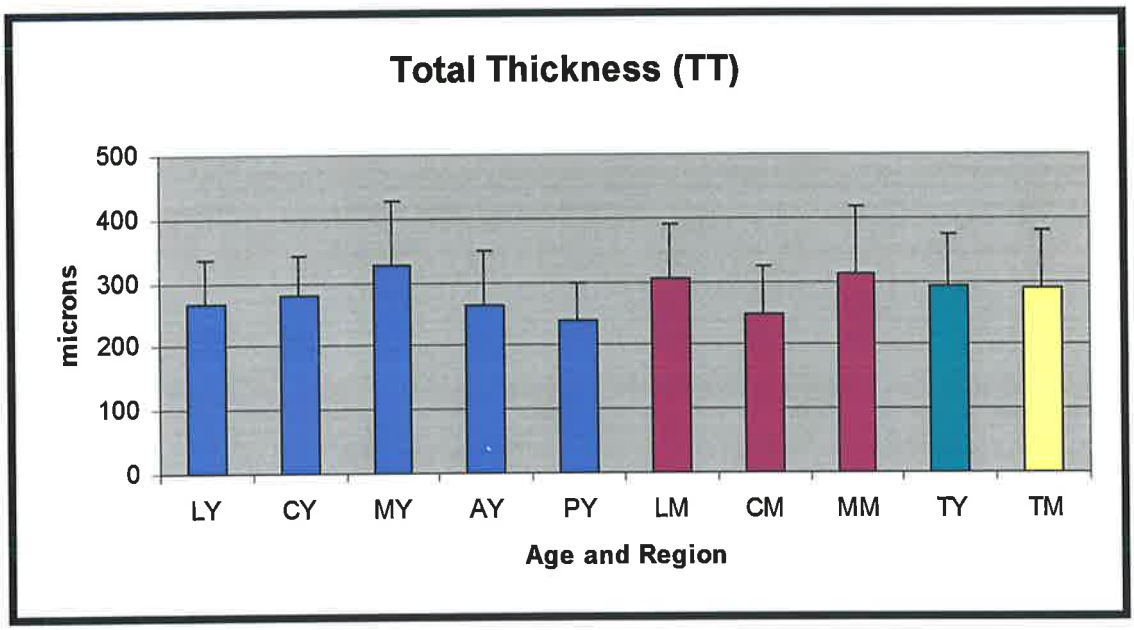
Total Thickness (TT)
500
400
300
200
100
0
microns
LY
CY
MY
AY
PY
LM
CM
MM
TY
TM
Age and Region

SECTION	Fibrous Zone (FZ) μm	Hypertrophic Zone (HZ) μm	Total Thickness (TT) μm
Lateral Young (L)	**143 (45.9)$^{+}$**	125 (48.9)	268 (67.4)
Central Young (C)	148 (50.0)	133 (52.7)	281 (63.3)
Medial Young (M)	**207 (123.6)$^{+}$**	119 (43.5)	326 (102.7)
Total Young	166 (85.1)	126 (48.0)	292 (82.3)
Lateral Mature (L)	**156 (44.7)***	**150 (59.7)‡**	**306 (84.4)$^{\#}$**
Central Mature (C)	**130 (50.1)*†**	**120 (44.8)‡**	**250 (73.2)$^{\#\wedge}$**
Medial Mature (M)	**174 (78.0)†**	138 (53.7)	**312 (107.0)$^{\wedge}$**
Total Mature	153 (61.6)	136 (53.9)	289 (92.7)

Table 3. Mean and standard deviation (in brackets) of all cartilage thickness measurements for lateral, central and medial sections in young and mature sheep. Figures in bold indicate a statistical significance at $p<0.05$ (across like symbols).

SECTION	Fibrous Zone (FZ) μm	Hypertrophic Zone (HZ) μm	Total Thickness (TT) μm
Anterior Young (A)	114 (41.9)	149 (60.4)	264 (85.5)
Posterior Young (P)	110 (41.3)	129 (24.1)	240 (58.5)

Table 4. Mean and standard deviation (in brackets) of all cartilage thickness measurements for anterior and posterior sections in young sheep. No statistically significant differences were found at $p<0.05$ (across like symbols).

SECTION	Fibrous Zone (FZ)	Hypertrophic Zone (HZ)	Total Thickness (TT)
Young Sheep			
anterior vs posterior	N	N	N
lateral vs central	N	N	N
lateral vs medial	**YES**	N	N
central vs medial	N	N	N
Mature Sheep			
lateral vs central	**YES**	**YES**	**YES**
lateral vs medial	N	N	N
central vs medial	**YES**	N	**YES**
Young & Mature Sheep			
lateral vs lateral	N	N	N
central vs central	N	N	N
medial vs medial	N	N	N
all regions vs all regions	N	N	N

Table 5. Summary of statistical outcome between regional and age groups for all cartilage thickness values ($p<0.05$).

3.3 Cartilage matrix and cellularity

The mean and standard deviation of both the condylar cartilage matrix and cellular components for lateral, central and medial sagittal sections in young and mature sheep are given in **Table 6.** In addition, the mean and standard deviation of these values for anterior and posterior coronal sections in young sheep are given in **Table 7.** No significant differences of such data were found as is summarised in **Table 8.** Intraobserver and interobserver variability analysis yielded no significant difference when using the Quantimet 500MC to measure the proportions of cartilage matrix and cellular components (see Appendix VIII).

3.3.1 Matrix component

The cartilage matrix component means and standard deviations for all anatomical regions measured including the combined sagittal totals for both young and mature sheep ranged from 34.8-42.4 % (2.97-10.44) and are presented in **Graph 4**. Although not significant, there is a consistent trend of a higher matrix component in the sagittal sections of the mature sheep as compared with those of the young sheep.

3.3.2 Cellular component

The cartilage cellular component means and standard deviations for all anatomical regions measured including the combined sagittal totals for both young and mature sheep ranged from 57.6-65.2 % (4.11-19.56) and are presented in **Graph 5**. Conversely to the matrix component of the condylar cartilage, there is a consistent trend of a higher cellularity in the sagittal sections of the young sheep as compared with those of the mature sheep, albeit non significant.

GRAPH 4

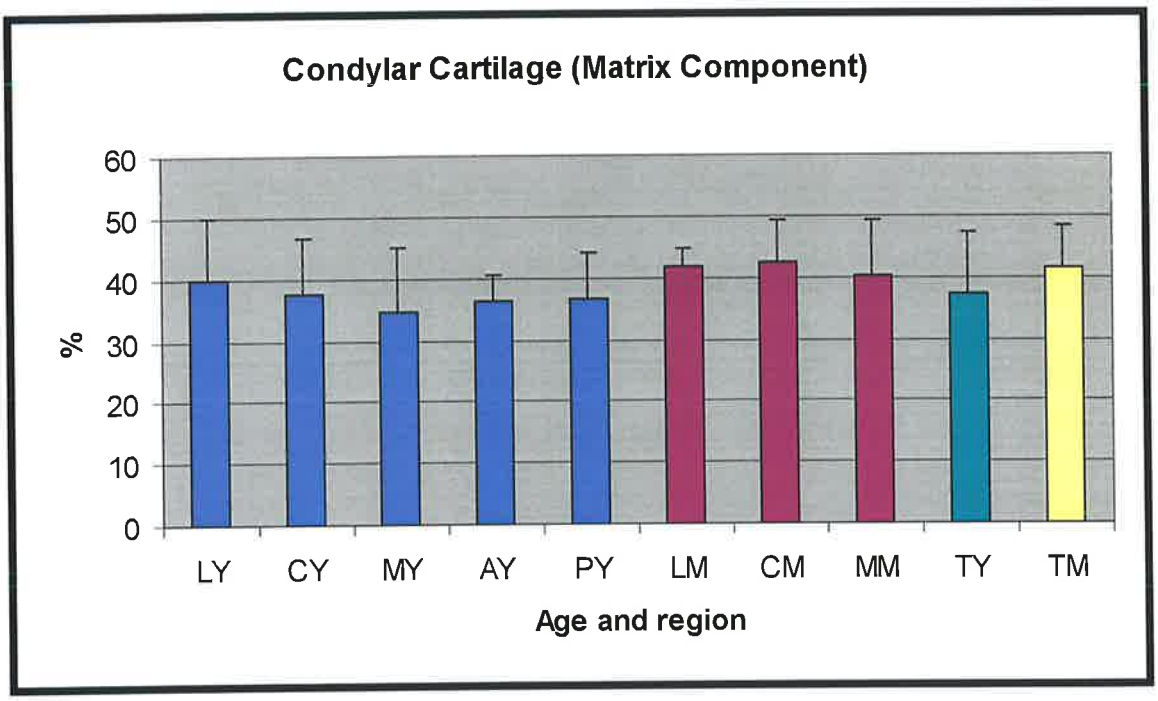

GRAPH 5

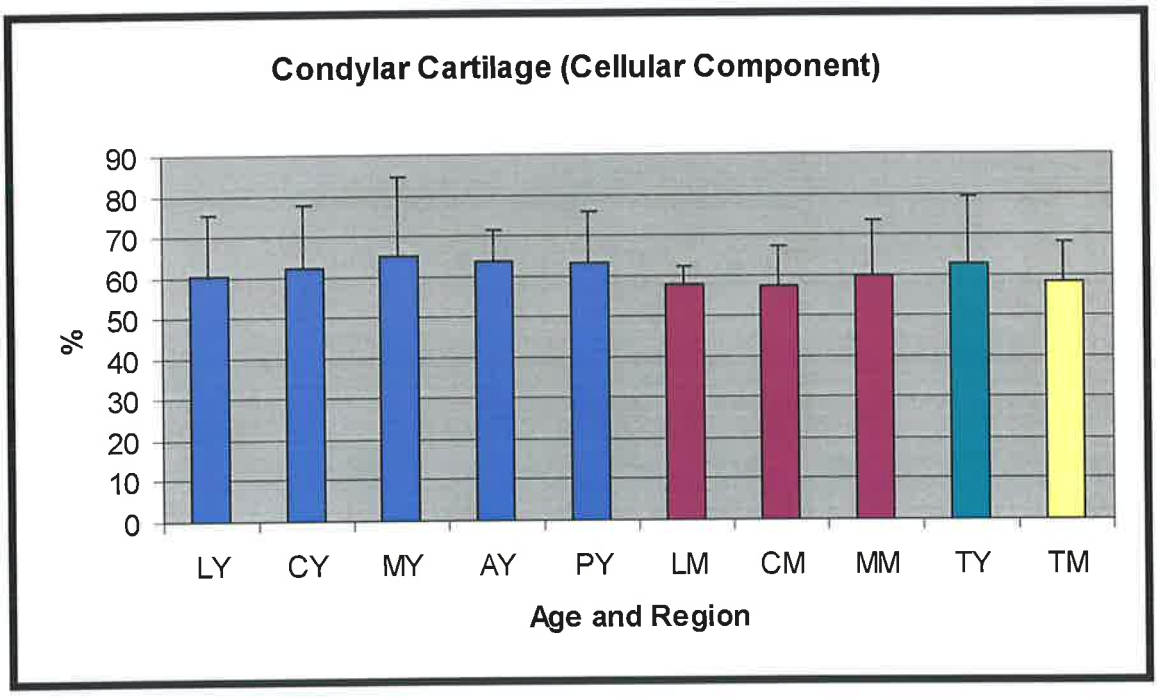

SECTION	Cartilage Matrix %	Cellular Component %
Lateral Young (L)	39.9 (10.15)	60.1 (15.29)
Central Young (C)	37.5 (9.27)	62.5 (15.45)
Medial Young (M)	34.8 (10.44)	65.2 (19.56)
Total Young	37.4 (10.0)	62.6 (16.74)
Lateral Mature (L)	41.8 (2.97)	58.0 (4.11)
Central Mature (C)	42.4 (6.96)	57.6 (9.44)
Medial Mature (M)	40.2 (9.22)	59.8 (13.69)
Total Mature	41.6 (6.72)	58.5 (9.45)

Table 6. Mean and standard deviation (in brackets) of all condylar cartilage matrix and cellular area percentages for lateral, central and medial sections in young and mature sheep. No statistically significant differences were found at $p<0.05$ (across like symbols).

SECTION	Cartilage Matrix %	Cellular Component %
Anterior Young (A)	36.2 (4.31)	63.8 (7.60)
Posterior Young (P)	36.8 (7.33)	63.2 (12.59)

Table 7. Mean and standard deviation (in brackets) of all condylar cartilage matrix and cellular area percentages for anterior and posterior sections in young sheep. No statistically significant differences were found at $p<0.05$ (across like symbols).

SECTION	Cartilage Matrix	Cellular Component
Young Sheep	N	N
lateral vs central	N	N
lateral vs medial	N	N
central vs medial	N	N
anterior vs posterior	N	N
Mature Sheep	N	N
lateral vs central	N	N
lateral vs medial	N	N
central vs medial	N	N
Young & Mature Sheep	N	N
lateral vs lateral	N	N
central vs central	N	N
medial vs medial	N	N
all regions vs all regions	N	N

Table 8. Summary of statistical outcome between regional and age groups for all cartilage matrix and cellular components ($p<0.05$).

3.4 Trabecular bone indices

In an attempt to refine the location of the qualitative differences noted in the trabecular bone, the mean and standard deviation for all the quantitative bone structural index for lateral, central and medial sagittal sections in young and mature sheep are given in **Table 9.** In addition, the mean and standard deviation for all the bone structural index values for anterior and posterior coronal sections in young sheep are given in **Table 10.** A summary of the significant differences of these data appear in **Table 11.** Intraobserver and interobserver variability analysis yielded no significant difference when using the Quantimet 500MC to measure bone index values (see Appendix VIII).

3.4.1 Bone Volume/Tissue Volume (BV/TV)

The BV/TV means and standard deviations for all anatomical regions measured including the combined sagittal totals for both young and mature sheep ranged from 43.21-63.3 % (8.20-14.69) and are presented in **Graph 6**. No statistically significant regional or age variations were found for BV/TV.

3.4.2 Bone Surface/Tissue Volume (BS/TV)

The BS/TV means and standard deviations for all anatomical regions measured including the combined sagittal totals for both young and mature sheep ranged from 3.46-4.6 mm^2/mm^3 (0.32-0.89) and are presented in **Graph 7**. A statistically significant ($p<0.05$) regional variation between the lateral and medial section BS/TV was found in the young sheep (see Appendix VII).

3.4.3 Bone Surface/Bone Volume (BS/BV)

The BS/BV means and standard deviations for all anatomical regions measured including the combined sagittal totals for both young and mature sheep ranged from

6.16-8.66 mm^2/mm^3 (1.07-2.29) and are presented in **Graph 8**. No statistically significant regional or age variations were found for BS/BV.

3.4.4 Trabecular Thickness (TbTh)

The TbTh means and standard deviations for all anatomical regions measured including the combined sagittal totals for both young and mature sheep ranged from 0.24-0.33 mm (0.03-0.08) and are presented in **Graph 9**. The only significant variation ($p<0.05$) when comparing each bone structural index value in similar anatomical regions of both young and mature sheep was found in the TbTh of the lateral regions (see Appendix VII).

3.4.5 Trabecular Separation (TbSp)

The TbSp means and standard deviations for all anatomical regions measured including the combined sagittal totals for both young and mature sheep ranged from 0.19-0.32 mm (0.05-0.10) and are presented in **Graph 10**. No statistically significant regional or age variations were found for TbSp.

3.4.6 Trabecular Number (TbN)

The TbN means and standard deviations for all anatomical regions measured including the combined sagittal totals for both young and mature sheep ranged from 1.73-2.21 #/mm (0.16-0.44) and are presented in **Graph 11**. A statistically significant ($p<0.05$) regional variation for the TbN was found between lateral and medial sections in the young sheep (see Appendix VII).

GRAPH 6

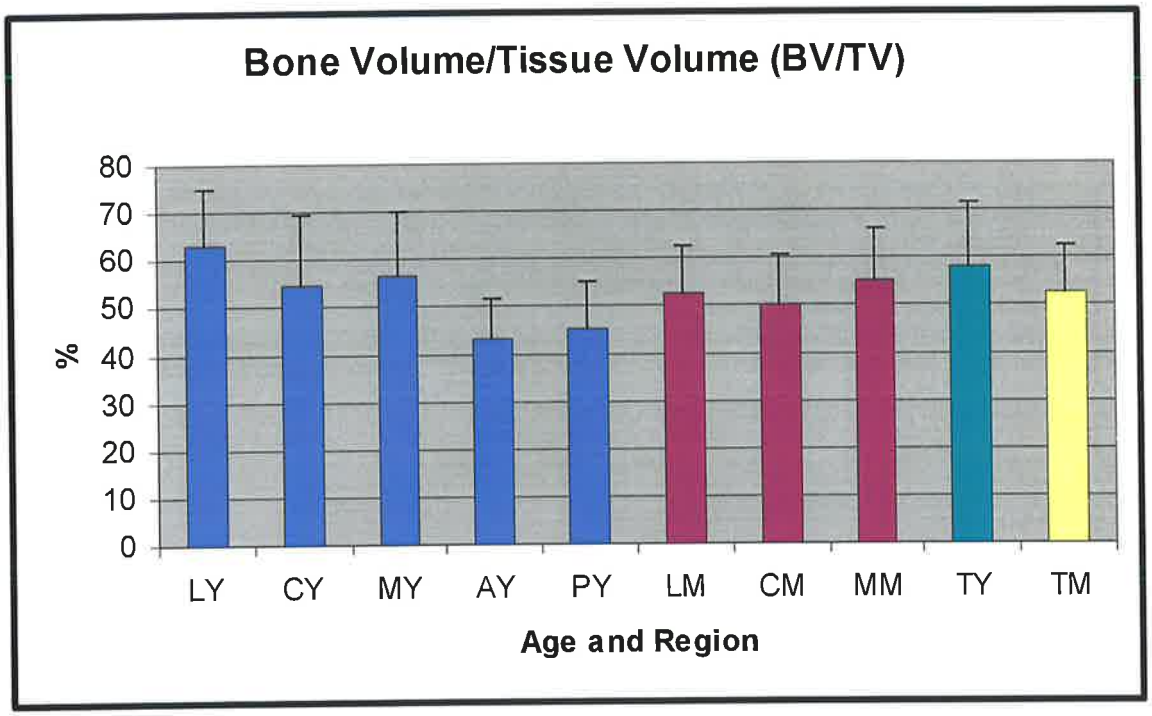

GRAPH 7

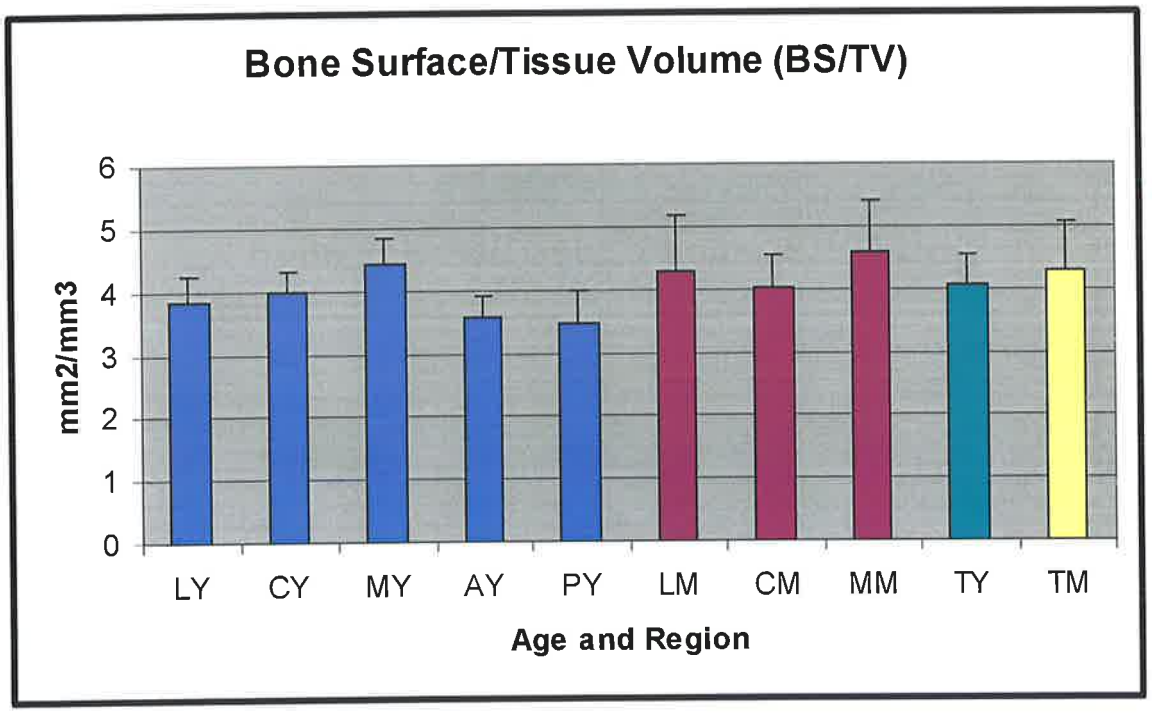

GRAPH 8

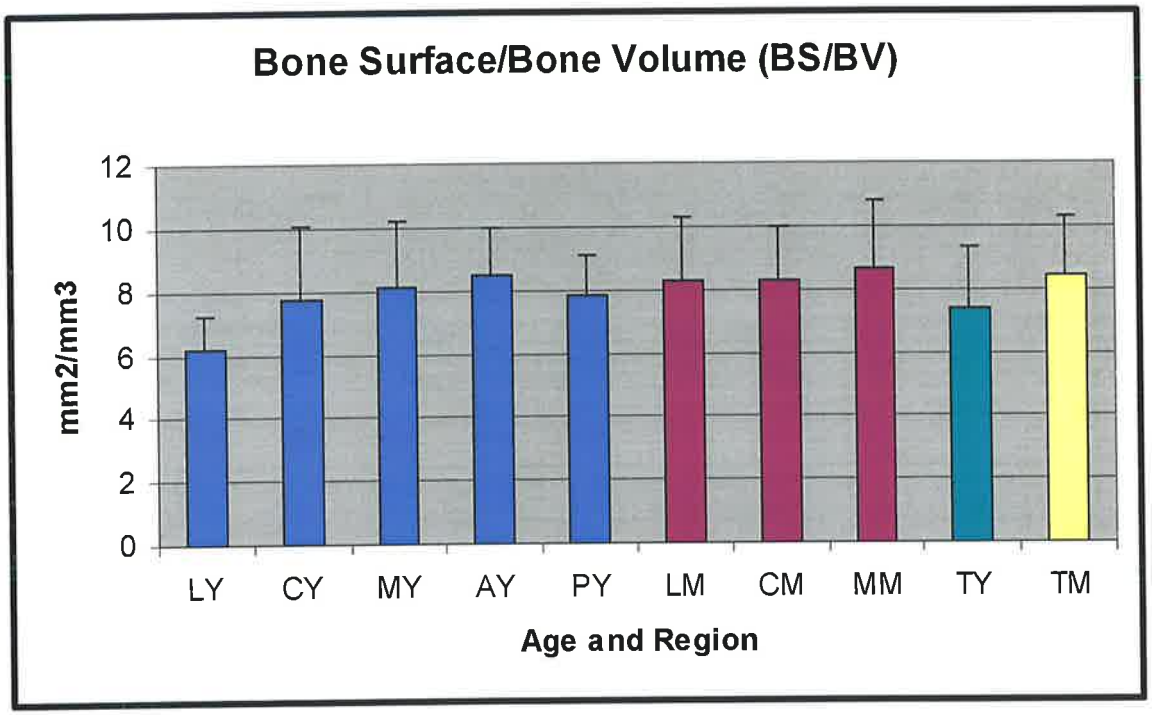

GRAPH 9

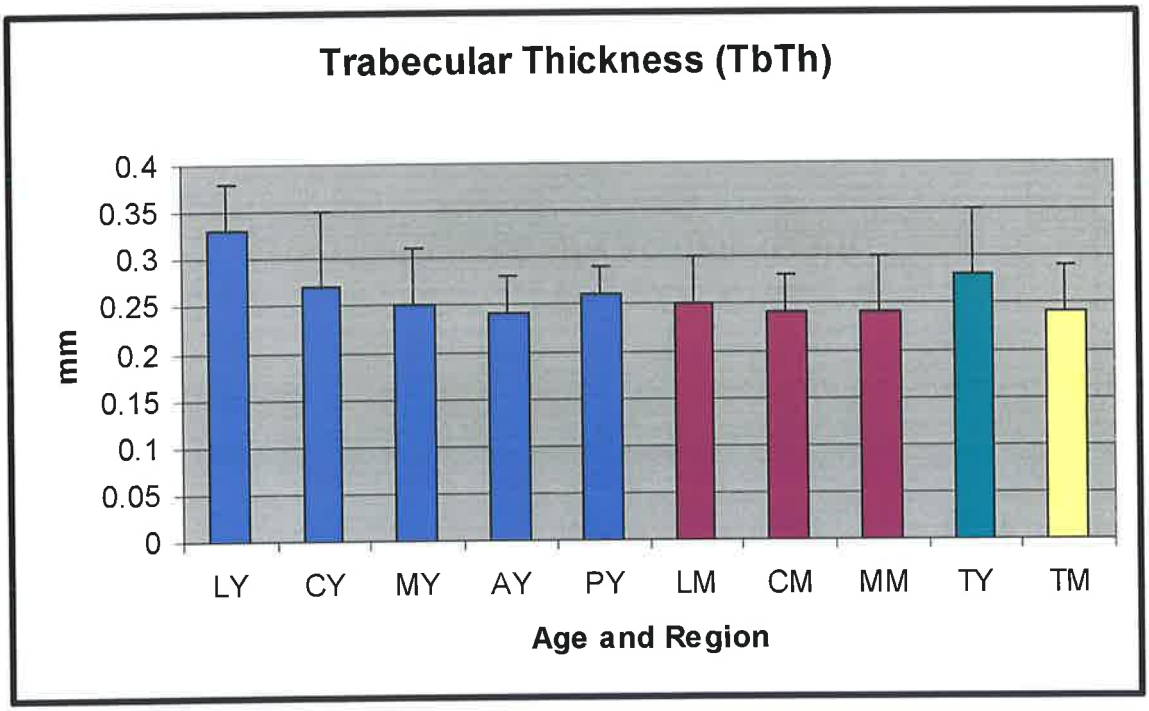

GRAPH 10

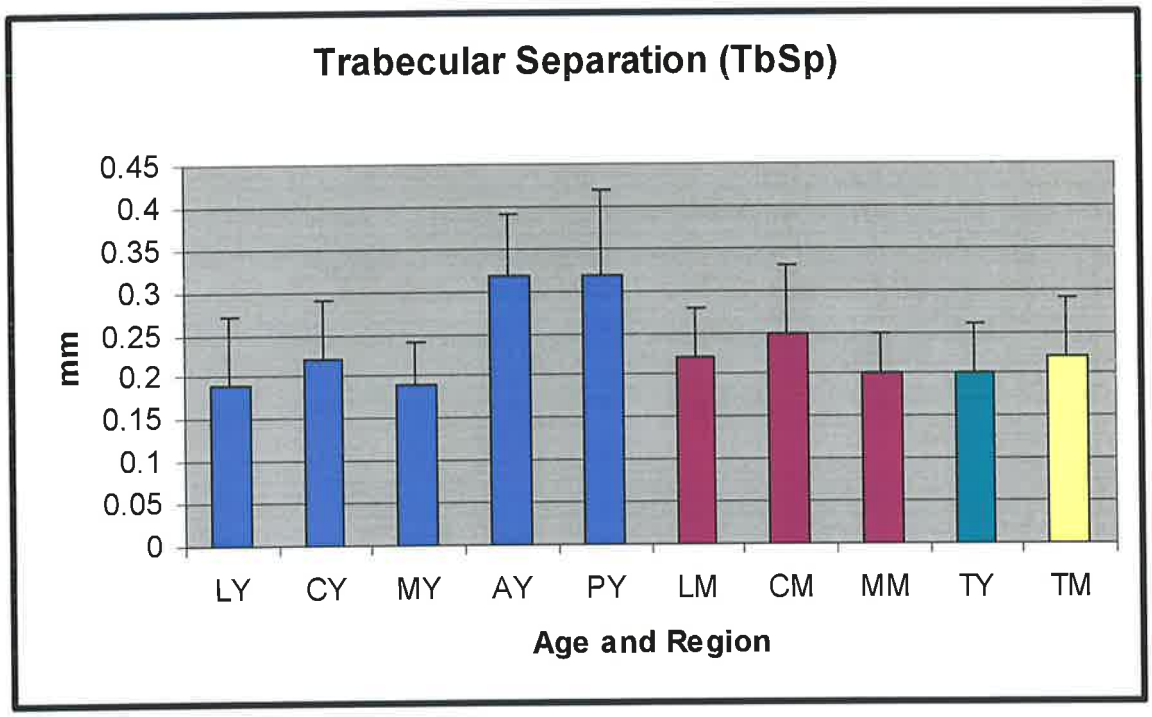

GRAPH 11

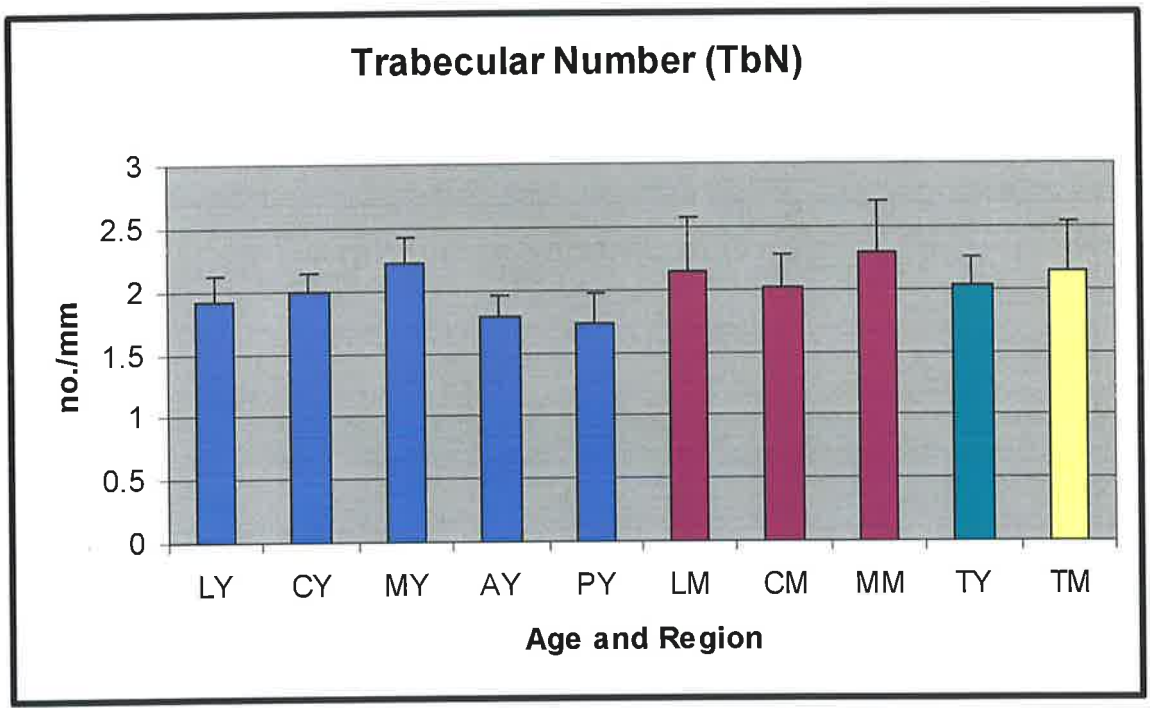

SECTION	BV/TV %	BS/TV mm^2/mm^3	BS/BV mm^2/mm^3	Tb.Th mm	Tb.Sp mm	Tb.N #/mm
Lateral Young (L)	63.3 (11.76)	**3.82 (0.43)***	6.16 (1.07)	**0.33 (0.05)**†	0.19 (0.08)	**1.91 (0.21)**‡
Central Young (C)	54.74 (14.69)	3.99 (0.32)	7.77 (2.29)	0.27 (0.08)	0.22 (0.07)	1.99 (0.16)
Medial Young (M)	56.86 (13.18)	**4.43 (0.42)***	8.15 (2.09)	0.25 (0.06)	0.19 (0.05)	**2.21 (0.21)**‡
Total Young	58.3 (13.01)	4.08 (0.45)	7.36 (1.98)	0.28 (0.07)	0.2 (0.06)	2.04 (0.22)
Lateral Mature (L)	52.89 (9.60)	4.28 (0.89)	8.29 (1.99)	**0.25 (0.05)**†	0.22 (0.06)	2.14 (0.44)
Central Mature (C)	50.05 (10.35)	4.02 (0.53)	8.3 (1.68)	0.24 (0.04)	0.25 (0.08)	2.01 (0.26)
Medial Mature (M)	55.01 (10.88)	4.6 (0.82)	8.66 (2.14)	0.24 (0.06)	0.2 (0.05)	2.3 (0.41)
Total Mature	52.65 (10.14)	4.3 (0.77)	8.42 (1.88)	0.24 (0.05)	0.22 (0.07)	2.15 (0.38)

Table 9. Mean and standard deviation (in brackets) of all bone structural index values for lateral, central and medial sections in young and mature sheep. Figures in bold indicate a statistical significance at $p<0.05$ (across like symbols).

SECTION	BV/TV %	BS/TV mm^2/mm^3	BS/BV mm^2/mm^3	Tb.Th mm	Tb.Sp mm	Tb.N #/mm
Anterior Young (A)	43.21 (8.29)	3.58 (0.33)	8.50 (1.46)	0.24 (0.04)	0.32 (0.07)	1.79 (0.16)
Posterior Young (P)	45.34 (10.02)	3.46 (0.51)	7.83 (1.27)	0.26 (0.03)	0.32 (0.10)	1.73 (0.25)

Table 10. Mean and standard deviation (in brackets) of all bone structural index values for anterior and posterior sections in young sheep. No statistically significant differences were found at $p<0.05$ (across like symbols).

SECTION	BV/TV	BS/TV	BS/BV	Tb.Th	Tb.Sp	Tb.N
Young Sheep						
lateral vs central	N	N	N	N	N	N
lateral vs medial	N	**YES**	N	N	N	**YES**
central vs medial	N	N	N	N	N	N
anterior vs posterior	N	N	N	N	N	N
Mature Sheep						
lateral vs central	N	N	N	N	N	N
lateral vs medial	N	N	N	N	N	N
central vs medial	N	N	N	N	N	N
Young & Mature Sheep						
lateral vs lateral	N	N	N	**YES**	N	N
central vs central	N	N	N	N	N	N
medial vs medial	N	N	N	N	N	N
all regions vs all regions	N	N	N	N	N	N

Table 11. Summary of statistical outcome between regional and age groups for all bone structural index values ($p<0.05$).

CHAPTER 4:

DISCUSSION

4.1 Introduction

In the literature, much has been published in the clinical and basic sciences on the growth of the TMJ. Many studies have utilised animal models to investigate changes in the tissue architecture instigated by orthodontic and surgical means. It is also important however, to look at normal tissues as they age naturally.

With increasing longevity, a potential increase in the incidence of degenerative joint diseases such as osteoarthritis may occur leading to a considerable morbidity and cost to society. These diseases usually involve both a loss of quantity, quality, and the ability of connective tissues to be sustained. It is thought that their genesis may occur in childhood when the cartilage and cancellous bone structure is developing under the influence of formative genetic and biomechanical factors (Byers et al., 2000).

The objective of this project was to look at aspects of age changes in normal tissue using the sheep as a model. Specifically, the aims were to qualitatively and quantitatively describe the structure of the condylar cartilage (including its thickness as well as cellular and matrix components) and trabecular bone indices. In addition a standardised protocol was developed and implemented to measure these structures. This is the first known project to have used the sheep as an animal model in order to histomorphometrically analyse these structures in young and mature animals. The relevance of this project is to further ameliorate the knowledge of the TMJ condyle during growth and development so that a better understanding of the structural changes that occur during disease processes can be gained to prevent and provide better clinical treatment for such diseases.

4.2 Findings of the study

4.2.1 Qualitative regional and ageing morphological patterns

At low magnification the articular surface covering the bony layer of the condyle in the sheep is comprised of a fibrous CT layer and a proliferative cell layer (deemed the FZ) as well as a hypertrophic cell layer (deemed the HZ). The FZ and HZ boundary was generally distinguishable in this study by the presence of a dense layer of flattened spindle shaped cells that transformed into an intensely stained ECM with enlarged circular cells, as Luder (1997) also described in the human.

The general cartilaginous structure and presence of both the FZ and HZ remained unchanged, except for the tapering of the cartilage at the ends of the articular surface where the HZ narrowed and disappeared as the FZ fused with the mucoperiosteum of the neck of the condyle. This was a feature consistent with Luder and Schroeder (1992) in the monkey and as Ma et al (2002a) in the sheep.

Qualitative studies have used histological methods to show various structural and metabolic changes of the condylar tissue occur in the guinea pig (Oberg et al., 1969), rat (Charlier et al., 1969), monkey (Carlson et al., 1978) and human (Oberg and Carlsson, 1979) with age. It was expected that qualitative differences would also be noted in the sheep. Some differences were noted in this study in regards to the FZ, HZ & TT proportions between different regions and different animals, particularly in the mature sheep (**Figure 23**). The central region of the mature sheep seemed consistently thinner than that of the lateral or medial regions. The articular surface often appeared more friable and undulated in the mature sheep (**Figure 23**) especially when compared with the young sheep (**Figure 24**). One young sheep had an unusually large medial FZ region which, although was not deemed to be pathological, was considered unusual. This could

have been the result of an increased load placed on this joint due to regional functional load differences.

Paulsen et al (1999) described the presence of the hypertrophic chondrocytes in humans up to 30 years of age suggesting that condylar growth potential existed up to this age. Luder (1998) however stated that in humans the hypertrophic growth cartilage had all but disappeared by the same age. In this study of sheep, the FZ and HZ layer comprising the active growth unit was found in all sheep suggesting that growth potential still exists in the sheep up to at least 4 years of age. Whether this growth potential remained indefinitely would be a case of further research using older animals.

In regards to the proportions of cellular and matrix components of cartilage, morphological variations were also seen. Some specimens displayed a highly cellular appearance, indicative of current growth whilst others had a more solid matrix architecture with chondrocytes having a smaller diameter, reflecting a condyle with less active growth (**Figure 25**). This was also found to be the case in humans by Luder in 1997. A greater qualitative variation tended to be seen in the mature age group as was previously found by Paulsen et al (1999). Examination of the Masson's trichrome stained specimens revealed little variation within the same animal for cartilage matrix and cellular components respectively as reflected by contrasting blue and red staining. Comparisons however, between the young and mature age groups did demonstrate some qualitative differences, particularly in regards to the colour saturation of the stains used (**Figure 24**).

Qualitative differences were noted in trabecular bone patterns of the condyle between young and mature sheep (**Figure 27**). Condylar trabeculae appeared thick and dense in

the young sheep with many small trabecular separations often displaying a poorly aligned connection of bony plates and rods. In the mature sheep however, the trabeculae tended to form longer and thinner cortical plates. Although the trabeculae still appeared denser, the more widely spaced trabeculae were usually aligned in a parallel fashion toward the articular surface. This is in agreement with other studies that noted trabecular bone structure changes with developmental age (Bergot et al., 1988; Feldkamp et al., 1989). Morphology of trabecular bone has also been shown to vary with anatomical location (Goldstein et al., 1993) which was also demonstrated in this study.

4.2.2 The thickness of condylar cartilage and the role of cartilage in load transfer

The cartilage thickness in the condyles of young and mature sheep appeared to be consistent with the histological observations. In regards to the HZ and FZ of the condyle, these measurements have not been performed in the literature. However the complete thickness of cartilage (equivalent to TT) has been performed. Ma et al (2002a) reported the total thickness of sagittal sections of the control sheep in his experimental study the order of 526.2μm. With regard to this experiment, a similar methodology was used to measure total thickness (ie from articular surface to SAB defined by vascularisation of tissues). In comparison the results from this study report a much thinner total thickness of both young and mature sheep (292μm and 289μm respectively). However, this project utilized 21 sheep for quantitation (11 young and 10 mature) whereas Ma and colleagues used only 8 sheep, with only serving 4 as controls. The findings are in close unity with those reported by McNamara and Carlson (1979) where they found an average thickness of 309.3μm for the thickness of cartilage in sagittal sections of their control group consisting of 14 animals.

Statistical analysis of the young sheep revealed only one significant regional difference between that of the lateral 143μm (45.9) and medial region 207μm (123.6) of the FZ. The explanation for this finding is due to one young sheep having a particularly large FZ which skewed the data. It is likely that all surfaces of the condyle are growing at an even rate and have only had a brief time in which the effects of loading during mastication have been employed. However, the mature sheep revealed a more consistent regional finding in regards to the thickness of the cartilage. All central zones were significantly thinner than either the lateral or medial sections for FZ, HZ and TT with the only exception being between the central and medial sections for HZ. Although this pattern could be due to excessive wear on the central surface of the joint from an increased load, it is much more likely that there is an increased load on the medial and lateral regions resulting in an increased growth response of the cartilage with a resultant increase in thickness of each of the zones. This explanation would be in accordance with the experimental studies of Ma et al (2002a) and McNamara and Carlson (1979) in regards to thickening of the condylar cartilage in response to an increased load (see below). Although comparisons cannot be made antero-posteriorly the results from the young sheep are very similar with the FZ and TT however being slightly thinner than for the latero-medial regions of the young sheep.

Interestingly, there was no thickness variation was found between young and mature sheep for any similar region or total zone the FZ, HZ or TT. This differs to the study on human autopsy specimens by Paulsen et al (1999) in which it was reported that a statistically significant correlation existed between age and fibrocartilage thickness ($r = -0.48$, $p<0.05$). The findings of this project are in some correlation with Luder's (1998) findings in that noted no significant differences in the latero-medial dimension of the human condyle with age in a semiquantitative light microscopic study. However,

Luder (1998) also noted that after 15-30 years of age the HZ had disappeared. This was not the case in the sheep although may have been so with older animals (4 years and above).

The results of this study on the thickness of condylar cartilage can potentially be explained in relation to its roles. Although articular cartilage serves as a load-bearing elastic material that is responsible for the frictionless movement of the surfaces of articulating joints (Huber, 2000), it only absorbs a negligible amount. It is predominantly a load transmitter which distributes load to the underlying bone (Standlee et al., 1981). The experiments performed by Ma et al (2002a) show the importance of cartilage in performing this role.

Ma and colleagues (2002a) found that when a functional appliance created an increase in loading of the joint by forward mandibular displacement in sheep, the average total thickness of the cartilage (proliferative and hypertrophic) in the anterior region of the condyle increased from 401.3μm in the control group to 538.3μm in the experimental group. Furthermore, the intermediate and posterior regions only showed an 11.6μm and 15.2μm variation between the groups respectively. They concluded however, that while the observed increased thickness might be the result of a changed rate of cell differentiation, the reason for thickening of the condylar cartilage was unclear. This was also shown to be the case in rats by Kantomaa (1984). No significant findings were found in relation to the thickness of condylar cartilage in the anterior or posterior coronal sections in young sheep in this study, although this is not surprising since no external influence to create loading of the condyle was performed. However, natural forces during mastication (up to 914N being reported by Finn, 1995) still occurred. With age, the TT of cartilage was still maintained (289μm for mature sheep compared

with 292μm for young sheep) also suggesting along with Standlee et al (1981) that cartilage is not only important for growth but is required for load transfer to the trabecular bone of the condyle.

The standard deviation associated with all of the regional and total measurements varied form 24.1-123.6μm. In regards to the variability of linear measurements using ImageJ 1.33u, the measurement error for condylar cartilage thickness was estimated to be 12.16μm for the FZ and 13.01μm for the HZ (see Appendix VI). This indicates that it is not the methodology that created large standard deviations seen in the results from measurement error but in fact the true variability of the thicknesses associated within each individual sheep. Thus, image analysis systems provide an efficient and accurate method for determining the various thicknesses of condylar cartilage zones.

4.2.3 The quantity of cellular and matrix components in condylar cartilage and its growth potential

Few studies have quantitated the condylar cartilage for its proportions of cellular and matrix components. The most recent study by Leidhold et al (2004) investigated this measurement in six domestic pigs (0-24mths) using H&E stained sections. This study used a measuring grid and stereological calculations from the average sectional area and number of cut cells per unit area to determine this. Their results showed that up until puberty the cell volume makes up the predominant contribution to cartilage in the domestic pig compared with the matrix (2.55:1, cell:matrix). However when late pubertal stage is reached then matrix synthesis exceeds the cell volume (0.91:1, cell:matrix). Similar results have been found in rats (2:1, cell:matrix during growth falling to 0.6:1, cell:matrix with declining growth dynamism) (Luder, 1994). However, this measurement seems to be species dependent with the monkey (Bosshardt-Luehrs and Luder, 1991) having predominant matrix synthesis (1:3, cell:matrix).

Unlike previous research, the present study used an image analysis system to measure contrasting colours representative of the cellular and matrix components. The methodology, relevance and accuracy for the novel use of using a modified blue Masson's trichrome for measuring this feature of condylar cartilage in the present study will be further discussed in Chapter 4.4.3 and also see Appendix I.

As a result of other reported changes in growth potential of cartilage from other sites in the human (Rodriguez et al., 1992; Byers et al., 2000), a high proportion of matrix with a low cellularity was predicted in the mature sheep condyle. Byers et al (2000) also reported that with increasing age, there is a decrease in the growth plate volume (ie reduction of proliferative and hypertrophic zone thickness) in long bones most evident in the first year of postnatal life. It was also noted that there was an increased production of matrix with a corresponding decrease in cell number and chondrocyte lacunae profile diameter at later ages. This is a coordinated developmental process whereby growth during childhood continues until a peak bone mass and trabecular structure conducive to the biomechanical requirements of the adult is achieved.

This study however, demonstrates that there is firstly no decrease in the thickness of cartilage with age in the sheep, but also that there is only a mild trend and not a significant increase in matrix production (37.4 to 41.6%) or decrease in cellularity (62.6 to 58.5%). Although comparisons cannot be made antero-posteriorly, the results from the young sheep are very similar and are within the range for the latero-medial regions of the young sheep (34.8-42.4% for matrix and 57.6-65.2% for cellularity). The results of this study support those of (Bosshardt-Luehrs and Luder, 1991) in the monkey but are dissimilar to those which studied the pig (Leidhold et al., 2004) and rat (Luder, 1994) suggesting that species variation as well as age have an effect on the proportions of

cartilage matrix and cellular levels. The results of this study also reflect the conclusions of Paulsen et al (1999) in that the condyle of the human still has growth potential in the adult (up to the age of 30 years) although there was some minimal decrease with age.

4.2.4 Regional and age differences of trabecular bone in the condyle and its role in load resistance and load dispersion

The architecture of trabeculae in arthrodial joints predominantly reflects the stress trajectories imposed on the articular surface. Further, the trabecular bone remodels to adapt and resist the average external force applied. It assumes a morphology that is optimal for the flow of force applied to the bone (Croucher et al., 1996; Nakajima et al., 1998). On the presumption that any load applied across the TMJ is directed radially through the condylar head, the histology (**Figure 27**) illustrates this impression.

Changes in trabecular structure occur with developmental age (Bergot et al., 1988; Feldkamp et al., 1989). Such changes from a plate-like structure to a denser rod-like pattern have been reported with increasing age in human vertebrae (Bergot et al., 1988; Feldkamp et al., 1989; Ding et al., 1997). Physical properties of trabecular bone have also been shown to vary with anatomical location (Goldstein et al., 1993). Other studies have demonstrated a decrease in trabecular bone density in the mandibular condyle and a reduction of trabecular width in edentulous specimens as compared with dentulous specimens (Hongo et al., 1989a) as well as with advancing age (Hongo et al., 1989b). The parallel plate model of bone (Parfitt et al., 1983) was adopted as the basis for quantitation of mandibular condyles in this study.

The bone volume densities in the condyles of young and mature sheep were within the ranges of 55-63% and 50-55% respectively which appear to be consistent with the histological observations. These were larger than the ranges reported elsewhere for bone

volume density in human condyles (17-30%) (Hongo et al., 1989b; Kawashima et al., 1997; Giesen and van Eijden, 2000).

As a result of developmental changes that will have occurred in mature sheep, a lower bone volume density might be predicted in young sheep. However, the mature sheep condyles showed no such age related change. Indeed, these findings in the model sheep accord with a histomorphometric study of the human mandibular condyle where no significant differences occur in trabecular structure with age (Hongo et al., 1989b). Although Paulsen et al (1999) found a moderately statistical correlation between bone volume and age in 20 autopsy samples from humans aged 18-31 years ($r = -0.52$, $p<0.05$). The bone surface density and the bone surface to bone volume ratio were greater in the mature sheep than in the young sheep, which again, is in accord with the qualitative observations. Also, in the young sheep, there was a significant variation in the bone surface density between the lateral ($3.82mm^2/mm^3$) and medial sections ($4.43mm^2/mm^3$) of the condyle. This is accounted for by the bone volume density being greatest in the lateral region (63%) of young sheep. One interpretation of this anatomical feature may be explained as a result of an overall lateral growth pattern of the developing sheep's condyle with an associated requirement for condylar strength in this area from a presumed greater magnitude of forces. However, the data cannot predict the nature of these forces and whether they are muscular or tortional due to mastication.

The mean trabecular thickness in the young sheep (0.28mm) and in the mature sheep (0.24mm) corresponded well with the interspecies ranges reported elsewhere for human (0.27-0.34mm) (Hongo et al., 1989b; Kawashima et al., 1997) and pig (0.23-0.27mm) (Teng and Herring, 1995). However, another study on humans reported a much lower value (0.10mm) (Giesen and van Eijden, 2000). In humans, trunk and limb bone

trabeculae often decrease in thickness with age (Bergot et al., 1988). Such a generalised phenomenon may explain the 0.04mm trabecular thickness difference seen between the young and mature sheep. Furthermore, the significance of the variation that occurred between the lateral regions of the young (0.33mm) and mature (0.25mm) sheep may be due to an increase in muscle force acting upon this anatomical region during growth.

The mean trabecular separation in young sheep was 0.20mm as compared with 0.22mm in the mature sheep. Although age does not appear to significantly vary trabecular separation in the sheep, these values are small in comparison with those reported in the human (mean of 0.53mm) (Giesen and van Eijden, 2000). However, similarities do occur with those reported for the pig (0.23-0.27mm) (Teng and Herring, 1995). Decreased trabecular separation (or increased trabecular thickness) may suggest that in both the sheep and the pig, the forces achieved are either much more powerful over an extended usage (sheep chew for up to 23 hours per day) than those achieved by humans or are related to the developmental status in respect of secondary dentition in these animals. Finn (1995) found a maximum TMJ reaction force of 914N in sheep compared to 500N in the human. These increased forces could generate greater loads across the sheep and pig condyles, explaining the need for an increased trabecular thickness and decreased trabecular separation (Mongini, 1983).

In the young sheep, there was a significant variation in the trabecular number between the lateral (1.91/mm) and medial sections (2.21/mm) of the condyle. The trabecular number (2.04/mm in young sheep and 2.15/mm in mature sheep) was also greater when compared with that reported for the human condyle, namely, 1.66/mm (Giesen and van Eijden, 2000) and 1.8/mm (Feldkamp et al., 1989). Interestingly, as for the thickness and separation of trabeculae, the range reported for trabecular number in the pig condyle

(from 2.4-2.9/mm) (Teng and Herring, 1995) is also in accordance with the sheep. This further supports the notion that an increased number and thickness of trabeculae with a resultant decrease in separation corresponds to an increase in loading on the joint.

Underneath the articular surface, the cortical shells of most trabecular bone regions contribute little to the stiffness and strength of the structure. The complex arrangement of trabecular bone beneath the cortical shell deforms easily during loading allowing the forces that could damage the cartilage layer to be absorbed. Moreover, these loads can be redistributed and transferred to the thicker reinforced cortical plates. Various studies have reported a high bone volume density in the superior regions of the condyle adjacent to the articular surface (Hongo et al., 1989b; Giesen and van Eijden, 2000). Functional stresses have been previously shown to concentrate in the human condylar neck, but appear to be dissipated within the broader elliptical condylar head (Standlee et al., 1981). This questions the issue of whether the condyle is designed to receive light varied forces rather than heavy cyclical unidirectional forces. If so, is this the case in the sheep? Thus, the TMJ condyle should not be considered as a static morphological structure but rather viewed as a dynamic functional unit with many component parts which are subordinate to different sets of forces.

4.3 Validity of the study

4.3.1 Animals and specimens

The main aim of the present study was to compare histomorphometric data obtained from cartilage and trabecular bone of the TMJ condyle in young and mature animals using the characterized sheep model (Bosanquet and Goss, 1987). In regards to the sheep used in the study, the animals, age, habitat and diet were all considered and standardised as much as possible.

Skinned Merino sheep heads were obtained fresh and collected together at the same time of year and within twenty four hours of the animal being killed. These whole sheep heads were then delivered, intact and fresh to the experimental laboratory to avoid the use of a transport medium which could have artefactually shrunken cellular size in the cartilage. Also, the condyle remained enclosed as part of the joint until dissection, minimizing the time that the condylar tissues were left outside of their natural environment before fixation.

In regards to determination of age, the true chronological age of the animals was not known although the usual method of determining the age of sheep is from the teeth (May, 1970). Generally, the age of each animal was determined by assessing its level of dental development with respect to the erupted mandibular teeth present (**Table 1**). This provided a consistent method to age the animals with the young group having a range of 10 ± 2 months and the mature group ranging between 3 years ± 6 months. The term mature was adopted rather than the term old, as a sheep can live for 10 years and beyond. This group of sheep were not old but were mature however, as they had passed puberty which is around 60 weeks in sheep (Karaharju-Suvanto, 1994). Thus, both

groups of animals had no overlap of ages with a considerable age gap between them, but without a vast variation within the mature group.

The sheep used in this study were not segregated according to sex on an untested assumption that no gender discrepancy would be seen in the structure of the TMJ condyle, similar to that reported for humans (Wish-Baratz et al., 1996). However, cranial breadth measurements were not taken into consideration which may have had an effect on the size of the condyles and corresponding measurements. It was felt that age and not size of the joint was more likely to produce morphological variations within the condylar tissues studied.

The animals' habitats were also standardised as much as possible. All animals were reared in local regional pastures which do not have a large variation in climate and thus provide a consistent source of food, limiting variability in constant chewing and thus loading of the TMJ with season. Sheep were not used from remote areas as these areas are prone to both floods and droughts.

Diet was also considered an important variable in this study as differing hardness of foodstuffs could have an impact on the amount of load and corresponding joint stress and expected chewing patterns sustained by each animal. This factor was standardized such that all specimens came from sheep that were grass fed animals. No grain or concentrates were additionally supplied in supplement to their grazing so as to minimise bias in chewing patterns and loading on the TMJ.

An important reason why the sheep was used as the animal model is that as previously discussed, the TMJ of the sheep is of similar size to those of man (Bosanquet and Goss,

1987). Unfortunately, larger animals mean higher cost. The sample size affects the statistical significance and therefore this study which used 22 animals does not have as much power as one which used 100+ rodents. However, the larger condyle did allow for the ready application of histomorphometrical methods for detailed quantitative analysis using the sheep as compared with rodents that have a tiny condyle.

4.3.2 Tissue sampling

When removing the joints, great care was taken not to damage them. Also, standard protocols for fixation (Appendix II), demineralization and processing (Appendix III) were followed to. In the case where an incidental neoplasm was found affecting the structure of the joint in one young sheep (**Figure 16**), this animal was eliminated from the study.

As in all biological tissues, growth and remodelling is a dynamic process. The increase in the average volume of matrix and cellular volumes in relation to the individual cartilage zones is a dynamic process, with measurements of the tissues reflecting only a snapshot (Leidhold et al., 2004). This of course is unavoidable and longitudinal studies are not possible where removal, dissection and analysis of both condyles are required.

Previous studies have used the coronoid process as a reference point for dissection of the condyle into sagittal blocks (Ma et al., 2002ab). In order to standardise the location of the sagittal dissections in this study, the dissection was performed consistently such that the central cut was made in the centre of the head of the condyle, whilst the lateral and medial cuts were made 5mm in from the respective sagittal edges (**Figure 13**). This allowed for comparisons between different regions within each of the two age groups, as well as between each of the groups. The condyles dissected into anterior and posterior

coronal blocks were made consistently using a logical approach such that the dissections divided the head of the condyle into equal coronal thirds (**Figure 14**).

To improve the present study, it would have been useful to histomophometrically compare cartilage and trabecular bone in the coronal plane between young and mature sheep, similar to that performed in this study in the sagittal plane. Unfortunately this was not possible due to lack of animal material available.

No differences were found between the left and right hand sides of the condyle for any bone index value in a study by Ma et al (2002b). Based on the findings of these previous studies symmetry of the joints was not assessed in the current study. Nevertheless, it would have been interesting to look for asymmetry in the thickness and matrix to cellular proportions of the condylar cartilage.

4.3.3 Staining techniques

To achieve accurate results when quantitating 5μm sections of condylar cartilage and trabecular bone using an automatic image analysis system, two types of Masson's trichrome staining techniques were used. These provided a wide degree of histological contrast with collagen in the cartilage and bone staining intensely with good colour differential between tissue components (**Figures 22 & 26**). The Haematoxylin-Eosin/Phloxine stain (H&EP) that was used for initial assessment provided good intensity and definition of the tissues but not the degree of contrast needed to provide a grey phase to distinguish between the tissue elements as well as that of the background (**Figure 15**).

The standard light green and ponceau-fuchsin Masson's trichrome provided good contrast against the background of the section when quantitating the trabecular bone patterns (**Figure 26**). The modified aniline blue and ponceau-fuchsin Masson's trichrome technique (see Appendix V) however, not only provided a better contrast between the cartilage and bone (**Figure 22**) but also between the blue cartilage matrix and the red cellular components of the condylar cartilage (**Figures 23, 24 & 25**). Also no blue/black staining of the nuclei of chondrocytes was seen indicating that this novel staining technique provides an accurate method for quantitating the proportions of cartilage matrix and cellular components when using an image analysis system.

4.3.4 Histological parameters and definitions

Determining the regions of cartilage and trabecular bone was one of the first important steps in histoquantitating the stained specimens. A judgment was required by the operator in determining the different zones of condylar cartilage and the cortical boundary of the trabecular bone. To minimize any variability, consistent cartilaginous zones (**Figure 17**) were defined according to the structure of the cartilage layers visualized as well as being adapted to those described in previous studies (McNamara and Carlson, 1979; Luder, 1997; Ma et al., 2002a). Similarly, this was the case for the cancellous-cortical bone margin (Hongo et al., 1989ab; Kawashima et al., 1997; Ma et al., 2002b) with structural bone index values (**Table 2**) measured according to those described by Parfitt et al (1983).

Nevertheless, some zones of cartilage (**Figure 25**) and trabecular bone (**Figure 18**) were not as well defined in some specimens as others. Fortunately, these cases were not common and are unlikely to have any significant effect on the overall results. Differences in histological interpretation did occur for both the same operator as well as

between different operators, but were proven to be non-significant (see Appendix VIII). With increased experience it is likely that more consistent measurements were achievable, such that measurements performed early in the study were probably responsible for the small discrepancies seen, especially for the intraobserver variability.

4.3.5 Image analysis and histomorphometry

Inaccuracies can occur with any measurement. During quantitation using the Quantimet 500MC (**Figure 19**) and public domain software programme (ImageJ 1.33u), over or under measurement of the cartilage and trabecular bone parameters could have been performed by the operator. This was taken into consideration when determining how best to measure these tissues prior to quantitation. With regards to cartilage, the measurements for thickness were consistently taken at the region of the most prominent point of the external surface for each of the zones. They were also measured perpendicular to the articular surface but not within 1mm of each end according to that described previously (McNamara and Carlson, 1979; Ma et al., 2002a). The measurement of cellular and matrix proportions of the cartilage also used the same digital photomicrograph as that used for the thickness, with a consistent width of 500μm being used (**Figure 20**). Slight over-estimative effects in the region of cell and matrix boundaries and the resulting minimal inaccuracies in cell diameter and tissue structure were unavoidable with sections of 5μm in thickness as also noted by Leidhold et al (2004). The accuracy however, of these values was further improved as the measurements were taken at three points along the condylar cartilage surface for every section giving greater confidence to the results. In regards to the trabecular bone, a line of best fit was traced around its boundary and a line of best fit was deduced when the boundary became unclear. Although the ascertainment of absolutely correct values is

virtually impossible with any form of measurement, these factors may help to produce a more accurate measurement.

As well as concerns related to interpretation of tissues, there were a number of other potential problems that were addressed. The detection of contaminants or artefact of tissues (such as the folding of tissues) from the preparation of specimens sometimes occurred. All sections were visualised prior to measurement with minor blemishes or artefact being digitally edited (excluded) from the measurement. Where a section was deemed to be unsatisfactory, a new specimen was produced. Magnification was kept consistent (cartilage at 200x, trabecular bone at 25x), to ensure that magnification bias remained consistent with only random error occurring. Of course this is only true if the operator error is not of significance, so intraobserver and interobserver measurements were performed and statistically analysed using random sections against the original measurements. No significant differences were found indicating that the quantitation of condylar cartilage thickness, proportions of cellular and matrix components, as well as measuring trabecular bone indices using the Quantimet 500MC can be performed accurately and consistently.

4.4 Epilogue and future directions

This study is the first to produce qualitative morphological features and histoquantitative data of the condylar cartilage and trabecular bone TMJ of both young and mature sheep. The information presented in this thesis has further added to the international literature known about the growth and development of the condyle and the role of the sheep as an animal model in studies of the TMJ.

However, a number of areas evolving from this study are still in need of further investigation. Lessons learned from this experiment will hopefully allow further research and an improved design to better understand the growth and development of the sheep condyle. By improving our knowledge through such models as the sheep, better treatment through orthodontic and surgical means can be provided to patients who have growth and developmental problems as well as those that have degenerative conditions. Some future directions that have evolved from this research project are:

- It would be a good complimentary study to use animals which had similar weights (and corresponding size) of the TMJ to see if these had any influence on the cartilage parameters and bone indices measured.

- Sections cut in the transverse (horizontal) plane were not used in this study. It would be interesting to see if there are differences both within age groups as well as comparing between young and mature sheep.

- It would be interesting to see if there was any individual asymmetry between the LHS and RHS joints of the sheep.

- Cortical bone was not assessed in this study and if analysed would provide a complete picture of the TMJ during growth and development.

- The comparison of different stains for quantitative purposes involving cartilage and bone of the sheep condyle would be a novel study to determine which stains are best for image analysis systems such as the Quantimet 500MC.

- In this study it was not possible to distinguish histologically between intramembranous and endochondrally ossified bone. Further investigation using immunohistochemistry (eg for collagen type X) to identify intramembranous bone or areas not endochondrally ossified could confirm (or deny) that the bone formation in the condylar head is completely endochondrally ossified in the sheep as previous studies have suggested.

- The use of fluorochromes (eg Calcein, tetracycline and alizarin red S) could provide information regarding the rate of growth at a particular age and the level of remodelling occurring in the young and mature sheep respectively.

SUMMARY

(1) This project supports the notion that the sheep is a useful animal model in studies of the TMJ, especially for those involving the effects of growth and development on the morphological architecture of the condyle.

(2) A staining protocol using a modified aniline blue Masson's trichrome stain was developed which enhanced and enabled the histoquantitation of the cartilage matrix and cellular components. A regular light green Masson's trichrome was also shown to be useful for the delineation of trabecular bone and its histoquantitation.

(3) Qualitative morphological variations of both cartilage thicknesses and matrix and cellular components were noted in both young and mature age groups.

(4) There was no significant reduction of the thickness of cartilage with age in the condyle of the sheep.

(5) There was a significant decrease in the thickness of the FZ, HZ and TT of the central region as compared to the lateral and medial regions in the mature sheep. This is a combination of both an increased thickness of the cartilage zones of the poles of the TMJ (from increased loads and cartilage production) as well as a decrease in thickness in the central region (decreased cartilage production and increased wear).

(6) A trend was discovered showing a lower condylar cartilage cellular component (increased matrix) in the mature sheep as compared with that of the young sheep.

(7) A high cartilaginous cellularity still exists in the mature sheep indicative of continuing growth and regeneration potential of the TMJ even into adulthood.

(8) Qualitative morphological changes with age were evident in the trabecular bone architecture with plates aligning in a parallel fashion toward the articular surface interconnected by rods compared with that of the young sheep where a more a haphazard appearance was evident.

(9) There was a significant concordance in the histomorphometric bone structural index values between various coronal and sagittal anatomical regions within both young and mature sheep age groups.

(10) There was a significant concordance in the histomorphometric bone structural index values between the two age groups for similar anatomical regions suggestive that the qualitative changes present are the result of remodelling of bone to load rather than a variation in the quantity of bone that changes with increasing age.

APPENDICES

APPENDIX I

NOTES ON DYES COMMONLY USED IN MASSON'S TRICHROME STAINS

Ponceau 2R

Ponceau 2R has a spectral curve absorption maximum at approximately 499-504nm and transmits red light in its greatest colour density. Ponceau 2R is a monoazo dye and has been used classically as a histological counterstain in the Masson (1911) technique. Acid fuchsin has also been added to the ponceau 2R original dye to become a popular working plasma stain for the Masson's trichrome technique (Lillie, 1969).

Acid Fuchsin

Acid fuchsin owes its acid character to the fact that it is a sulfonated derivative of basic fuchsin. Acid fuchsin is a triaminotriphenylmethane (rosanilin) derivative of the triphenylmethane subdivision of the arylmethane group of dyes. By itself is a widely used plasma stain (as an acid dye it stains basic components), which has been recommended for a number of special uses. The best known is the Van Gieson connective tissue stain, which it is used with picric acid after haematoxylin to differentiate smooth muscle from CT. To the pathologist however it has been valuable as a constituent (with aniline blue and ponceau) of the Mallory connective tissue stain, but more importantly, combined with ponceau as a primary plasma stain in the Masson's trichrome technique. This working stain is more popular as the combination of dyes has a greater affinity for the basic components in the cytoplasm as compared with just the original Ponceau 2R stain, providing better contrast and better permeability of the dye (Lamar Jones, 2002).

Light Green

In regards to the fiber stain, light green was originally used by Masson in the 1911 technique. Light green is a diaminotriphenylmethane derivative of the triphenylmethane subdivision the arylmethane group of dyes. Light green has a spectral curve absorption maximum at 629-634nm and reflects green light in its greatest colour density. It is a derivative of brilliant green which is sulfonated and is therefore and acid dye. Light green is a valuable plasma stain often used for staining animal tissues in contrast to nuclear dyes. It photographs well. In pathologic history it finds its most important use as the collagen fiber stain in the Masson's trichrome modification of the Mallory aniline blue method. However, its greatest drawback is its lack of permeance (Lillie, 1969).

Aniline Blue

Aniline blue has also been used as a fibre stain as part of the Masson's trichrome technique. It is similar to light green but is a triaminotriphenylmethane (rosanilin) derivative of the triphenylmethane subdivision of the Arylmethane group of dyes. It has a spectral curve absorption maximum at approximately 600-610nm and transmits blue light in its greatest colour density. On account of the sulfonic groups, this dye is strongly acidic and thus makes a good counterstain. It is best known in histology for its counterstaining in the Mallory's aniline blue CT stain technique but also provides a useful alternative to the light green counterstain as it has better permeance (Lillie, 1969).

Phosphomolybdic Acid (PMA)-mordant

A critical element to generate a highly contrasting Masson's trichrome stained section is to firstly ensure that a mordant is used and is at a sufficient concentration. In

discussing the mechanism of differential staining of collagen and other CT components by the Masson trichrome procedure, Baker (1958) noted that the background dye is displaced by phosphomolybdic acid (PMA) so that collagen is coloured by the subsequent applied counterstain of light green or aniline blue. To ensure the weakening of the positive tissue and negative ponceau/fuchsin dye bonds in order to ensure uptake of the counterstain a mordant like 4% PMA is used. When a section is first treated with a levelling or plasma dye and then with PMA, this acid competes with the dye and gains access to the positively charged groups on the collagen easily, expelling the dye in the process. If treatment is stopped at the right time, only non tensile collagen will be free to stain when treated with a milling or fiber stain (Lamar Jones, 2002). Another important factor to achieve good contrast is to ensure that the counterstain used is effective at replacing the weakened primary-tissue bond such that only the strongest bonds maintain the primary dye. This is why fiber stains such as light green and aniline blue are used (Flint et al., 1975).

APPENDIX II

FIXATIVE SOLUTION

10% Buffered Formalin

Reagent Formulae

40% Formaldehyde	100ml
Distilled Water	900ml
Sodium dihydrogen phosphate monohydrate	4g
Disodium hydrogen phosphate anhydrous	6.5g

APPENDIX III

TISSUE PROCESSING PROTOCOL

Tissues were processed with the Shandon Citadel 2000® tissue processing unit according to the following protocol:

Container 1	10% Formalin	0.5 hours
Container 2	70% Alcohol	1 hour
Container 3	80% Alcohol	1 hour
Container 4	90% Alcohol	1 hour
Container 5	100% Alcohol	1 hour
Container 6	100% Alcohol	1 hour
Container 7	100% Alcohol	1 hour
Container 8	Histolene®	2 hours
Container 9	Histolene®	2 hours
Container 10	Wax	3 hours
Container 11	Wax	3 hours

(Histolene® is a registered product by Fronine Pty. Ltd., NSW, Australia)

APPENDIX IV

SLIDE SUBBING PROTOCOL

Slides were subbed using APT (3-amino propyltriethoxysaline) Sigma Cat. No. A3648.

Requirements (per run of 175 slides for APT coating):

- 175 glass slides in 7 clean black plastic racks soaked in Extran® (Merck Pty Ltd, Australia) and rinsed in free running tapwater for 20 minutes.
- 1800mls ethanol.
- One 300ml square glass container for 2% APT solution.
- Three disposable plastic containers for ethanol rinsing.

Preparation:

1) Check slides for scratches or marks, discard any imperfect slides.
2) Place good slides in clean black plastic racks.
3) Soak slides overnight in Extran® detergent in a 5 litre tub.
4) Wash slides in several changes of free running tap water for 20 minutes.
5) Place 500mls of ethanol in each of the three disposable containers.
6) Place 6mls of APT into the square glass container. Place the remaining 300mls of ethanol in the glass container.

Method:

1) Drain the rinsed slides but do not allow to dry.
2) Dip and swish 5 times in the first ethanol container.
3) Dip and swish 5 times in 2% 3-APT solution.
4) Dip and swish 5 times in the last two ethanol containers.
5) Drain well, dip in a final wash of distilled water.
6) Drain slides well.
7) Dry slides in an oven at 37 C°.

APPENDIX V

a) PROTOCOL FOR HAEMATOXYLIN AND EOSIN-PHLOXINE

Sections

Formalin fixed sections decalcified in Ethylene-Diamine Tetra-Acetic acid (EDTA)

Embedded in paraffin and cut using a microtome at 5 μm

Positive control used for all tests

Method

1) Place cut sections in a heater rack to melt the paraffin wax and to achieve better adhesion of the tissue to the slide
2) Decerate any residual wax by using a series of two xylene solutions for 4 minutes and 3 minutes respectively
3) Dehydrate the sections by placing in a series of alcohol solutions (absolute alcohol for 3 minutes, 95% alcohol for 3 minutes then 70% alcohol for 3 minutes)
4) Wash gently in running tap water for 1 minute
5) Rinse in distilled water and check for complete removal of wax and xylene
6) Stain with Mayer Lillie Haematoxylin for 10 minutes
7) Wash in running tap water for 4 minutes
8) Differentiate in 0.5% HCl acid alcohol solution (2 dips)
9) Rinse well in running tap water for 3 minutes
10) Blue sections in Scott's tap water (3 dips)
11) Rinse well in running tap water for 3 minutes
12) Rinse in 70% alcohol for 3 minutes
13) Stain with Eosin-Phloxine for 2 minutes

14) Dehydrate in a series of alcohol (95% alcohol then two absolute alcohol solutions) for 2 minutes each

15) Clear in a series of two xylene solutions for 2 minutes

16) Mount sections with coverslips using a depex adhesive

Reagent Formulae

Lillie-Mayer's Haematoxylin:

Aluminium ammonium sulphate	200g
Haematoxylin	20g
Ethanol	100mls
Sodium iodate	4g
Glacial Acetic acid	80mls
Glycerol	1200mls
Distilled water	2800mls

Alcohol Acetified Eosin-Phloxine solution:

1% Eosin	50ml
1% Phloxine B	5mls
95% Alcohol	390mls
Glacial acetic acid	2mls

Scott's Tap Water:

Potassium Bicarbonate	2g
Magnesium Sulphate	20g
Distilled Water	1000mls

Results

Collagen = pink

Erythrocytes = cherry red

Acidophilic cytoplasm = pinky-red

Basophilic cytoplasm = purple

Nuclei =blue

APPENDIX V

b) PROTOCOL FOR MASSON'S TRICHROME (RED/GREEN WITH NUCLEAR STAIN)

Sections

Formalin fixed sections decalcified in Ethylene-Diamine Tetra-Acetic acid (EDTA)

Embedded in paraffin and cut using a microtome at 5 μm

Positive control used for all tests

Method

1) Place cut sections in a heater rack to melt the paraffin wax and to achieve better adhesion of the tissue to the slide
2) Decerate any residual wax by using a series of two xylene solutions for 4 minutes and 3 minutes respectively
3) Dehydrate the sections by placing in a series of alcohol solutions (absolute alcohol for 3 minutes, 95% alcohol for 3 minutes then 70% alcohol for 3 minutes)
4) Wash gently in running tap water for 1 minute
5) Rinse in distilled water and check for complete removal of wax and xylene
6) Stain with Harris Haematoxylin for 5 minutes
7) Wash in running tap water for 4 minutes
8) Rinse in 1% v/v acetic acid (poured generously over slide)
9) Stain with 1% Ponceau/Fuchsin solution in 1% acetic acid for 2 minutes
10) Rinse in 1% v/v acetic acid (poured generously over slide)
11) Mordant in 4% aqueous phosphomolybdic acid for 2 minutes
12) Rinse in 1% v/v acetic acid (poured generously over slide)
13) Stain with 2% light green in 2% acetic acid for 2 minutes
14) Rinse slides in 1% v/v acetic acid (poured generously over slide)

15) Dehydrate in a series of alcohol (90% alcohol then two absolute alcohol solutions) for 2 minutes each

16) Clear in a series of two xylene solutions for 2 minutes

17) Mount sections with coverslips using a depex adhesive

Reagent Formulae

Harris Haematoxylin:

Aluminium ammonium sulphate	50g
Haematoxylin	2.5g
Absolute Alcohol	50mls
Distilled water	500mls
Mercuric Oxide	1.5g
Glacial Acetic Acid	20ml

Ponceau-Fuchsin

Ponceau 2R	0.7gm
Acid Fuchsin	0.35gm
Distilled Water	100mls
Glacial acetic acid	1.0mls

Light Green

Light Green	2.0gm
Distilled Water	100mls
Glacial acetic acid	2.0mls

Results

Collagen, cartilage, mucin and basophil granules = Green

Cytoplasm, muscle and acidophilic granules = Red

Nuclei = Blue black

APPENDIX V

c) PROTOCOL FOR MASSON'S TRICHROME (RED/BLUE WITHOUT NUCLEAR STAIN)

Sections

Formalin fixed sections decalcified in Ethylene-Diamine Tetra-Acetic acid (EDTA)

Embedded in paraffin and cut using a microtome at 5 μm

Positive control used for all tests

Method

1) Place cut sections in a heater rack to melt the paraffin wax and to achieve better adhesion of the tissue to the slide
2) Decerate any residual wax by using a series of two xylene solutions for 4 minutes and 3 minutes respectively
3) Dehydrate the sections by placing in a series of alcohol solutions (absolute alcohol for 3 minutes, 95% alcohol for 3 minutes then 70% alcohol for 3 minutes)
4) Wash gently in running tap water for 1 minute
5) Rinse in distilled water and check for complete removal of wax and xylene
6) Rinse in 1% v/v acetic acid (poured generously over slide)
7) Stain with 1% Ponceau/Fuchsin solution in 1% acetic acid for 2 minutes
8) Rinse in 1% v/v acetic acid (poured generously over slide)
9) Mordant in 4% aqueous phosphomolybdic acid for 2 minutes
10) Rinse in 1% v/v acetic acid (poured generously over slide)
11) Stain with 2.5% aniline blue in 2.5% acetic acid for 2 minutes
12) Rinse slides in 1% v/v acetic acid (poured generously over slide)
13) Dehydrate in a series of alcohol (90% alcohol then two absolute alcohol solutions) for 2 minutes each
14) Clear in a series of two xylene solutions for 2 minutes

15) Mount sections with coverslips using a depex adhesive

Reagent Formulae

Ponceau-Fuchsin

Ponceau 2R	0.7gm
Acid Fuchsin	0.35gm
Distilled Water	100mls
Glacial acetic acid	1.0mls

Aniline Blue

Aniline Blue	2.5gm
Distilled Water	100mls
Glacial acetic acid	2.5mls

Results

Collagen, cartilage, mucin and basophil granules = Blue

Cytoplasm, muscle and acidophilic granules = Red

APPENDIX VI

STATISTICAL ANALYSIS: MEASUREMENT ERROR

Variability of linear measurements
Measurements of Cartilage thickness using ImageJ 1.33u

$$S = \sqrt{\sum d^2 / 2n}$$

S = Measurement Error
d = Difference between the repeated measurements
n = Number of repeated measurements

FZ 1	FZ 2	FZ Difference	HZ 1	HZ 2	HZ Difference
190	191	1	76	79	3
211	216	5	62	67	5
177	179	2	67	69	2
145	154	9	97	93	4
151	155	4	84	80	4
196	193	3	99	105	6
166	164	2	58	60	2
87	84	3	62	56	6
123	119	4	54	56	2
183	185	2	104	101	3
153	157	4	111	113	2
72	75	3	61	58	3
74	76	2	57	63	6
75	72	3	51	55	4
71	66	5	66	63	3
60	63	3	88	87	1
75	74	1	83	81	2
93	86	7	81	78	3
69	67	2	91	96	5
167	162	5	79	71	8
84	85	1	78	85	7
76	73	3	67	71	4
92	97	5	86	85	1
127	130	3	96	94	2
114	110	4	78	82	4
		Sum of Diff = 86			**Sum of Diff = 92**

d = 86 microns
n = 25 times

S = 12.16 microns for FZ

d = 92 microns
n = 25 times

S = 13.01 microns for HZ

APPENDIX VII

STATISTICAL ANALYSIS: STUDENT'S T-TESTS (TWO SAMPLE)

Statistically significant results for Bone and Cartilage measurements

BSTV
lateral vs medial sections (young sheep)
Two-Sample Assuming Unequal Variances

	BSTV 1	BSTV 2
Mean	3.8200105	4.4306835
Variance	0.190959	0.1809968
Observations	12	12
Hypo. Mean Diff.	0	
df	22	
t Stat	-2.452667	
P(T<=t) one-tail	0.0170509	
t Critical one-tail	1.8124615	
P(T<=t) two-tail	**0.0341018**	
t Critical two-tail	2.2281392	

TbN
lateral vs medial sections (young sheep)
Two-Sample Assuming Unequal Variances

	TbN 1	TbN 2
Mean	1.9133386	2.2170084
Variance	0.047972	0.043837
Observations	12	12
Hypo. Mean Diff.	0	
df	22	
t Stat	-2.454904	
P(T<=t) one-tail	0.0169857	
t Critical one-tail	1.8124611	
P(T<=t) two-tail	**0.0339715**	
t Critical two-tail	2.2281388	

TbTh
lateral sections (mature vs young sheep)
Two-Sample Assuming Unequal Variances

	TbTh 1	TbTh 2
Mean	0.2593844	0.3250056
Variance	0.0025681	0.0032852
Observations	20	12
Hypo. Mean Diff.	0	
df	30	
t Stat	-2.220506	
P(T<=t) one-tail	0.0231981	
t Critical one-tail	1.7822867	
P(T<=t) two-tail	**0.0463962**	
t Critical two-tail	2.1788128	

FZ Thickness
lateral vs central sections (mature sheep)
Two-Sample Assuming Unequal Variances

	FZ 1	FZ 2
Mean	155.61907	129.64149
Variance	2000.1014	2513.2844
Observations	30	30
Hypo. Mean Diff.	0	
df	57	
t Stat	2.1179124	
P(T<=t) one-tail	0.0192779	
t Critical one-tail	1.6720287	
P(T<=t) two-tail	**0.0385557**	
t Critical two-tail	2.0024663	

FZ Thickness
central vs medial sections (mature sheep)
Two-Sample Assuming Unequal Variances

	FZ 1	FZ 2
Mean	129.64149	174.39332
Variance	2513.2844	6080.9417
Observations	30	30
Hypo. Mean Diff.	0	
df	49	
t Stat	-2.64404	
P(T<=t) one-tail	0.005487	
t Critical one-tail	1.6765512	
P(T<=t) two-tail	**0.010974**	
t Critical two-tail	2.009574	

HZ Thickness
lateral vs central sections (mature sheep)
Two-Sample Assuming Unequal Variances

	HZ 1	HZ 2
Mean	149.84276	120.28315
Variance	3559.5	2007.2971
Observations	30	30
Hypo. Mean Diff.	0	
df	54	
t Stat	2.1699842	
P(T<=t) one-tail	0.0172131	
t Critical one-tail	1.6735657	
P(T<=t) two-tail	**0.0344261**	
t Critical two-tail	2.004881	

APPENDIX VII

Total Thickness (TT)
lateral vs central sections (mature sheep)
Two-Sample Assuming Unequal Variances

	TT 1	TT 2
Mean	305.46182	249.92464
Variance	7123.1225	5363.7004
Observations	30	30
Hypo. Mean Diff.	0	
df	57	
t Stat	2.7221902	
P(T<=t) one-tail	0.0042942	
t Critical one-tail	1.6720287	
P(T<=t) two-tail	**0.0085884**	
t Critical two-tail	2.0024663	

Total Thickness (TT)
central vs medial sections (mature sheep)
Two-Sample Assuming Unequal Variances

	TT 1	TT 2
Mean	249.92464	312.49091
Variance	5363.7004	11458.149
Observations	30	30
Hypo. Mean Diff.	0	
df	51	
t Stat	-2.64219	
P(T<=t) one-tail	0.0054554	
t Critical one-tail	1.6752847	
P(T<=t) two-tail	**0.0109109**	
t Critical two-tail	2.0075822	

FZ Thickness
lateral vs medial sections (young sheep)
Two-Sample Assuming Unequal Variances

	FZ 1	FZ 2
Mean	142.60697	207.37518
Variance	2104.7969	15265.077
Observations	18	18
Hypo. Mean Diff.	0	
df	22	
t Stat	-2.08497	
P(T<=t) one-tail	0.0244441	
t Critical one-tail	1.7171443	
P(T<=t) two-tail	**0.0488882**	
t Critical two-tail	2.0738731	

APPENDIX VIII

STATISTICAL ANALYSIS: STUDENT'S T-TESTS (TWO SAMPLE)

Tests for Intraobserver and Interobserver variability
Measurements of Cartilage components using the Quantimet 500MC

INTRAOBSERVER VARIABILITY
Two-Sample Assuming Unequal Variances

	Total Area 1	Total Area 2
Mean	1475117	1489548
Variance	3.407E+11	4.006E+11
Observations	10	10
Hypothesized Mean [	0	
df	18	
t Stat	-0.053003	
P(T<=t) one-tail	0.4791566	
t Critical one-tail	1.7340636	
P(T<=t) two-tail	**0.9583132**	
t Critical two-tail	2.100922	

INTEROBSERVER VARIABILITY
Two-Sample Assuming Unequal Variances

	Total Area 1	Total Area 2
Mean	1475117	1506191
Variance	3.407E+11	3.545E+11
Observations	10	10
Hypothesized Mean [	0	
df	18	
t Stat	-0.117856	
P(T<=t) one-tail	0.4537435	
t Critical one-tail	1.7340636	
P(T<=t) two-tail	**0.907487**	
t Critical two-tail	2.100922	

INTRAOBSERVER VARIABILITY
Two-Sample Assuming Unequal Variances

	Field Area 1	Field Area 2
Mean	593471	612400
Variance	2.895E+10	4.577E+10
Observations	10	10
Hypothesized Mean [	0	
df	17	
t Stat	-0.218977	
P(T<=t) one-tail	0.4146378	
t Critical one-tail	1.7396067	
P(T<=t) two-tail	**0.8292757**	
t Critical two-tail	2.1098156	

INTEROBSERVER VARIABILITY
Two-Sample Assuming Unequal Variances

	Field Area 1	Field Area 2
Mean	593471	627639
Variance	2.895E+10	3.875E+10
Observations	10	10
Hypo. Mean Diff.	0	
df	18	
t Stat	-0.415273	
P(T<=t) one-tail	0.3414253	
t Critical one-tail	1.7340636	
P(T<=t) two-tail	**0.6828505**	
t Critical two-tail	2.100922	

APPENDIX VIII

STATISTICAL ANALYSIS: STUDENT'S T-TESTS (TWO SAMPLE)

Tests for Intraobserver and Interobserver variability
Measurements of Bone Indices using the Quantimet 500MC

INTRAOBSERVER VARIABILITY
Two-Sample Assuming Unequal Variances

	Field 1	Field 2
Mean	37942600	36897600
Variance	1.869E+14	1.929E+14
Observations	10	10
Hypo. Mean Diff.	0	
df	18	
t Stat	0.1695642	
P(T<=t) one-tail	0.433622	
t Critical one-tail	1.7340636	
P(T<=t) two-tail	**0.867244**	
t Critical two-tail	2.100922	

INTEROBSERVER VARIABILITY
Two-Sample Assuming Unequal Variances

	Field 1	Field 2
Mean	79361100	73823400
Variance	1.823E+15	1.056E+15
Observations	10	10
Hypo. Mean Diff.	0	
df	18	
t Stat	0.3263278	
P(T<=t) one-tail	0.37397	
t Critical one-tail	1.7340631	
P(T<=t) two-tail	**0.74794**	
t Critical two-tail	2.1009237	

INTRAOBSERVER VARIABILITY
Two-Sample Assuming Unequal Variances

	Area 1	Area 2
Mean	43611600	44462700
Variance	2.046E+14	1.495E+14
Observations	10	10
Hypo. Mean Diff.	0	
df	18	
t Stat	-0.143013	
P(T<=t) one-tail	0.4439343	
t Critical one-tail	1.7340631	
P(T<=t) two-tail	**0.8878687**	
t Critical two-tail	2.1009237	

INTEROBSERVER VARIABILITY
Two-Sample Assuming Unequal Variances

	Area 1	Area 2
Mean	25595300	20358100
Variance	1.825E+14	7.26E+13
Observations	10	10
Hypo. Mean Diff.	0	
df	15	
t Stat	1.0368599	
P(T<=t) one-tail	0.158114	
t Critical one-tail	1.7530503	
P(T<=t) two-tail	**0.316228**	
t Critical two-tail	2.1314495	

INTEROBSERVER VARIABILITY
Two-Sample Assuming Unequal Variances

	Perimeter 1	Perimeter 2
Mean	368359	283966
Variance	4.573E+10	1.251E+10
Observations	10	10
Hypo. Mean Diff.	0	
df	18	
t Stat	1.1058548	
P(T<=t) one-tail	0.1416756	
t Critical one-tail	1.7340631	
P(T<=t) two-tail	**0.2833512**	
t Critical two-tail	2.1009237	

INTEROBSERVER VARIABILITY
Two-Sample Assuming Unequal Variances

	Perimeter 1	Perimeter 2
Mean	134362.49	166319.2
Variance	5.065E+09	3.045E+09
Observations	10	10
Hypothesized Mean [	0	
df	17	
t Stat	-1.122156	
P(T<=t) one-tail	0.1386981	
t Critical one-tail	1.7396067	
P(T<=t) two-tail	**0.2773962**	
t Critical two-tail	2.1098156	

REFERENCES

Alini M, Matsui Y, Dodge GR, Poole AR. The extracellular matrix of cartilage in the growth plate before and during calcification: changes in composition and degradation of type II collagen. *Calcif Tissue Int.* 1992; **50(4):** 327-35.

Alini M, Marriott A, Chen T, Abe S, Poole AR. A novel angiogenic molecule produced at the time of chondrocyte hypertrophy during endochondral bone formation. *Dev Biol.* 1996; **176(1):** 124-32.

al-Mobireek AF, Darwazeh AM, Hassanin MB. Experimental induction of rheumatoid arthritis in temporomandibular joint of the guinea pig: a clinical and radiographic study. *Dentomaxillofac Radiol.* 2000; **29(5):** 286-90.

Amstutz HC and Sissons HA. The structure of the vertebral spongiosa. *J Bone Joint Surg Br.* 1969; **51(3):** 540-50.

Arnett GW and Tamborello JA. Progressive class II development-female idiopathic condylar resorption. In: West RA (Editor) Oral maxillofacial clinics of North America. Philadelphia: WB Saunders, 1990; 699-716.

Arnett GW, Tamborello JA, Rathbone JA. Temporomandibular joint ramifications of orthognathic surgery. In: Bell WH (Editor) Modern practice in orthognathic and reconstructive surgery. Philadelphia: WB Saunders, 1992; 523-93.

Arnett GW, Milam SB, Gottesman L. Progressive mandibular retrusion-idiopathic condylar resorption. Part I. *Am J Orthod Dentofacial Orthop.* 1996; **110(2):** 117-27.

Atkinson PJ. Variation in trabecular structure of vertebrae with age. *Calcif Tissue Res*. 1967; **1:** 24–32.

Baker JR. Principles of Biological Microtechnique. London: Methuen, 1958.

Bergman RJ, Gazit D, Kahn AJ, Gruber H, McDougall S, Hahn TJ. Age-related changes in osteogenic stem cells in mice. J *Bone Miner Res.* 1996; **(5):** 568-77.

Bergot C, Laval-Jeantet AM, Preteux F, Meunier A. Measurement of anisotropic vertebral trabecular bone loss during aging by quantitative imageanalysis. *Calcif Tissue Int.* 1988; **43(3):** 143-9.

Bermejo A, Gonzalez O, Gonzalez JM. The pig as an animal model for experimentation on the temporomandibular articular complex. *Oral Surg, Oral Med, Oral Path.* 1993; **75(1):** 18-23.

Bonse U, Busch F, Gunnewig O, Beckmann F, Pahl R, Delling G, Hahn M, Graeff W. 3D computed X-ray tomography of human cancellous bone at 8 microns spatial and 10^{-4} energy resolution. *Bone Miner.* 1994; **25(1):** 25-38.

Bosanquet AG and Goss AN. The sheep as a model for temporomandibular joint surgery. *Int J Oral Maxillofac Surg.* 1987; **16(5):** 600-3.

Bosshardt-Luehrs CPB and Luder H. Cartilage matrix production and chondrocyte enlargement as contributors to mandibular condylar growth in monkeys (Macaca fascicularis). *Am J Orthod Dentofacial Orthop.* 1991; **100:** 362-369.

Brighton CT. The growth plate. *Orthop Clin North Am.* 1984; **15(4):** 571-95.

Brookes M and Revel W. Blood supply of bone; specific aspects review and update. London: Springer, 1998.

Brown RA, Kayser M, McLaughlin B, Weiss JB. Collagenase and gelatinase production by calcifying growth plate chondrocytes. *Exp Cell Res.* 1993; **208(1):** 1-9.

Bullough PG. The role of joint architecture in the etiology of arthritis. *Osteoarthritis Cartilage.* 2004; **12:** S2-9.

Burr D. Subchondral bone in the pathogenesis of osteoarthritis. Mechanical aspects. In: Brandt KD, Doherty M, Lohmander LS (Editors) Osteoarthritis, 2nd Edition. Oxford: Oxford University Press, 2003; 125–132.

Byers S, van Rooden JC, Foster BK. Structural changes in the large proteoglycan, aggrecan, in different zones of the ovine growth plate. *Calcif Tissue Int.* 1997; **60(1):** 71-8.

Byers S, Moore AJ, Byard RW, Fazzalari NL. Quantitative histomorphometric analysis of the human growth plate from birth to adolescence. *Bone.* 2000; **27(4):** 495-501.

Carlevaro MF, Albini A, Ribatti D, Gentili C, Benelli R, Cermelli S, Cancedda R, Cancedda FD. Transferrin promotes endothelial cell migration and invasion: implication in cartilage neovascularization. *J Cell Biol.* 1997; **136(6):** 1375-84.

Carlson DS, McNamara JA, Jaul DH. Histological analysis of the growth of the mandibular condyle in the resus monkey (*Macaca mulatta*). *Am J Anat.* 1978; **151:** 103-118.

Charlier JP, Petrovic A, Herrmann-Stutzmann J. Effects of mandibular hyperpropulsion on the prechondroblastic zone of young rat condyle. *Am J Orthod.* 1969; **55(1):** 71-4.

Crompton AW and Parker P. Evolution of the mammalian masticatory apparatus. *Am Sci.* 1978; **66:** 192-201.

Croucher PI, Garrahan NJ, Compston JE. Assessment of cancellous bone structure: comparison of strut analysis, trabecular bone pattern factor and marrow space star volume. *J Bone Miner Res.* 1996; **11(7):** 955-61.

Culling CFA. Handbook of histopathological and histochemical techniques, 3rd Edition. London: Butterworths, 1974.

Dahlberg G. Statistical methods for medical and biological studies. New York: Interscience Publications, 1940.

de Bont LG, Boering G, Liem RS, Eulderink F, Westesson PL. Osteoarthritis and internal derangement of the temporomandibular joint: a light microscopic study. *J Oral Maxillofac Surg.* 1986; **44(8):** 634-43.

de Bont LG and Stegenga B. Pathology of temporomandibular joint internal derangement and osteoarthrosis. *Int J Oral Maxillofac Surg.* 1993; **22(2):** 71-4.

Dick R and Jones DN. Temporomandibular joint condyle changes in patients undergoing chronic haemodialysis. *Clin Radiol.* 1973; **24:** 72-76.

Dieppe P, Cushnaghan J, Young P, Kirwan J. Prediction of the progression of joint space narrowing in osteoarthritis of the knee by bone scintigraphy. *Ann Rheum Dis.* 1993; **52:** 557–563.

Ding M, Dalstra M, Danielsen CC, Kabel J, Hvid I, Linde F. Age variations in the properties of human tibial trabecular bone. *Bone Joint Surg Br.* 1997; **79(6):** 995-1002.

Dovitch V and Herzberg F. A radiographic study of the bony trabecular pattern in the mandibular rami of certain herbivores, carnivores and omnivores. *Angle Orthod.* 1968; **38:** 205–210.

Drury RAB and Wallington EA. Carleton's histological technique. New York: Oxford University Press, 1967.

Feldkamp LA, Goldstein SA, Parfitt AM, Jesion G, Kleerekoper M. The direct examination of three-dimensional bone architecture in vitro by computed tomography. *Bone Miner Res.* 1989; **4(1):** 3-11.

Felson DT, McLaughlin S, Goggins J, LaValley MP, Gale ME, Totterman S, Li W, Hill C, Gale D. Bone marrow edema and its relation to progression of knee osteoarthritis. *Ann Intern Med.* 2003; **139:** 330–336.

Festing, M. Doing better animal experiments; together with notes on the genetic nomenclature of laboratory animals. *ANZCCART News*. 2000; **13:** 1-8.

Finn B. The Anatomy and Biomechanics of the Masticatory Apparatus in the Australian Merino Sheep [Master of Dental Surgery]. Adelaide: The University of Adelaide; 1994.

Flint MH, Lyons MF, Meaney MF, Williams DE. The Masson staining of collagen-an explanation of an apparent paradox. *Histochemical Journal.* 1975; **7:** 529-546.

Flygare L, Hosoki H, Rohlin M, Petersson A. Bone histomorphometry using interactive image analysis. A methodological study with application on the human temporomandibular joint. *Eur J Oral Sci.* 1997; **105(1):** 67-73.

Fontenot MG. Viscoelastic properties of human TMJ discs and disc replacement materials (abstract). *J Dent Res.* 1985; **64:** 163.

Fujisawa T, Kuboki T, Kasai T, Sonoyama W, Kojima S, Uehara J, Komori C, Yatani H, Hattori T, Takigawa M. Repetitive, steady mouth opening induced an osteoarthritis-like lesion in the rabbit temporomandibular joint. *J Dent Res.* 2003; **82(9):** 731-5.

Furstman L, Bernick S, Zipkin I. The effect of hydrocortisone and fluoride upon the rat's mandibular joint. J *Oral Therap Pharm.* 1965; **1:** 515-525.

Gibson GJ and Flint MH. Type X collagen synthesis by chick sternal cartilage and its relationship to endochondral development. *J Cell Biol.* 1985; **101(1):** 277-84.

Giesen EB and van Eijden TM. The three-dimensional cancellous bone architecture of the human mandibular condyle. *J Dent Res.* 2000; **79(4):** 957-63.

Gillbe GV. A comparison of the disc in the craniomandibular joint of three mammals. *Acta Anat.* 1973; **86:** 394-409.

Glorieux FH, Travers R, Taylor A, Bowen JR, Rauch F, Norman M, Parfitt AM. Normative data for iliac bone histomorphometry in growing children. *Bone.* 2000; **26:** 103–109.

Goldstein SA, Goulet R, McCubbrey D. Measurement and significance of three-dimensional architecture to the mechanical integrity of trabecular bone. *Calcif Tissue Int.* 1993; **53:** S127-32.

Gong H, Zhang M, Yeung HY, Qin L. Regional variations in microstructural properties of vertebral trabeculae with aging. *J Bone Miner Metab.* 2005; **23(2):** 174-80.

Goose DH and Appleton J. Human dentofacial growth. Oxford: Pergamon Press, 1982.

Griffin CJ, Hawthorn R, Harris R. Anatomy and histology of the human temporomandibular joint. *Monogr Oral Sci.* 1975; **4:** 1-26.

Gruber HE and Rimoin DL. Quantitative histology of cartilage cell columns in the human costochondral junction: Findings in newborn and pediatric subjects. *Pediatr Res.* 1989; **25:** 202–204.

Hacker SA, Healey RM, Yoshioka M, Coutts RD. A methodology for the quantitative assessment of articular cartilage histomorphometry. *Osteoarthritis Cartilage.* 1997; **5(5):** 343-55.

Hecker JF. The sheep as an experimental animal. London: Academic press, 1983.

Heinegard D, Bayliss M, Lorenzo P. Biochemistry and metabolism of normal and osteoarthritic cartilage. In: Brandt KD, Doherty M, Lohmander LS (Editors) Osteoarthritis, 2nd Edition. Oxford: Oxford University Press, 2003; 73–82.

Herring SW. Animal models of temporomandibular disorders: how to choose. In: Sessle BJ, Bryant PS, Dionne RA (Editors). Temporomandibular Disorders and Related Pain Conditions. Seattle: IASP Press, 1995; 323-328.

Herring SW. Critical Commentary 1: The role of the human lateral pterygoid muscle in the control of horizontal jaw movements. *J Orofac Pain.* 2001; **15:** 292-295.

Herring SW, Decker JD, Liu ZJ and Ma T. The temporomandibular joint in miniature pigs: anatomy, cell replication, and relation to loading. *Anat Rec.* 2002; **266:** 152-166.

Herring SW. TMJ anatomy and animal models. *J Musculoskelet Neuronal Interact.* 2003; **3(4):** 391-4.

Hert J. A new explanation of the cancellous bone architecture. *Funct Devel Morph.* 1992; **2:** 17-24.

Hert J. A new attempt at the interpretation of the functional architecture of the cancellous bone. *J Biomech.* 1994; **27:** 239-242.

Hongo T, Yotsuya H, Shibuya K, Kawase M, Ide Y. Quantitative and morphological studies on the trabecular bones in the condyloid processes of the Japanese mandibles. Comparisons between dentulous and edentulous specimens. *Bull Tokyo Dent Coll.* 1989a; **30(2):** 67-76.

Hongo T, Orihara K, Onoda Y, Nakajima K, Ide Y. Quantitative and morphological studies of the trabecular bones in the condyloid processes of the Japanese mandibles; changes due to aging. *Bull Tokyo Dent Coll.* 1989b; **30(3):** 165-74.

Huber M, Trattnig S, Lintner F. Anatomy, biochemistry, and physiology of articular cartilage. *Invest Radiol.* 2000; **35(10):** 573-80.

Hunziker EB, Schenk RK, Cruz-Orive LM. Quantitation of chondrocyte performance in growth-plate cartilage during longitudinal bone growth. *J Bone Joint Surg Am.* 1987; **69(2):** 162-73.

Hunziker EB and Schenk RK. Physiological mechanisms adopted by chondrocytes in regulating longitudinal bone growth in rats. *J Physiol.* 1989; **414:** 55–71.

Hylander WL. Experimental analysis of temporomandibular joint reaction force in macaques. *Am J Phys Anthrop.* 1979; **51:** 433-456.

Hylander WL and Bays R. An in vivo strain gauge analysis of squamosal-dentary joint reaction force during mastication and incision in *Macaca mulatta* and *Macaca fascicularis*. *Arch Oral Bio.* 1979; **24:** 689-697.

Iannotti JP. Growth plate physiology and pathology. *Orthop Clin North Am.* 1990; **21(1):** 1-17.

Isaacson KG, Reed RT, Stephens CD. Functional orthopaedic appliances. Oxford: Blackwell Scientific Publications, 1990.

Ishibashi H, Takenoshita Y, Ishibashi K, Oka M. Age-related changes in the human mandibular condyle: a morphologic, radiologic, and histologic study. *J Oral Maxillofac Surg.* 1995; **53(9):** 1016-23.

Ishimaru J and Goss AN. A model for osteoarthritis of the temporomandibular joint. *J Oral Maxillofac Surg.* 1992; **50(11):** 1191-5.

Judex S, Boyd S, Qin YX, Turner S, Ye K, Muller R, Rubin C. Adaptations of trabecular bone to low magnitude vibrations result in more uniform stress and strain under load. *Ann Biomed Eng.* 2003; **31(1):** 12-20.

Kantomaa T. Effect of increased posterior displacement of the glenoid fossa on mandibular growth: a methodological study on the rabbit. *Eur J Orthod.* 1984; **6(1):** 15-24.

Karaharju-Suvanto T. Cephalometric changes after gradual lengthening of the mandible: an experimental study in sheep. *Dentomaxillofac Radiol.* 1994; **23(3):** 159-62.

Kawashima T, Abe S, Okada M, Kawada E, Saitoh C, Ide Y. Internal structure of the temporomandibular joint and the circumferential bone: comparison between dentulous and edentulous specimens. *Bull Tokyo Dent Coll.* 1997; **38(2):** 87-93.

Kember NF and Sissons HA. Quantitative histology of the human growth plate. *J Bone Jt Surg.* 1976; **58**: 426–435.

Kneissel M, Roschger P, Steiner W, Schamall D, Kalchhauser G, Boyde A, Teschler-Nicola M. Cancellous bone structure in the growing and aging lumbar spine in a historic Nubian population. *Calcif Tissue Int.* 1977; **61:** 95–100.

Kraus WJ and Cutts JH. Concise text of histology. Baltimore: Williams & Wilkins, 1981.

Kuhn JL, DeLacey JH, Leanellett EE. Relationship between bone growth rate and hypertrophic chondrocyte volume in New Zealand white rabbits of varying ages. *J Orthop Res.* 1996; **14:** 706–711.

Lamar Jones M. Connective tissues and stains. In: Bancroft D and Gamble M (Editors) Theory and practice of histological techniques. London: Churchill Livingstone, 2002; 139-162.

Lanyon LE. Control of bone architecture by functional load bearing. *J Bone Min Res.* 1992; **7(2):** S369-375.

Leidhold K, Krey KF, Dannhauer KH, Keller F. Investigations into growth and differentiation in the cartilage of the condylar process in the domestic pig. A quantitative study of endochondral cartilage growth and cell distribution. *J Orofac Orthop.* 2004; **65(5):** 363-75.

Lewinson D and Silbermann M. Chondroclasts and endothelial cells collaborate in the process of cartilage resorption. *Anat Rec.* 1992; **233(4):** 504-14.

Lieberman DE and Crompton AW. Why fuse the mandibular symphysis? A comparative analysis. *Am J Phys Anthropo.* 2000; **112(4):** 517-40.

Liebgott WB. The anatomical basis of dentistry. Philadelphia: WB Saunders, 1982.

Lillie, RD. H.J. Conn's Biological Stains, 8th Edition. Baltimore: Williams & Wilkins, 1969.

Luder HU. Perichondrial and endochondral components of mandibular condylar growth: morphometric and radioautographic quantitation in rats. *J Anat.* 1994; **185:** 587-598.

Luder HU. Frequency and distribution of articular tissue features in adult human mandibular condyles: a semiquantitative light microscopic study. *Anat Rec.* 1997; **248(1):** 18-28.

Luder HU. Age changes in the articular tissue of human mandibular condyles from adolescence to old age: a semiquantitative light microscopic study. *Anat Rec.* 1998; **251(4):** 439-47.

Luder HU and Schroeder HE. Light and electron microscopic morphology of the temporomandibular joint in growing and mature crab-eating monkeys (*Macaca fascicularis*): the condylar calcified cartilage. *Anatomy and Embryology.* 1992; **185:** 189-199.

Ma B, Sampson W, Fazzalari N, Wilson D, Wiebkin O. Induced mandibular condylar growth in a sheep model after functional appliance treatment. *Aust Orthod J.* 2001; **17(2):** 81-8.

Ma B, Sampson W, Fazzalari N, Wilson D, Wiebkin O. Experimental forward mandibular displacement in sheep. *Arch Oral Biol.* 2002a; **47(1):** 75-84.

Ma B, Sampson W, Wilson D, Wiebkin O, Fazzalari N. A histomorphometric study of adaptive responses of cancellous bone in different regions in the sheep mandibular condyle following experimental forward mandibular displacement. *Arch Oral Biol.* 2002b; **47(7):** 519-27.

Masson, P. Some histological methods. Trichrome stainings and their preliminary technique. *J tech Meth.* 1929; **12:** 75-90.

May, N. The anatomy of the sheep: a dissection manual, 3rd Edition. St. Lucia: University of Queensland Press, 1970; 97-99.

Mayhew T. 3D structure from thin sections: applications of stereology. In: Heath J (Editor) Asia/Pacific Microscopy and Analysis. Surrey: Rolston Gordon Communications, 2000; 11-14.

Mazzuca SA, Brandt KD, Schauwecker DS, Buckwalter KA, Katz BP, Meyer JM, Lane KA. Bone scintigraphy is not a better predictor of progression of knee osteoarthritis than Kellgren and Lawrence grade. *J Rheumatol.* 2004; **31(2):** 329-32.

McKay GS, Yemm R, Cadden SW. The structure and function of the temporomandibular joint. *Br Dent J.* 1992; **173(4):** 127-32.

McMillen C. The sheep-an ideal model for biomedical research? *ANZCCART News.* 2001; **14(2):** 1-4.

McNamara JA Jr and Carlson DS. Quantitative analysis of temporomandibular joint adaptations to protrusive movement. *Am J Orthod.* 1979; **76:** 593-611.

McNeill C. Temporomandibular disorders: guidelines for classification, assessment and management, 2nd Edition. Chicago: Quintessence Books, 1993; 27-31.

Merida-Velasco JR, Rodriguez-Vazquez JF, Merida-Velasco JA, Sanchez-Montesinos I, Espin-Ferra J, Jimenez-Collado J. Development of the human temporomandibular joint. *Anat Rec.* 1999; **255(1):** 20-33.

Miralles-Flores C and Delgado-Baeza E. Histomorphometric analysis of the epiphyseal growth plate in rats after prenatal alcohol exposure. *J Orthop Res.* 1992; **10:** 325–336.

Mongini F. Influence of function on temporomandibular joint remodelling and degenerative disease. *Dent Clin North Am.* 1983; **27(3):** 479-94.

Nakajima K, Onoda Y, Okada M, Abe S, Ide Y. A study of the internal structure of the mandibular ramus in Japanese. *Bull Tokyo Dent Coll.* 1998; **39(1):** 57-65.

Nickel JC and McLachlan KR. In vitro measurement of the stress-distribution properties of the pig temporomandibular joint disc. *Arch Oral Biol.* 1994; **39(5):** 439-48.

Oberg T, Fajers CM, Friberg U, Lohmander S. Collagen formation and growth in the mandibular joint of the guinea pig as revealed by autoradiography with 3H-proline. *Acta Odontol Scand.* 1969; **27(4):** 425-42.

Oberg T and Carlsson GE. Macroscopic and microscopic anatomy of the temporomandibular joint. In: Zarb GA and Carlsson GE (Editors) Temporomandibular Joint function and dysfunction. Copenhagen: Munksgaard, 1979; 101-118.

Oberholzer M, Ostreicher M, Christen H, Bruhlmann M. Methods in Quantitative image analysis. *Histochem Cell Bio.* 1996; **105:** 333-355.

Odgaard A. Three-dimensional methods for quantification of cancellous bone architecture. *Bone.* 1997; **20(4):** 315-28.

Oztan HY, Ulusal BG, Aytemiz C. The role of trauma on temporomandibular joint ankylosis and mandibular growth retardation: an experimental study. *J Craniofac Surg.* 2004; **15(2):** 274-82.

Palla S, Gallo LM, Gossi D. Dynamic stereometry of the temporomandibular joint. *Orthod Craniofac Res.* 2003; **6:** 37-47.

Parfitt AM, Mathews CH, Villanueva AR, Kleerekoper M, Frame B, Rao DS. Relationships between surface, volume, and thickness of iliac trabecular bone in aging and in osteoporosis. Implications for the microanatomic and cellular mechanisms of bone loss. *J Clin Invest.* 1983; **72(4):** 1396-409.

Parkes EW. Braced Frameworks. Oxford: Pergamon Press, 1974.

Parkinson IH and Fazzalari NL. Cancellous bone structure analysis using image analysis. *Australas Phys Eng Sci Med.* 1994; **17(2):** 64-70.

Paulsen HU, Thomsen JS, Hougen HP, Mosekilde L. A histomorphometric and scanning electron microscopy study of human condylar cartilage and bone tissue changes in relation to age. *Clin Orthod Res.* 1999; **2(2):** 67-78.

Peat G, McCarney R, Croft P. Knee pain and osteoarthritis in older adults: a review of community burden and current use of primary health care. *Ann Rheum Dis.* 2001; **60:** 91–97.

Perry HT, Xu Y, Forbes DP. The embryology of the temporomandibular joint. *Cranio.* 1985; **3(2):** 125-32.

Petersson I. Occurrence of osteoarthritis of the peripheral joints in European populations. *Ann Rheum Dis.* 1996; **55:** 659–661.

Phinney DG, Kopen G, Isaacson RL, Prockop DJ. Plastic adherent stromal cells from the bone marrow of commonly used strains of inbred mice: variations in yield, growth, and differentiation. *J Cell Biochem.* 1999; **72(4):** 570-85.

Piette E. Anatomy of the human temporomandibular joint. An updated comprehensive review. *Acta Stomatol Belg.* 1993; **90(2):** 103-127.

Pritzker K. Pathology of osteoarthritis. In: Brandt K, Doherty M, Lohmander LS (Editors) Osteoarthritis, 2nd Edition. Oxford: Oxford University Press, 2003; 49–58.

Puzas JE. Biology and pathology of the temporomandibular joint: is there an animal model to study this affliction? *J Musculoskelet Neuronal Interact.* 2003; **3(4):** 395-400.

Rodriguez JI, Razquin S, Palacios J, Rubio V. Human growth plate development in the fetal and neonatal period. *J Orthop Res.* 1992; **10:** 62–71.

Roesler H. Some historical remarks on the theory of cancellous bone structure (Wolff's law). In: Cowin SC (Editor) Mechanical properties of bone. New York: The American Society of Mechanical Engineers, 1981; 27-42.

Sandy J. Proteolytic degradation of normal and osteoarthritic cartilage matrix. In: Brandt KD, Doherty M, Lohmander LS (Editors) Osteoarthritis, 2nd Edition. Oxford: Oxford University Press, 2003; 82–92.

Sasaki T, Kim TW, Debari K, Nagamine H. Cartilage-bone replacement in endochondral ossification of mandibular condylar heads in young beagle dogs. *J Electron Microsc (Tokyo).* 1996; **45(3):** 213-22.

Seipp JH. The Temporomandibular Joint. In: Provenza DV (Editor) Oral Histology, inheritance and development. Philadelphia: JB Lippincott Company.

Silbermann M and Livne E. Age-related degenerative changes in the mouse mandibular joint. *J Anat.* 1979; **129(3):** 507-520.

Smit TH, Odgaard A, Schneider E. Structure and function of vertebral trabecular bone. *Spine.* 1997; **22(24):** 2823-33.

Sontag W. Age-dependent morphometric change in the lumbar vertebrae of male and female rats: Comparison with the femur. *Bone.* 1994; **15:** 593–601.

Standlee JP, Caputo AA, Ralph JP. The condyle as a stress-distributing component of the temporomandibular joint. *J Oral Rehab.* 1981; **8(5):** 391-400.

Stratmann U, Schaarschmidt K, Santamaria P. Morphometric investigation of condylar cartilage and disc thickness in the human temporomandibular joint: significance for the definition of ostearthrotic changes. *J Oral Pathol Med.* 1996; **25(5):** 200-5.

Ten Cate AR. Oral histology: development, structure and function, 6th Edition. St. Louis: Mosby, 2003.

Teng S and Herring SW. A stereological study of trabecular architecture in the mandibular condyle of the pig. *Arch Oral Biol.* 1995; **40(4):** 299-310.

Thilander B, Carlsson GE, Ingervall B. Postnatal development of the human temporomandibular joint. I. A histological study. *Acta Odontol Scand.* 1976; **34(2):** 117-126.

Thomason JJ, Grovum LE, Deswysen AG, Bignell WW. In vivo surface strain and stereology of the frontal and maxillary bones of sheep: implications for the structural design of the mammalian skull. *Anat Rec.* 2001; **264(4):** 325-38.

Tominaga K, Hirashima S, Fukuda J. An experimental model of osteoarthrosis of the temporomandibular joint in monkeys. *Br J Oral Maxillofac Surg.* 2002; **40(3):** 232-7.

Turner CH. On Wolff's law of trabecular architecture. *J Biomech.* 1992a; **25:** 1-9.

Turner CH. Functional determinants of bone structure: beyond Wolff's law of bone transformation. *Bone.* 1992b; **13:** 403-409.

van der Gulden WJ, Beynen AC, Bosland MC. Animal models. In: van Zutphen LF, Baumans V, Beynen AC (Editors) Principles of laboratory animal science Amsterdam: Elsevier, 1993; 189-196.

von Wowern N and Stoltze K. Pattern of age related bone loss in mandibles. *Scand J Dent Res.* 1980; **88(2):** 134-46.

Watt I and Doherty M. Plain radiographic features of osteoarthritis. In: Brandt K, Doherty M, Lohmander LS (Editors) Osteoarthritis, 2nd Edition. Oxford: Oxford University Press, 2003; 211–225.

Westacott CI. Subchondral bone in the pathogenesis of osteoarthritis. Biological effects. In: Brandt KD, Doherty M, Lohmander LS (Editors) Osteoarthritis, 2nd Edition. Oxford: Oxford University Press, 2003; 133–142.

Wish-Baratz S, Hershkovitz I, Arensburg B, Latimer B, Jellema LM. Size and location of the human temporomandibular joint. *Am J Phys Anthropol.* 1996; **101(3):** 387-400.

Wright DM and Moffett BC Jr. The postnatal development of the human temporomandibular joint. *Am J Anat.* 1974; **141(2):** 235-49.